



NTNU – Trondheim
Norwegian University of
Science and Technology

Rigid Pipelay Curve Stability

Christian Andersson

Marine Technology

Submission date: June 2014

Supervisor: Svein Sævik, IMT

Co-supervisor: Trond Ståle Nessmo, Subsea 7

Norwegian University of Science and Technology
Department of Marine Technology

NORWEGIAN UNIVERSITY OF SCIENCE AND
TECHNOLOGY

MASTER THESIS SPRING 2014:

Rigid Pipelay Curve Stability

Christian Andersson

June 10, 2014



NTNU – Trondheim
Norwegian University of
Science and Technology



MASTER THESIS SPRING 2014

for

Stud. tech. Christian Andersson

Rigid Pipelay Curve Stability

Kurve stabilitet under legging av stive rør

Field developments with constraints from existing subsea infrastructure or natural seabed features may introduce rigid pipeline routes with small curve radiuses. Rigid pipelines are commonly stable during pipe laying by weight for curve radiuses from 1000m and above. At smaller curve radiuses additional measures like turnpoints (lateral supports) may be required.

Project experience shows that the calculate required number of turnpoints, based on both pipeline structural integrity and turn point's capacity to withstand horizontal contact force, is conservative compared to what is seen offshore. It is believed that a better method for calculating contact force from pipeline on turn points would reduce the number of turnpoints installed offshore. The master thesis work is to be carried out as follows::

- 1) Literature study: A general study on pipeline design topics, i.e. on-bottom stability, free span assessment, wall thickness design, trawl interaction, in-place condition with local buckling criteria (this is suggested as there is not literature study required for turn points evaluation)
- 2) Establish basis in terms of case study input data.
- 3) Installation analysis by use of Orcaflex or Simla to define bottom tension during pipelay operations. The bottom tensions are input to analysis of load acting on turnpoints.
- 4) Establishment of methodology for calculating turn point loading:
 - a) Evaluate effect of turnpoints installation tolerances
 - b) Evaluate level of dynamic tension to be applied in analysis. E.g. max tension minus one/two standard deviations may give a sufficient safety level to avoid failure of turnpoints.
- 5) Establish local FE model to model interaction between pipeline with external coating and turnpoint. (can be seen in connection with your project thesis done last autumn, with collapse of pipelines with thick coating).
- 6) Perform analysis with respect to the stress/local buckling utilization versus the turnpoint load
- 7) Conclusions and recommendations for further work

It is assumed that the input data for the case study is provided by Subsea7.

The work scope may prove to be larger than initially anticipated. Subject to approval from the supervisors, topics may be deleted from the list above or reduced in extent.

In the thesis the candidate shall present his personal contribution to the resolution of problems within the scope of the thesis work

Theories and conclusions should be based on mathematical derivations and/or logic reasoning identifying the various steps in the deduction.

The candidate should utilise the existing possibilities for obtaining relevant literature.

Thesis format

The thesis should be organised in a rational manner to give a clear exposition of results, assessments, and conclusions. The text should be brief and to the point, with a clear language. Telegraphic language should be avoided.

The thesis shall contain the following elements: A text defining the scope, preface, list of contents, summary, main body of thesis, conclusions with recommendations for further work, list of symbols and acronyms, references and (optional) appendices. All figures, tables and equations shall be numerated.

The supervisors may require that the candidate, in an early stage of the work, presents a written plan for the completion of the work.

The original contribution of the candidate and material taken from other sources shall be clearly defined. Work from other sources shall be properly referenced using an acknowledged referencing system.

The report shall be submitted in two copies:

- Signed by the candidate
- The text defining the scope included
- In bound volume(s)
- Drawings and/or computer prints which cannot be bound should be organised in a separate folder.

Ownership

NTNU has according to the present rules the ownership of the thesis. Any use of the thesis has to be approved by NTNU (or external partner when this applies). The department has the right to use the thesis as if the work was carried out by a NTNU employee, if nothing else has been agreed in advance.

Thesis supervisors:

Prof. Svein Sævik, NTNU
Trond Ståle Nessmo, Subsea7

Deadline: June 10th , 2014

Trondheim, January , 2014

Svein Sævik

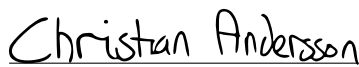
Preface

This report is the result of the Master's thesis work done by stud.techn. Christian Andersson during the spring semester 2014 at the department of Marine Technology, Norwegian University of Science and Technology.

During the early stages of the thesis work, a lot of time was spent reading relevant literature in the field of pipeline design. In addition, much time was spent to get familiarised with the SIMLA software. When the final hand were laid on the static analyses, setting up the dynamic analyses went a bit faster. However, the process of running the dynamic analysis was much more time-consuming than expected. It was first attempted to reduce the computational time by reducing the sea state from 3 to 1 hour. In addition, the number of pipe-elements was reduced compared to the static analysis. This saved a lot of time, but the time spent running the dynamic analysis was still significant. Late in the work process, it became evident that the most critical response would occur at the same time, during a sea state with the same seed, i.e. same waves generated. One analysis, with a 3 hour sea state was therefore performed in order to obtain the most critical response. Then, all the other dynamic analyses were set up with a short time-interval around this critical time-period. This was a real time saver and was essential in order to get finished with the results. It was originally planned to establish a local Finite Element model to study the interaction between the pipeline with external coating and the turnpoint. However, as other parts of the scope of work have been very time consuming, this has been removed in agreement with the supervisors.

I would like to thank my fellow students in my office, for multiple academic discussions, and especially Sindre M. Dahl, for letting me run some SIMLA analyses at his computer. A great thank must be addressed to Trond Ståle Nessmo in Subsea 7, for all the help he has provided during the thesis work. Meetings and email correspondence have been of great help. I would also like to thank professor Svein Sævik for excellent counselling and all the help he has offered me during the thesis work. Weekly guidance time and discussions has been invaluable for the completion of this thesis. Especially his expertise within SIMLA, has been of very good use regarding modelling tips and code debugging. In addition, Marintek should be acknowledged regarding license of SIMLA.

Trondheim, June 10, 2014



Christian Andersson

Summary

Pipeline installation would generally involve curved sections in the horizontal plane, due to existing subsea infrastructure or natural seabed characteristics. At a small curve radius, the lateral seabed friction could be insufficient providing on-bottom stability of the pipeline. Hence, additional measures like lateral supports, so called turnpoints, may be required. The effect of installing such turnpoints have been studied in this thesis, using a computer software called SIMLA. Both static and dynamic analyses have been performed in order to preserve the curve stability and control the load effect on the pipeline and the turnpoints. In the static analyses, the pipe is being fed out from the Seven Navica lay vessel. In this way, history effects get introduced as the pipe elements experience the operation from being fed out until it rests on the seabed. The dynamic analyses is carried out at the stage in the laying process that results in the highest dynamic response.

The pipeline investigated is a 10" ID production pipeline laid between two templates. The route is assumed to have a constant water depth, and consists of two straight distances having a curved section with a curve radius of 400 [m] in between. In the route, originally 10 turnpoints have been installed. In order to investigate whether this is a over-conservative number, the analyses performed in this thesis have been conducted for 3-10 turnpoints along the route.

In the static feeding analysis, the axial friction is turned off during laying. This is done since the results obtained with axial friction activated gave less credible results, as the simulations indicated that the static axial force distribution was changed with increased number of turnpoints. Given that the pipe is assumed laid at a constant water depth, deactivating the axial friction can be justified. The reason is that the constant water depth gives rise to a stable departure angle, and thus an approximately constant tension in the pipe during laying.

From the static results, it is found that introducing more turnpoints along the route resulted in a flattening of the equivalent moment-curve. This makes sense, since the distance between the turnpoints is reduced. In the same manner, the contact force between the turnpoints and the pipeline gets reduced, as the force is more distributed and shared between additional supports. It is further noted that both the contact force and the moment is symmetrically distributed over the pipeline curvature. Based on this, symmetry of the problem could probably be exploited, reducing the size of the static model.

Several parameter studies have been carried out in order to obtain the overall worst case results. Based on the parameter study, the dynamic analysis was set up. The following parameters have been applied in the dynamic analyses:

- A current direction of 90° , pushing the pipe towards the turnpoint.
- A touchdown position right behind the last turnpoint.
- A wave heading of 45° from behind on the vessel, introducing both roll and pitch motion. With a significant wave height of $H_S = 2.5$ [m] and a wave period of $T_P = 7$ [s].

The dynamic analysis has been carried out during a 3-hour sea state, prescribed by the Jonswap-spectrum. In order to reduce the computational time running the analyses, the worst response during the sea state was found, and then all the analyses was carried out in a short time interval, based on the most critical time.

The dynamic tension in the pipeline increases as more turnpoints are installed, i.e. the system gets stiffer. As the system gets stiffer with more turnpoints installed, the contact force between the turnpoints and the pipeline is actually at its lowest when only 3 turnpoints are installed. This can be explained by the increase of tension in the pipeline. A stiffer system gives higher dynamic response. As far as the moment distribution is concerned, the same applies as for the static analyses, i.e. the moment gets reduced when the number of turnpoints is increased.

A local buckling check has been performed in order to control the results against DNV's standard for local buckling. It is found that neither 3 nor 4 turnpoints along the route is sufficient to satisfy the local buckling criteria. Hence, 5 or more turnpoints must be installed. In addition to this criteria, the turnpoints used in the case investigated have a geotechnical capacity of 80 [kN]. The contact force between the turnpoint and pipe must therefore be kept below this capacity.

As the turnpoints are installed with a certain turnpoint tolerance, an analysis investigating the effect of such tolerance has been performed. As the tolerance was set to 0.5 [m] in the lateral direction, there was an increase in the contact forces, the moment and the tension in the pipeline. The contact force remained within the geotechnical limitations of the turnpoints utilized. However, the results showed that 5 turnpoints along the curvature is not sufficient to fulfil the local buckling criteria. Hence, installation of 6 turnpoints is proposed. This is lower than the originally 10 turnpoints that have been installed for the case investigated. Hence, the method utilized by Subsea 7 is found to be over-conservative.

In order to create a picture of how the turnpoint tolerance affects the results, an analysis has been carried out for 1 [m] lateral tolerance as well. This resulted in a significant increase of moments and contact force between the pipe and the turnpoints. Furthermore, the local buckling utilization is considerably increased when the tolerance is as high as 1 [m] in the lateral direction. It is evident that the turnpoint tolerance is of high importance. Keeping the tolerance as low as possible is essential in order to install as few turnpoints as possible.

Sammendrag

Installasjon av rørledninger vil generelt involvere kurvede seksjoner i horisontalplanet, som følge av eksisterende undervanns-installasjoner, eller som følge av naturlige sjøbunnsforhold. I tilfeller der radiusen til kurvaturen blir liten, kan den laterale friksjonen på sjøbunnen bli for liten med hensyn på å kunne sikre stabilitet av rørledningen. Ved slike tilfeller, er det nødvendig med forebyggende tiltak. Støtter som hindrer røret fra å bevege seg sideveis på havbunn, såkalte turnpoints, er en mulig løsning.

I denne oppgaven er SIMLA benyttet til å studere effekten av å installere slike støtter på havbunnen når det er nødvendig med horisontal kurvatur av rørledningen. Simla er et program som er spesialtilpasset analyser av offshore rørledninger under design, installasjon og operasjon. Både statisk og dynamisk analyse av problemet er utført slik at kurvstabilitet bevares og lasteffekt på rørledningen og turnpunktene holdes på et akseptabelt nivå. I den statiske analysen blir røret matet ut fra leggefartøyet Seven Navica, slik at historie-effekter inkluderes. På denne måten opplever rør-elementene hele prosessen fra å bli matet ut fra skipet til det hviler på havbunn. Den dynamiske analysen blir så utført på det stadiet av leggeprosessen som resulterer i høyest dynamisk respons, slik at verste tilfelle av dynamisk effekt blir introdusert i systemet.

Røret som undersøkes er et 10" indre diameter produksjonsrør, som skal ligge mellom to subsea templates. Ruten som røret skal legges antas å ha et konstant vanddyb og består av to rette strekninger med en kurvet seksjon i midten, som har en kurv-radius på 400 [m]. I tilfellet som undersøkes er det opprinnelig installert 10 turnpoints. For å undersøke om dette er et over-konservativt antall, har det blitt utført analyser for installasjon av 3-10 turnpoints langs ruten.

I den statiske legg-analysen deaktiveres aksial friksjon, ettersom lite troverdige resultater ble funnet da dette var aktivert. Resultatene indikerte at kraftfordelingen i aksialplanet endret seg med økt antall turnpoints. Antagelsen om å deaktivere aksial friksjon kan forsvares, tatt i betraktning at røret legges langs et konstant vanddyb. Dette fører til at røret har en konstant avgangsvinkel fra fartøyet, og dermed også en tilnærmet konstant aksial spenning i røret gjennom legging.

Fra de statiske analysene ble det også funnet at økt antall turnpoints gir en utflatning av moment-kurven. Dette er logisk, i og med at avstanden mellom støttene reduseres. På tilsvarende måte blir kontaktkreftene mellom turnpoints og røret lavere, da kraften fordeles blant flere støtter. Videre ser man at moment og kontakt-kraft er symmetrisk fordelt over rørets kurvatur. Dette kan tyde på at problemets symmetri kan utnyttes, hvilket vil redusere modellens størrelse.

En rekke parametre har blitt studert for at det verste tilfellet skal bli vurdert. Ut fra parameterstudiene ble den dynamiske analysen satt opp. Følgene parametre har blitt implementert i den dynamiske analysen:

- En strømretning på 90° , som dytter røret mot turnpoint.
- Et nedslagspunkt på røret rett etter siste turnpoint.
- En bølgeretning 45° bakfra på skipet, slik at både rull og stamp introduseres.

Den dynamiske analysen ble utført basert på en 3 timers sjøtilstand som er beskrevet av Jonswap-spekteret. For å redusere beregningstiden det tar å kjøre analysene, blir en full sjøtilstand benyttet som utgangspunkt for å sette opp de andre analysene over et kort tidsintervall, der den dynamiske responsen viste seg å være størst.

Den dynamiske spenningen i røret økes etter hvert som flere turnpoints installeres. Dette innebærer et stivere system, som igjen fører til høyere dynamisk respons. Det er derfor slik at kontaktkraften mellom turnpoints og rør er på sitt laveste når kun 3 turnpoints er installert. Momentfordelingen, på sin side, blir som i den statiske analysen redusert ved et økt antall turnpoints.

En kontroll mot lokal knekking av røret har blitt utført for å kontrollere opp mot DNVs offshore standard. I tillegg til dette kriteriet, har turnpointene en geoteknisk kapasitet på 80 [kN] som kontaktkraften mellom turnpoints og røret ikke kan overskride. Det ble funnet at hverken 3 eller 4 turnpoints langs kurvaturen var tilstrekkelig for å oppfylle DNVs knekk- kriterium. Altså må 5 eller flere turnpoints må installeres.

Ettersom turnpoints er installert med en viss turnpoint-toleranse, er det utført analyser med formål om å finne innvirkningen en slik toleranse har på resultatene. Med en lateral toleranse på 0.5 [m] ble det funnet en økning av både kontaktkraft, spenning og moment. Resultatet viste at kontaktkraften forble innenfor kravet til den geotekniske kapasiteten til turnpointene, men viste samtidig at 5 turnpoints ikke var tilstrekkelig til å overholde det lokale knekkingskriteriet. På bakgrunn av dette, er det foreslått å installere 6 turnpoints, som er lavere enn de opprinnelige 10 som er blitt installert. Det kan dermed virke som at metoden som brukes av Subsea 7 i dag er i overkant konservativ, hvilket var forventet basert på erfaringer som er gjort offshore.

For å danne et bilde av hvordan turnoints-toleransen påvirker strukturen, er det også blitt utført analyser med 1 [m] lateral toleranse. En slik toleranse ga betraktelig økning i rørets moment og kontaktkraft mellom turnpoints og rør. Dermed er også den lokale knekkingsgraden kraftig økt. Det er derfor åpenbart at turnpoints-toleranse er av meget høy betydning, og det vil være essensielt å holde toleransen tilstrekkelig lav, for å kunne installere så få turnpoints som mulig.

Contents

1	Introduction	1
1.1	Project Objective	1
1.2	Build up of Thesis	2
2	Theory	3
2.1	Pipeline Design Process	3
2.1.1	Limit State Criteria	3
2.2	Pipeline Stress Components	6
2.2.1	Hoop Stress	6
2.2.2	Longitudinal Stress	7
2.2.3	Equivalent Stress	8
2.3	Wall Thickness Design	9
2.3.1	Characteristic wall thickness	10
2.3.2	Classification of Location	10
2.3.3	Pressure Containment	11
2.4	Expansion Analysis	11
2.5	Buckling Analysis	12
2.5.1	Global Buckling	13
2.5.2	Local Buckling	13
2.5.3	Upheaval buckling	14
2.5.4	Lateral buckling	14
2.5.5	Collapse	15
2.5.6	Propagating Buckling	17
2.6	On-Bottom Stability	17
2.7	Free-Span Analysis	19
2.8	Pipeline Installation	21
2.8.1	J-lay	21
2.8.2	S-lay	22
2.8.3	Reeling	22
2.8.4	Assessment of the methods	23
2.8.5	Combined loading criteria	24
3	Non-Linear Finite Element Method	25
3.1	General	25

3.1.1	Equilibrium	25
3.1.2	Kinematic compatibility	26
3.1.3	Stress strain relationship	27
3.2	Non-linearities	29
3.3	Lagrange Formulation	29
3.4	Solution Procedures	30
3.4.1	Static Solution Procedure	31
3.4.2	Dynamic Solution Procedure	31
3.4.3	Incremental time integration: HHT- α Method	33
4	SIMLA	35
4.1	Building the Model	35
4.2	The different analyses	36
4.2.1	Initial configuration	36
4.2.2	Static analysis	36
4.2.3	Dynamic analysis	37
4.3	Input Data	37
4.3.1	Route	38
4.3.2	Pipe Properties	39
4.3.3	Environmental Conditions	40
4.3.4	Soil	42
4.3.5	Turnpoints	44
4.4	Running the Analyses	45
5	Turnpoints Calculations	47
5.1	Background	47
5.2	Horizontal curve stability	47
5.3	Current method	48
5.4	Method applied	49
6	Results	51
6.1	Parameter study	51
6.1.1	Current Direction	51
6.1.2	Touchdown position	52
6.1.3	Wave period	54
6.1.4	Wave Direction	54
6.1.5	Summary of the parameter study	55

6.2	Static analysis	56
6.2.1	Configuration of axial friction	56
6.2.2	Axial force	58
6.2.3	Moments	59
6.2.4	Contact force	61
6.3	Dynamic analysis	63
6.3.1	Representation of the sea state	63
6.3.2	Axial force	65
6.3.3	Moments	66
6.3.4	Contact force	68
6.4	Local Buckling check	71
6.5	Turnpoint tolerance	72
7	Conclusion	79
8	Recommendations for Further Work	81
	Appendices	I
	Appendix A Lay Configuration	II
	Appendix B SIMLA Input Files	III
	B.1 J-Feed_3Turn.sif	III
	B.2 Dynamic_Restart_3Turn.spi	XII
	Appendix C MATLAB files	XXII
	C.1 Simla_Route_Input_Calculations	XXII
	C.2 Local_Buckling_Calculations	XXV

List of Figures

1.1	Curve stability & Turnpoints	1
2.1	Stress Components	6
2.2	Hoop stress distribution with internal overpressure	7
2.3	Description of Ovality	16
2.4	Absolute Stability	19
2.5	J-lay	21
2.6	S-lay	22
2.7	Reel Straightening	23
3.1	Pipe element parameters; definition of local coordinate system	27
3.2	Isotropic and kinematic hardening.	28
3.3	Illustration of Newton Raphson iteration	31
4.1	Seven Navica - Lay configuration	37
4.2	Seven Navica	38
4.3	Pipeline Route in the xy-plane	38
4.4	Vertical spring stiffness	43
4.5	Unit force factors	43
4.6	Turnpoint tolerance calculated from Matlab	45
5.1	Minimum horizontal radius	48
5.2	Coordinate system, moments definition	50
6.1	Current Cases	51
6.2	Touchdown positions investigated	53
6.3	Wave directions	55
6.4	Feed analysis	56
6.5	Axial force in the pipeline - with axial friction activated	57
6.6	Static moment distributions with and without axial friction activated	58
6.7	Axial force in the pipeline vs number of turnpoints, Static results	59
6.8	Equivalent moment in pipeline vs number of turnpoints, Static results	60
6.9	Contact force vs number of turnpoints, Static results	61
6.10	Assumed model applied by Subsea 7	62
6.11	Response during a 3 hour sea state	64
6.12	Comparison of full vs a short interval representing the same sea state	65

6.13	Axial force in the pipeline vs number of turnpoints, Dynamic results	66
6.14	Equivalent moment in pipeline vs number of turnpoints, Dynamic results	67
6.15	Contact force at the last turnpoint, Dynamic results, 3-10 turnpoints	68
6.16	Contact force against KP-value at t=1087 s, for 3-10 turnpoints . .	69
6.17	Turnpoint tolerance cases investigated, 5, 6 and 7 Turnpoints	72
6.18	Impact from different tolerance cases, 5 turnpoints	73
6.19	Impact from different tolerance cases, 6 turnpoints	73
6.20	Effect of turnpoint tolerance	75
6.21	Local buckling utilization as a function of turnpoint tolerance . . .	76
6.22	Contact force as a function of turnpoint tolerance	77

List of Tables

2.1	Classification of Loads	5
2.2	Load Effect Factor	5
2.3	γ_c - Condition Load Effect Factor	5
2.4	Characteristic wall thickness	10
2.5	Classification of Safety Classes	10
2.6	Fabrication factors	16
4.1	Pipeline Dimensions	39
4.2	Steel Properties	39
4.3	Coating Properties	39
4.4	Current Profile	41
6.1	Parameters applied	55
6.2	Static results	62
6.3	Dynamic results	70
6.4	Control of Local Buckling	71
6.5	Results from the worst case turnpoint positions	74
6.6	Results from the worst case turnpoint position	74

List of Abbreviations

ALS:	Accidental Limit State
ERW:	Electric Resistance Welding
FBE:	Fusion Bonded Epoxy
FEED:	Front End Engineering Design
FLS:	Fatigue Limit State
KP:	Kilometre Point
LRFD:	Load and Resistance Factor Design
PP:	Polypropylene
RAO:	Response Amplitude Operator
SLS:	Serviceability Limit State
SMLS:	Seamless Pipe
SMTS:	Specified Minimum Tensile Strength
SMYS:	Specified Minimum Yield Stress
TRB:	Three Roll Bending
ULS:	Ultimate Limit State
UO:	Pipe fabrication process for welded pipes
UOE:	Pipe fabrication process for welded pipes - expanded

List of Symbols

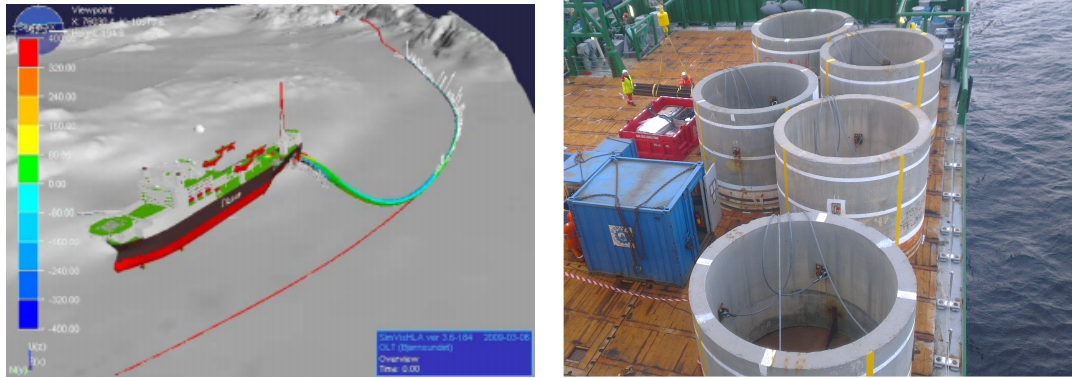
α :	Parameter to control damping properties
α_{fab} :	Fabrication Factor
ε :	Strain
γ_c :	Condition Load Effect Factor
γ_E :	Environmental Load Effect Factor
γ_F :	Functional Load Effect Factor
γ_m :	Material factor
γ_{SC} :	Safety class factor
γ_W :	Safety factor on weight
μ :	Soil friction
ν :	Poisson ratio
ρ :	Density
σ :	Stress
σ_e :	Equivalent stress
σ_h :	Hoop Stress
σ_l :	Longitudinal stress
ϕ_k :	Phase angle
ϕ_k^p :	Position dependent phase angle
ω_p :	Peak frequency
\mathbf{a} :	Acceleration field
\mathbf{C} :	Damping matrix
\mathbf{f} :	Volume force vector
$\boldsymbol{\varepsilon}$:	Strain tensor of natural strain
\mathbf{K} :	Stiffness matrix

$M:$	Mass matrix
$R:$	External applied load vector
$R^E:$	External force vector
$R^I:$	Internal force vector
$r:$	Displacement vector
$\dot{r}:$	Velocity vector
$\ddot{r}:$	Acceleration vector
$S:$	2nd Piola-Kirchoff stress tensor
$\sigma:$	Stress tensor of Cauchy stress
$\sigma_0:$	Initial stress tensor
$t:$	Surface traction
$u:$	Displacement vector
$b:$	Buoyancy per unit length
$C_0:$	Initial configuration
$C_n:$	Last obtained equilibrium configuration
$D:$	Nominal outside diameter
$E:$	Young's modulus
$f_0:$	Ovality of the pipe
$f_u:$	Tensile strength
$f_y:$	Yield stress
$H_s:$	Significant wave hight
$M_{Sd}:$	Design Moment
$N_\omega:$	Number of wave components
$p_b:$	Burst Pressure
$p_c:$	Collapse Pressure

p_e :	External Pressure
P_{el} :	Elastic Collapse Pressure
p_i :	Internal Pressure
p_{min} :	Minimum Internal Pressure
P_p :	Plastic Collapse Pressure
R_{min} :	Minimum horizontal curve radius
S_{sd} :	Design Effective axial force
t :	Thickness
T_0 :	Bottom tension
t_{corr} :	Thickness corrosion allowance
t_{fab} :	Fabrication thickness tolerance
T_p :	Peak period
T_z :	Zero-up crossing period
w_s :	Submerged weight

1 Introduction

Offshore pipelines are essential for the transportation of oil and gas worldwide. Depending on the application, the pipelines are classified and range from small diameter in-field flowlines, to large diameter export lines, for transportation from offshore installations to onshore processing plants. The pipelines can be either rigid or flexible. Rigid pipelines are used between fixed structures, while flexible pipes can be used for operation from both fixed and floating structures. Natural seabed features, or congested areas where existing subsea infrastructure makes restrictions of the pipe laying, may introduce rigid pipeline routes with small horizontal curve radius. Rigid pipelines are commonly stable during pipe laying by weight for curve radius of 1000 [m] or greater. To ensure horizontal curve stability, measures like lateral supports, so called turnpoints (see Figure 1.1b), along the pipeline route may be required when the curve radius becomes lower than this.



(a) Curve stability during installation in SIMLA (from Sævik (2012))

(b) Turnpoints (from Nessmo (2014))

Figure 1.1: Curve stability & Turnpoints

In this thesis, curve stability by implementing turnpoints along the pipeline route is investigated. Project experience shows that calculating the required number of turnpoints is conservative compared to what is seen offshore. It is believed that a better method for calculating the interaction between the pipe and the turnpoints could reduce the number of turnpoints installed, hence also the installations costs.

1.1 Project Objective

The objective of the master thesis work is to study the interaction between the pipe and the turnpoints installed. This is investigated by use of a special purpose software for offshore pipelines; SIMLA (see Figure 1.1a). The goal is to develop a

method where a proper number of turnpoints along the route ensures both horizontal curve stability, structural integrity of the pipeline and that the contact force between the pipe and the turnpoints remains less than the geotechnical capacity of the turnpoints. To control the results, a local buckling utilization of the pipeline will be performed.

1.2 Build up of Thesis

Chapter 2: This chapter gives an introduction to theory regarding pipeline design. This has been studied in order to get a general understanding of the rigid pipeline design process and the necessary design checks that comes with.

Chapter 3: The content of this chapter is about the non-linear finite element method. This is included in order to enhance the knowledge of methods applied in the software used throughout the thesis work; SIMLA. The main focus in the chapter is associated to the basic methods applied in SIMLA.

Chapter 4: This chapter contains information on the analyses performed, how the model is built, how different features are included and which assumptions that are made.

Chapter 5: A brief description of how Subsea 7 currently performs their turnpoint-calculations is given. Further, a more detailed description on how the calculations are performed during this thesis work, is provided. It also presents the parameters that have been studied in separate parameter studies, in order to set up the analyses based on the worst case scenario.

Chapter 6: The results from the simulations are presented in this chapter. In the beginning of the chapter, the results from the parameter studies are described before the final results are presented from both the static and the dynamic analyses.

Chapter 7: Conclusions from the work carried out and the results obtained in this thesis can be found in this chapter.

Chapter 8: Based on the experiences from the work carried out, a recommendation of further work is presented.

2 Theory

In this chapter there will be given some background theory of pipeline design. The theory presented is a result of the literature study carried out during this thesis. A general study of pipeline design was chosen as a result of the fact that there are limited literature available regarding turnpoints evaluation and it gives an overall understanding of rigid pipeline design process and design checks.

2.1 Pipeline Design Process

The pipeline design process is a multi-disciplinary process that requires a diversity of engineering skills and knowledge, including structural mechanics, thermodynamics, material technology, hydrodynamics, etc. The purpose of the design process for a pipeline is to determine the optimal pipeline characteristics that meet the needs of its purpose and at the same time ensures safe operation throughout its lifetime (Sævik; 2012). Finding the optimal pipeline characteristics is an iterative process, where several parameters need to be accounted for, such as:

- Diameter and thickness dimensions
- Material selection and welding
- Route selection
- Flowline protection
- Installation method

The pipeline design process is a dynamic process where iterations of, among other, the above mentioned parameters need to meet the requirements from its associated stress analysis. The design phase will according to DNV (2012) typically be split into a FEED-phase (Front End Engineering Design), basic design and detail design. The design tasks are repeated in each design phase, with an increased level of details for each new phase.

2.1.1 Limit State Criteria

Limit state design of the pipeline implies that the pipe is controlled against all potential failure modes. The limit states are distinguished into four categories, where the importance and the degree of criticality of the failure modes varies. The four limit states are:

- Serviceability Limit State, SLS

- Ultimate Limit State, ULS
- Fatigue Limit State, FLS
- Accidental Limit State, ALS

The two latter limit states, FLS and ALS, are sub-categories of ULS accounting for respectively cyclic loading effects and accidental loads (DNV; 2012).

A distinction is commonly made between Load Controlled and Displacement Controlled condition. When the structural response is mainly governed by the loads imposed on the pipe, one has a load controlled condition. On the other hand, if the structural response is mainly governed by imposed geometric displacement, one has a displacement controlled condition. A load controlled is more conservative than a displacement controlled condition, and a displacement controlled condition should therefore only be applied when the deformation is well known. Based on this, a load controlled condition can according to DNV (2012) always be applied instead of a displacement controlled design criterion.

DNV-OS-F101 (DNV; 2012) utilize a Load and Resistance Factor Design (LRFD) format, with the basic concept of verifying that the design load effects do not exceed the design resistance for any failure modes in any load scenarios. Each limit state should according to DNV (2012) be controlled against the design load effect, where the design load in terms of moment and effective axial force comes at the same format and are defined as follows:

$$M_{Sd} = M_F \cdot \gamma_F \cdot \gamma_c + M_E \cdot \gamma_E + M_I \cdot \gamma_F \cdot \gamma_c + M_A \cdot \gamma_A \cdot \gamma_c \quad (2.1a)$$

$$S_{Sd} = S_F \cdot \gamma_F \cdot \gamma_c + S_E \cdot \gamma_E + S_I \cdot \gamma_F \cdot \gamma_c + S_A \cdot \gamma_A \cdot \gamma_c \quad (2.1b)$$

Where the various γ -signs represents load effect factors (see Table 2.2 and 2.3) and the subscripts refers to:

Table 2.1: Classification of Loads

Subscript	Load Category	Definitions from DNV (2012):
F	Functional Loads	<i>Loads that are arising from the physical existence of the pipeline system and its intended use.</i>
E	Environmental Loads	<i>Those loads on the pipeline system which are caused by the surrounding environment, and that are not otherwise classified as functional or accidental loads.</i>
I	Interference Loads	<i>Loads which are imposed on the pipeline system from 3rd party activities shall be classified as interference loads.</i>
A	Accidental Loads	<i>Loads which are imposed on a pipeline system under abnormal and unplanned conditions and with an probability of occurrence less than 10^{-2} within a year shall be classified as accidental loads.</i>

Table 2.2: Load Effect Factor (from DNV (2012))

Limit State	γ_F	γ_E	γ_I	γ_A
ULS (System Check)	1.2	0.7		
(Local Check)	1.1	1.3	1.1	
FLS	1.0	1.0	1.0	
ALS	1.0	1.0	1.0	1.0

Table 2.3: γ_c - Condition Load Effect Factor (from DNV (2012))

Condition	γ_c
Pipeline resting on uneven seabed	1.07
Reeling on and J-tube pull-in	0.82
System pressure test	0.93
Otherwise	1.00

The load effect combination referred to as system check in table 2.2, does only need to be checked when system effects are present, i.e. when a major part of a pipeline is exposed to identical functional load and potential failure occurs in connection with the lowest structural capacity. This is relevant in pipeline design, since a pipeline generally will fail at the lowest capacity, expressed as the weakest link principle. Hence, system effects must be taken into consideration in the design of a pipeline, but will, however, according to DNV (2012), typically only apply during installation.

2.2 Pipeline Stress Components

Offshore pipelines are exposed to a set of various loading conditions through its lifetime, that may trigger various failure modes, such as excessive yielding, plastic straining, local buckling, fatigue, fracture, corrosion etc. (Sævik; 2012). Different loading conditions results in various stress components in the pipe, and hence it will vary which stresses that are the governing in the pipeline. The various stress components that a pipe is subjected to includes (Bai and Bai; 2005):

- Hoop Stress (σ_h).
- Longitudinal Stress (σ_l).
- Equivalent Stress (σ_e), which is a combination of the two above.

They all have in common that they need to be accounted for in pipeline design, and basically forms the foundation of the initial wall thickness sizing.

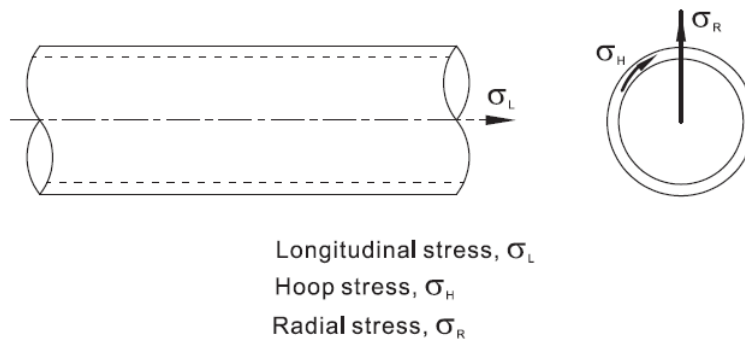


Figure 2.1: Stress Components, figure from Bai and Bai (2012)

The magnitude of the radial stress (see Figure 2.1) in a pipeline is usually small compared to the hoop and the longitudinal stresses, and is therefore not particularly limiting in design codes.

2.2.1 Hoop Stress

Hoop stresses are stresses in the circumferential direction of the pipe wall, see Figure 2.1. In order to avoid bursting, i.e. excessive yielding in hoop direction, the hoop stress could be calculated by Equation 2.2. Depending on which standard that is utilized, a typical safety factor would be applied to the yield stress of the

material. The hoop stress, σ_h , can be described by thin and thick walled shell theory. DNV-OS-F101 (DNV; 2012) operates with a formula based on thin walled theory:

$$\sigma_h = \frac{D - t}{2t}(p_i - p_e) \quad (2.2)$$

Where:

D = Nominal outside diameter

t = Thickness

$(p_i - p_e)$ = Differential Pressure

By considering thick walled shell theory (see Equation 2.3), it can be seen that the hoop stress varies across the pipe wall:

$$\sigma_h(r) = \frac{p_i D_i^2 - p_e D_e^2}{D_e^2 - D_i^2} + (p_i - p_e) \frac{D_i^2 D_e^2}{(2r)^2 (D_e^2 - D_i^2)} \quad (2.3)$$

The thick walled equation for the hoop stress is often called the Lamé equation, where it is seen that the stress varies over the cross section. It can be noted that the maximum hoop stress always occurs on the inner surface of the pipe wall, where the radius, r , is lowest, see Figure 2.2:

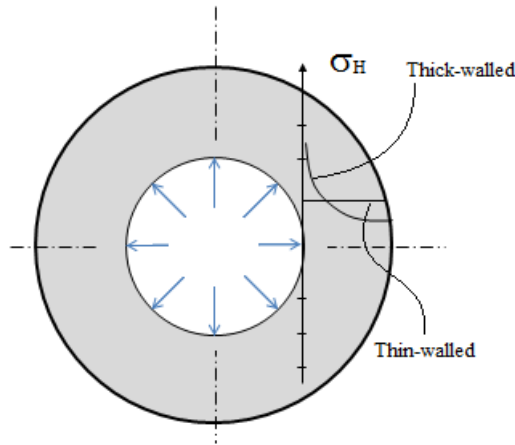


Figure 2.2: Hoop stress distribution with internal overpressure, distinction between thin- and thick-walled theory.

2.2.2 Longitudinal Stress

Axial or longitudinal stress, σ_l , is the stress in the axial direction of the pipe wall, and consist of the following contributors:

- Hoop stress, σ_{lh}
- Thermal stress, σ_{lt}
- Bending stress, σ_{lb}
- End cap force induced stress, σ_{lc}

The longitudinal stress can according to Bai and Bai (2005) be determined by:

$$\sigma_l = \nu\sigma_{lh} + \sigma_{lt} + \sigma_{lb} + \sigma_{lc} \quad (2.4)$$

Where ν is the Poisson ratio.

The Poisson effect is in fact together with the temperature what longitudinal stresses primarily arise from. Longitudinal stress consists mainly of two stress contributors, where the first is related to the pressure and the second is related to the temperature (Palmer and King; 2008). A pipeline free to expand in all directions will tend to expand, both circumferentially and axially, with increased temperature. The expansion is usually unconstrained in the circumferential direction, but is, however, constrained by seabed friction in the longitudinal direction. Hence, longitudinal stress will be induced in the pipeline, and can potentially be very large.

2.2.3 Equivalent Stress

Equivalent stress are commonly calculated in order to establish how the combined stress level becomes compared to the yield strength. If the equivalent stress reaches the yield criteria, the pipe will start to deform plastically. The combined stress is determined differently depending on the different standards. In order to perform stress investigation of excessive yielding, the Von Mises's equivalent stress criteria is normally used, as it provides a good description of the yield process due to multi-axial stresses in metals (Sævik; 2012). The combined equivalent stress can according to DNV (2012) be expressed as:

$$\sigma_e = \sqrt{\sigma_h^2 + \sigma_l^2 - \sigma_h\sigma_l + 3\tau_{hl}^2} \quad (2.5)$$

Where, τ_{hl} = Tangential shear stress

When it comes to bursting of a pipeline, it has been demonstrated that the hoop stress criterion provides good control against this in a displacement controlled situation for a pipe under combined internal pressure and bending. However, in a

load controlled situation of the pipe, equivalent stress criterion may be applied to assure adequate burst strength under combined internal pressure and axial loads. During the operating phase, it is in general conservative to use the equivalent stress criteria in order to prevent bursting, since the dominating load is internal pressure combined with bending (Bai and Bai; 2005).

2.3 Wall Thickness Design

"The pipe wall thickness and material selected by the designer should provide adequate strength to prevent deformation and collapse by handling stresses, external reactions, and thermal expansions and contractions" (Mohitpour et al.; 2007, Chapter 3).

Wall thickness selection is an essential part of the design process of offshore pipelines. Determining the optimal wall thickness and steel grade can be considered as one of the main objective in pipeline design. The wall thickness is the most relevant parameter affecting the capacity to resist the loads imposed throughout installation and operation, as well as a significant factor impacting on the investment costs (Torselletti et al.; 2003). From the economic point of view, the interest in optimizing the wall thickness becomes evident, considering that the steel costs can amount to as much as 50 % of an entire pipeline project costs according to Braestrup et al. (2005).

Current design practice is based on the concept of limiting the hoop stress for design against the differential pressure, and the equivalent stress for design against combined loads (Bai and Bai; 2005). The minimum required wall thickness can in most cases be determined by inserting a usage factor applied to the Specified Minimum Yield Stress (SMYS) into the hoop stress formula. For the vast majority, it will be the hoop stresses in circumferential direction caused by internal overpressure that are governing when choosing the the wall thickness of the pipe. However, at very deep water, the required wall thickness may be governed by local buckling due to the external pressure. Beside the above mentioned aspects, other considerations, such as loads related to installation, bending loads due to uneven seabed and external impact due to e.g. trawling, may also influence the design of the wall thickness.

Taking into account the diversity of considerations that need to be treated during wall thickness design, one can conclude that the calculations of optimal wall thickness is far from being a trivial task.

2.3.1 Characteristic wall thickness

DNV-OS-F101 (DNV; 2012) operates with two different characterisations of wall thickness, t_1 and t_2 , where t_1 is used when system effects are present and failure likely would occur in connection with low capacity, while t_2 is used when failure likely would occur in connection with an extreme load effect at a location with average thickness. The characterisation distinguish between operation and prior to operation, where the latter are intended for cases where corrosion is negligible. However, if corrosion does exists, this should be subtracted the same way as for the operation phase, see Table 2.4:

Table 2.4: Characteristic wall thickness (from DNV (2012)).

	Prior to operation	Operation
t_1	$t - t_{fab}$	$t - t_{fab} - t_{corr}$
t_2	t	$t - t_{corr}$

Where:

t_{fab} = Fabrication thickness tolerance.
 t_{corr} = Thickness corrosion allowance.

2.3.2 Classification of Location

Pipeline wall thickness design builds on the concept of classifying the pipeline into specific safety classes, depending on location and the transported medium. DNV-OS-F101 (DNV; 2012) states that: *"Pipeline design shall be based on potential failure consequence. This is implicit by the concept of safety class. The safety class may vary for different phases and locations."* Where the safety classes are defined as follows:

Table 2.5: Classification of Safety Classes (from DNV (2012)).

Safety Class	Definition
Low	Where failure implies insignificant risk of human injury and minor environmental and economic consequences
Medium	Where failure implies low risk of human injury, minor environmental pollution or high economic or political consequences.
High	Classification for operating conditions where failure implies risk of human injury, significant environmental pollution or very high economic or political consequences.

Further, codes distinguish between graphical zones, and DNV deals with two location classes(DNV; 2012):

Location Class 1: The area where no frequent human activity is anticipated. For the majority of offshore pipelines the risk associated to human injury is minor in case of failure, and will thereby be assigned within this category. Zone 1 is classified as Normal/Medium Safety class during operating phases.

Location Class 2: The part of the pipeline/riser in the near platform (manned) zone or in areas with frequent human activity. The extent of this zone should be based on appropriate risk analyses. If no such analyses are performed, a minimum horizontal distance of 500 [m] shall be adopted. Zone 2 is classified as High Safety Class during operation.

2.3.3 Pressure Containment

The general requirement for wall-thickness selection of a pipe is that the pipe should sustain stresses for pressure containment. Bursting of a pipeline by excessive internal pressure can occur if the pipe is not properly designed, or if the maximum internal pressure is substantially underestimated (Sævik; 2012). DNV-OS-F101 (DNV; 2012) operates with the following pressure containment criteria in order to avoid excessive yielding (bursting) in the hoop direction:

$$p_i - p_e \leq \frac{p_b(t_1)}{\gamma_m \gamma_{SC}} \quad (2.6)$$

Where the pressure containment resistance is given by:

$$p_b(t) = \frac{2}{\sqrt{3}} \frac{2t}{D-t} f_{cb} \quad (2.7)$$

f_{cb} is given as the smallest value of f_y and $f_u/1.15$:

$$f_{cb} = \text{Min} \left[f_y; \frac{f_u}{1.15} \right] \quad (2.8)$$

A sufficient safety level is ensured in equation 2.6 by means of a material factor, γ_m , coping with material uncertainties and a safety class factor, γ_{SC} , that depend on the application.

2.4 Expansion Analysis

Expansion of pipelines may be initiated by internal pressure and temperature. In addition to these, the magnitude of the expansion depends on the weight of the pipeline and friction forces along the pipe. Thus, several input parameters are needed in order to conduct a expansion analysis, such as pipeline and coating properties, temperature and pressure profile, contents weight and geotechnical data of the seabed conditions.

A pipe resting on the seabed is partially restrained from axial movement by soil friction. When the pipeline is exposed to high operating temperature and internal pressure, high axial compressive forces may develop in the pipe. At some critical axial force level the pipe will release its potential axial expansion by buckle laterally or vertically. This is not desirable, since it may lead to critical damage of the pipeline, and should therefore be prevented. One way to avoid critical effects is to release the expansion force in a controlled manner by installing the pipeline with curves, such that one initiate lateral deflection at pre-defined intervals. The same effect can also be obtained by installing local trigger points which the pipeline is crossing. This will also ensure that the pipeline buckles at a predefined interval. The local imperfection is reducing the buckling load (axial force) which then makes the pipe to release expansion force at that location. Other usual methods of preventing this failure mode is to constraint the pipe from buckle laterally and/or vertically by for instance trenching, rockdumping, concrete mats or pipe supports (Fyrileiv et al.; 1996). However, all of these actions are associated with high costs.

Pipeline extension will affect several design issues, such as tie-in design, lateral and upheaval buckling assessment, free-span assessment, crossing design and bottom roughness/stress assessment (Bai and Bai; 2005).

2.5 Buckling Analysis

Compressive axial loads are usually induced in pipelines due to frictional resistance of axial expansion due to changes in the temperature and/or the internal pressure of the pipe. In presence of initial imperfections, which certainly are present in pipelines laid on the seabed, buckling may be introduced. The buckling may be initiated as an upward movement from the seabed or as snaking lateral movements along the seabed. For normal friction coefficients, occurrence of the lateral mode will happen at a lower axial load than the vertical mode unless the line is laid in a trench (Hobbs; 1981). A combination of the two, i.e. upheaval in combination with lateral buckling, may also occur.

When it comes to buckling of pipelines, control of local and global buckling need to be performed. Global buckling involves a substantial length of the pipeline with no major deformations of the cross section. Local buckling mode, on the other hand, is limited to a short length of the pipeline exposed to significant deformation of the cross section.

2.5.1 Global Buckling

Global buckling is a load response and not a failure mode. The response is due to compressive axial force in the pipeline, which reduces the axial carrying capacity. The compressive axial force is due to the operational temperature and pressure, which are above the ambient. Hence, the pipe will try to expand, but when the pipeline is restrained and not free to expand, the pipe will develop axial compressive force. *"As more pipelines operates at higher temperatures, the likelihood of buckling becomes more pertinent"* (Bai and Bai; 2012). Pipelines with high effective axial compressive forces or pipelines with low buckling capacity, are particularly exposed to potential global buckling.

Global buckling may either prevail horizontally, as lateral buckling on the seabed, or vertically, in terms of upheaval buckling of buried pipelines or downwards in a free-span. The global buckling behaviour is very dependent of the pipe-soil interaction. This interaction includes major uncertainties regarding characterisation as well as variation along the route, and is the most vital aspect of global buckling or expansion design (DNV; 2007).

Even though global buckling is not a failure mode itself, it may, however, give rise to ultimate failure modes, such as (DNV; 2007):

- Local Buckling
- Fracture
- Fatigue

2.5.2 Local Buckling

Pipelines subjected to combined pressure, axial force and bending may be exposed to local buckling. Yielding of the cross section and buckling on the compressive side of the pipeline are potential failure modes (Bai and Bai; 2005).

Local buckling implies gross deformation of the cross section, and DNV (2012) operates with the following criteria to be fulfilled:

- System Collapse
- Propagation Buckling
- Combined load criteria

2.5.3 Upheaval buckling

Upheaval buckling occurs due to the interaction between the axial compressive force and overbend imperfections in the pipeline profile. The pipe will tend to move upward if the force acting on the soil from the pipe exceeds the vertical downwards force due to the submerged weight of the pipe, its bending stiffness, and the resistance of the soil cover (Palmer et al.; 1990). This may introduce considerable vertical displacements. A complete description of the upheaval behaviour of buried pipelines is complex and requires a detailed study of all of the parameters involved, such as (Braestrup et al.; 2005):

- Pipe cross section properties
- Non-linear pipe material behaviour (involving temperature dependence)
- Pipeline out-of-straightness
- Geometric pipe imperfection
- Soil characteristics along the pipeline route
- Varying soil cover along the pipeline

Upheaval buckling is considered as an Ultimate Limit State failure and may occur both for pipelines left exposed on the seabed, prior to developing lateral buckling, and buried pipelines. The vertical soil resistance is usually much lower than the lateral for a covered pipeline. Buried pipelines will therefore tend to move vertically rather than laterally and try to break out of the soil cover, i.e. upheaval buckling.

2.5.4 Lateral buckling

Unburied pipelines, left exposed on the seabed, may buckle laterally rather than vertically, unless the lateral friction coefficient is very high or the pipe is sufficiently restrained in the lateral direction. The resistance against sideways movement is basically the lateral friction coefficient multiplied with the submerged weight of the pipeline.

Lateral global buckling of an exposed pipeline resting on even seabed, often termed snaking, can in some situations be analysed by use of analytical methods. However, there are several limitations to such methods due to the assumptions these analytical models are based on (DNV; 2012). By example, analytical models assumes an elastic material behaviour, which neglects the plastic hinge effects caused by high strains and coupling between longitudinal and circumferential material behaviour (Sævik and Levold; 1995). The lateral buckling phenomena is usually a highly non-linear phenomenon due to sources like (Fyrileiv et al.; 1996):

- Lateral soil friction which may include softening response.
- Geometrical non-linearities including pipeline buckling.
- Plastic yielding in the pipe cross-section.
- Localisation of deformation during post-buckling response.

If only one or more of the limitations for the analytical methods in (DNV; 2012) are not fulfilled, more sophisticated analysis is required. As at least one of the above mentioned factors usually applies in a project, will the finite element analysis in practise always be used.

2.5.5 Collapse

Pipeline collapse refers to flattening of the pipeline due to excessive external pressure. The pipeline design should provide a wall thickness where system collapse criterion is fulfilled at all times. However, due to the fact that the pipeline in operation is pressurised, and therefore not that vulnerable against collapse buckling, normal design practice is thus based on performing collapse check during the installation phase only. The uncertainty in load effect for collapse due to external pressure is considerably lower than for other failure modes due to the fact that the water depth is well known, and thus also the pressure level (Marley et al.; 2012).

The collapse pressure of a pipe is a function of several parameters, such as Young's Modulus, Poisson's ratio, Yield stress, ovality and diameter-to-thickness-ratio.

External pressure cause compressive Hoop-stress in the pipe wall, hence both the yield strength and circumferential stiffness affect the pipeline capacity.

The Hoop-stiffness increase with increased pipe thickness and are therefore not particularly large for thin-walled pipes. Hence, the elastic collapse arise at an average hoop stress well below the proportional limit (Murphy and Langner; 1985). The elastic collapse pressure, P_{el} , is given by:

$$P_{el} = \frac{2E}{1 - \nu^2} \left(\frac{t}{D}\right)^3 \quad (2.9)$$

For thick-walled pipes, however, the Hoop-stiffness is sufficiently large. Hence, the average hoop stress generally exceeds the yield stress at the initiation of collapse. The plastic collapse pressure, P_p , are given in equation 2.10. This formula is based on the assumption that the pipe enter the plastic zone before collapse occur, in other words it assumes that the pipe is not able to deform elastically until collapse

pressure. Plastic strains are introduced in order to reach the desired level of deformation:

$$P_p = 2\alpha_{fab}f_y\left(\frac{t}{D}\right) \quad (2.10)$$

Where α_{fab} is the fabrication factor, which has the purpose of covering the effect of material derating due to the production process. Maximum fabrication factors for pipes manufactured by specific fabrication methods are given in the following table:

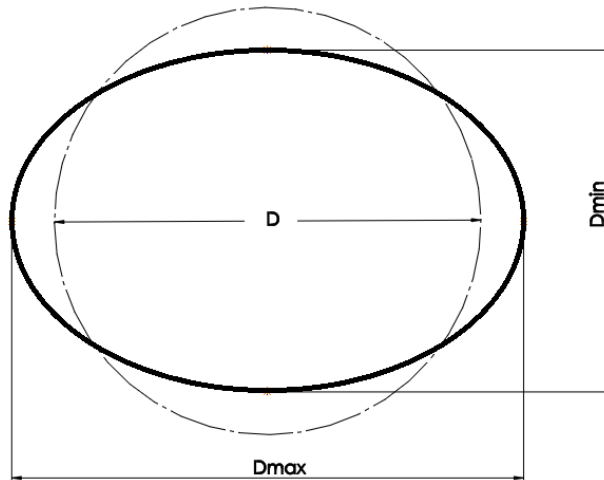
Table 2.6: Fabrication factors (from α_{fab} (DNV; 2012))

Pipe	Seamless	UO, TRB, ERW	UOE
α_{fab}	1.00	0.93	0.85

At D/t -ratios in between the thick- and thin-walled pipe, there is a gradual transition from elastic to plastic collapse. In this range, both the elastic collapse pressure and the plastic collapse pressure are non-conservative (Murphy and Langner; 1985). Hence, several approaches for collapse predictions have been developed. DNV is currently using a collapse formula for pipelines exposed to external pressure that assumes that the collapse capacity is a function of the elastic and plastic capacity, as well as the D/t -ratio and the ovality of the pipeline:

$$(P_c - P_{el})(P_c^2 - P_p^2) = P_c P_{el} P_p f_0 \frac{D}{t} \quad (2.11)$$

Where f_0 express the ovality of the pipe and are defined by:



$$f_0 = \frac{D_{max} - D_{min}}{D} \quad (2.12)$$

Figure 2.3: Description of Ovality

Note that two different definitions of ovality can be found in the literature today, and that the ovality, f_0 , presented above is according to DNV-OS-F101, and is half the size of the other expression (Aamlid et al.; 2011).

2.5.6 Propagating Buckling

When a pipe is exposed to combined action of bending and external pressure, the buckling process will accelerate. Impacts or abrupt bending deformation may initiate the buckling process to start and propagate along the pipe at a lower pressure than the theoretical collapse pressure, a phenomenon termed buckle propagation (Sævik; 2012). The risk of local buckling initiation is considerably high during installation, where accidents like losing the pipe during installation due to failure in the vessel tensioner system may occur. Hence, buckle arrestors, i.e. thicker sections applied at certain intervals in order to stop this process, will be designed to limit the extent of the damage of a propagating buckle (Bai and Bai; 2005).

Propagation buckling can not be initiated unless local buckling already has occurred. Buckle arrestors should according to DNV (2012) be installed if the external pressure exceeds the propagating buckle criterion, given as:

$$p_e - p_{min} \leq \frac{p_{pr}}{\gamma_m \gamma_{SC}} \quad (2.13)$$

where the propagating pressure is defined as:

$$p_{pr} = 35 f_y \alpha_{fab} \left(\frac{t_2}{D} \right)^{2.5} \quad (2.14)$$

for $15 < \frac{D}{t_2} < 45$.

p_{min} is the minimum internal pressure, usually taken as zero during installation.

The spacing between the arrestors should then be determined based on cost and spare philosophy (DNV; 2012).

2.6 On-Bottom Stability

Pipelines resting on the seabed are subjected to hydrodynamic loads from both waves and current. In areas on the seabed where lateral or vertical movement of the pipeline may result in damage of the pipe, it is required that the weight of the pipeline is sufficient to assure stability under the impact of the worst possible environmental condition. The object of a pipeline stability analysis is to decide how much weight that is required and to be added through the coating of the pipe.

Calculations regarding on-bottom stability of the pipeline need to be conducted in order to form the basis for the required submerged mass. The required submerged

mass will directly influence the required pipelay tensions, installation stresses and the pipe configuration at the seabed. From the installation point of view, the priority is to minimize the required submerged mass of the pipeline (Bai and Bai; 2005).

On-bottom stability concerns both vertical and lateral stability of the pipeline. When it comes to vertical stability, the pipeline should be checked for the possibility of sinking and floatation. Sinking of the pipe should be considered towards maximum content density, while the possibility of floatation should be considered towards minimum content density, e.g. empty condition. The submerged weight of the pipeline shall according to DNV (2012) meet the following criterion in order to avoid floatation in water:

$$\gamma_W \cdot \frac{b}{w_{sub} + b} \leq 1.00 \quad (2.15)$$

Where:

γ_W = Safety factor on weight, 1.1

b = Buoyancy per unit length

w_{sub} = Submerged weight per unit length

The objective of a lateral stability analysis is to estimate the lateral displacement of a pipe susceptible to hydrodynamic load from a combination of current and waves during a sea state. On-bottom stability may follow one of three distinct approaches (DNV; 2010):

1. **Absolute stability:** This is the traditional approach, which is based on force equilibrium between applied hydrodynamic loads and soil resistance, ensuring that the hydrodynamic loads are less than the soil resistance during an extreme design sea state. See Figure 2.4.
2. **No break-out:** This approach permits minor displacements response due to the largest waves during a sea state. However, max displacement should be less than about half a diameter, which ensures that the pipe does not move out of its cavity. The pipe remains virtually stable and this approach may take the benefit of the build-up of passive resistance during the small displacement that the pipe will experience.
3. **Accumulated displacement:** When this approach is used, one specifies a certain, larger, permitted displacement during the sea state considered, and the pipe will then break out of its cavity several times during the sea state. In this context, one has to be aware of the fact that the displacement is an accumulated damage and that a sea state less harsh than the one considered also could move the pipe.

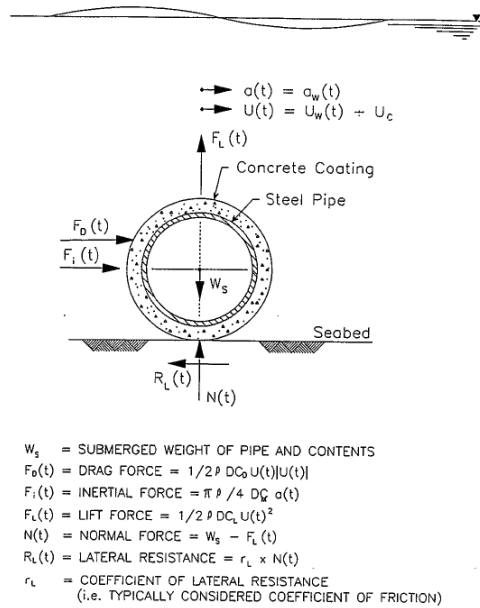


Figure 2.4: Absolute Stability, figure from Palmer et al. (1989)

2.7 Free-Span Analysis

Free-span of a pipeline is a phenomena that occurs when the contact between a pipeline and the seabed is lost over a substantial length. Free span assessment is usually an essential aspect in design of pipelines. For pipelines that are exposed on the seabed, span survey and assessment is of high importance during the operation phase. Free spans may become a challenge in pipeline design and operation as a result of pipeline installation on uneven seabed or seabed scouring effects. The costs associated with seabed adjustments and span intervention are in many projects substantial. On the other hand, these costs are insignificant compared to the potential costs related to a fatigue failure of a pipeline. Despite this, free spans are often designed applying unreasonable over-conservative concepts and often very simple analytical tools (Fyrileiv et al.; 2005).

Free span assessment must be based on a realistic evaluation of the effective axial force, and any changes due to sagging in spans, lateral buckling, end expansion, etc. must be properly accounted for. Changes in pressure and temperature during operation may cause significant changes in the span characteristics and must therefore be taken into consideration in the free span assessment(DNV; 2006a).

Normal code requirements regarding free spans demands that the pipeline is investigated against (Bai and Bai; 2012):

- Excessive yielding under different loads.
- Fatigue due to vortex induced vibrations (VIV).
- Interference with human activities, e.g. trawling.

Considerations of these requirements will be the basis of an resulting allowable free-span length. DNV-RP-F105 (DNV; 2006a), which considers free spanning pipelines subjected to combined wave and current loading, operates with a design criteria where a free span assessment addressing the integrity of the pipe with respect to fatigue (FLS) and local buckling (ULS), shall be performed for all temporary and permanent free spans.

Local fatigue design check should be performed for all free-spanning sections along the pipeline route, computing damage contributions from all potential vibration modes linked to the respective spans. The objective of designing the pipeline against fatigue design is to assure sufficient safety towards fatigue failure during the design life. To ensure this, it is essential that all imposed stress fluctuations capable of provoking fatigue damage within the entire design life are accounted for.

A essential question to be asked related to free spanning pipelines is, according to Fyrileiv et al. (2005), whether vortex induced vibrations (VIV) with corresponding fatigue is an actual problem or not. The number of known failures due to VIV is in fact rather low. This may somewhat be because of the fact that design codes and industry practice up to recently have been based on no onset of VIV. Free span design has in other words probably been over-conservative. An additional factor is that pipelines often have been buried or installed on flat seabed without free spans.

The vortex shedding frequency due to a flow perpendicular to a free span is governed by the Strouhal's number, the outer diameter of the pipe and the flow velocity. When considering an increasing flow velocity, the shedding frequency accordingly reach one of the natural frequencies of the span. Thereby, the span will begin to vibrate and the vortex shedding along the span gets correlated by the vibration of the span. The vortex shedding frequency and the vortex induced vibration gets locked-in with the natural frequencies of the span over a certain range of flow velocities. This may result in failure of the span due to fatigue. Fatigue failures of free spans are rare events but may occur if the problem is not treated properly (Fyrileiv et al.; 2005).

2.8 Pipeline Installation

Subsea pipeline installation is performed by specialized lay-vessels, with several possible methods, with the most common methods being S-lay, J-lay, reeling and tow-methods. The pipeline would be subjected to several loads during the installation process, such as hydrostatic pressure, tension and bending. The loads depend on the installation method, where each method has its pros and cons. The planning of an installation requires detailed static and dynamic analysis in order to determine under which weather conditions the operation may take place. In case of bad weather forecasts prior to the operation, such that the conditions are not within the accepted weather window, the operation must be postponed until the conditions improve. Taken the day rates of a laying barge into account, the costs of such delays may be substantial (Passano et al.; 2008).

2.8.1 J-lay

As the name implies, the pipe is in this case installed in a J-shaped configuration, i.e. the pipe enters the water in a close to vertical position (see Figure 2.5). The top angle that the pipe enters the water with is governed by the water depth, the submerged weight of the pipeline and the applied horizontal tension. Lower horizontal tension yields a higher top angle and a shorter layback length, i.e. the horizontal distance between the touchdown point and where the pipe leaves the vessel. The pipe are welded together on the vessel and number of welding stations are limited by the tower height.

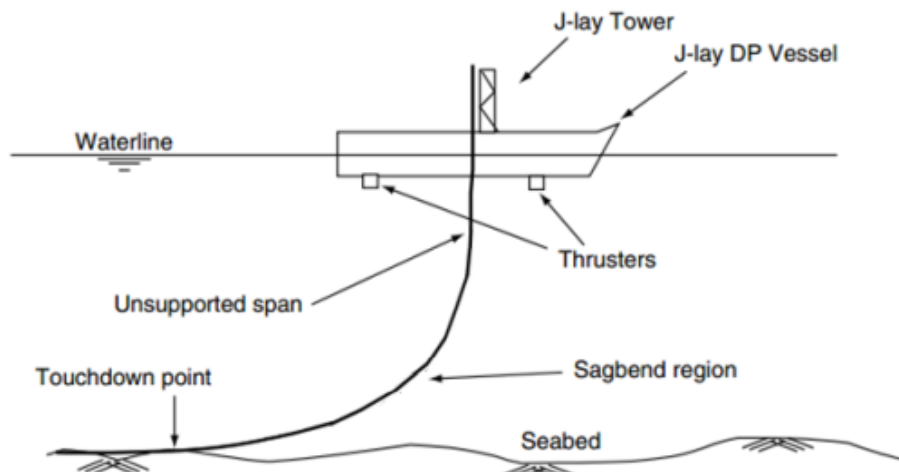


Figure 2.5: J-lay (from Guo (2014))

2.8.2 S-lay

For the S-lay method the pipe is installed in a S-curve down to the seabed (see Figure 2.6). The pipe is in other words guided horizontally out from the vessel. The pipe is in the upper part supported by a stinger, a steel structure protruding from the vessels aft, that is fitted with rollers to minimize damage of the pipe and guides the pipeline into the water. The stinger provides a smooth transition from the horizontal position to a certain departure angle. The curvature in the lower section (the sagbend) is controlled by lay tension transmitted to the pipeline by tension machines (Braestrup et al.; 2005). The horizontal laying from the vessel allows for several welding stations along the deck.

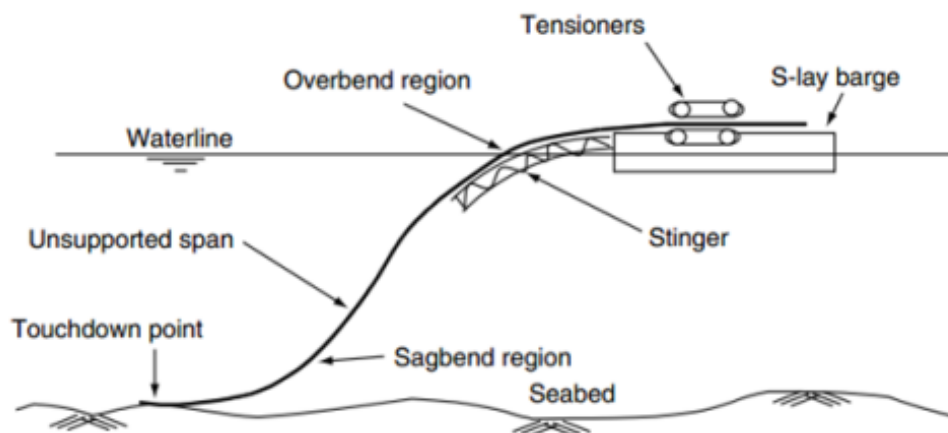


Figure 2.6: S-lay (from Guo (2014))

2.8.3 Reeling

The pipe reeling method is based on a method where the pipeline is made up onshore and reeled onto a huge drum on a purpose-built vessel. The pipe undergoes plastic deformation as the pipe is reeled onto the drum. When unreeling the pipe during installation, the pipe gets straightened using a special straightening ramp. Normally, this gets done by first bending the pipe sections to a common bending radius, as the pipes stored at the outermost layers have larger radius than the inner layer. Straightening all sections to the same radius, the straightening configuration will become equal for all sections. The straightener may consist of three rollers, where the one in the middle is on top of the pipe with the purpose of bending the pipe in the opposite direction, see Figure 2.7.

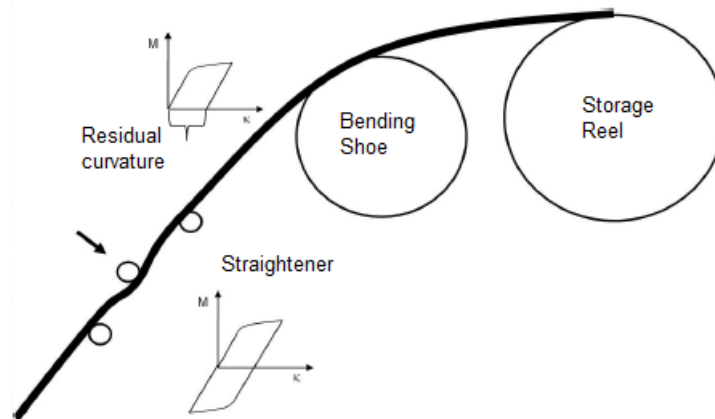


Figure 2.7: Reel Straightening (from Sævik (2012))

When reeling the pipeline, one major attention must be given to the plastic deformation of the pipe, and it is decisive that the deformation is kept within the limits specified in associated offshore codes, such as DNV-RP-F108 (DNV; 2006b). It is stated in this code that a potential failure mode during a reeling installation is fracture of the girth welds. During the reeling process, the pipe will be subjected to cyclic loading, i.e. reeling-on, reeling-off, bending over an aligner and finally straightening. The code requires that the pipeline system has sufficient resistance against both crack extension by tearing and unstable fracture during both the installation phase and during operation.

2.8.4 Assessment of the methods

The reeling method does have one major advantage regarding installation time compared to the other methods as it allows pipelines manufacturing onshore, under controlled conditions. This provides a high installation rate and reduces the costs directly related to the installation process. However, the reeling method is limited to a maximum pipe diameter of about 18 inches due to the amount of plasticity that may be allowed.

When it comes to welding, the J-lay allows for a limited number of welding stations, and hence the lay rate tends to be lower than for S-lay. However, in case of large water depths, the limitation of the stinger length used in S-lay, implies a higher top angle and horizontal tension compared to the J-lay method. This means that J-lay will be more applicable since it allows for smaller horizontal tension, and is thus preferable with respect to pipeline curve stability at these water depths.

2.8.5 Combined loading criteria

In conjunction with installation it need to be performed a control of local buckling due to combined loading. Since the pipe is installed in an un-pressurized condition, often empty, it has to be controlled against combined loading with external overpressure. The control is performed by utilizing a load controlled criteria in DNV (2012), for pipe members subjected to bending moment, effective axial force and external overpressure. The following criteria is the one to be satisfied:

$$\left[\gamma_m \gamma_{SC} \frac{|M_{Sd}|}{\alpha_c M_p(t_2)} + \left(\frac{\gamma_m \gamma_{SC} S_{Sd}}{\alpha_c S_p(t_2)} \right)^2 \right]^2 + \left[\gamma_m \gamma_{SC} \frac{p_e - p_{min}}{p_c(t_2)} \right]^2 \leq 1 \quad (2.16)$$

Where:

M_{Sd} = Design Moment

S_{Sd} = Design Effective axial force

p_i = Internal Pressure

p_e = External Pressure

p_c = Characteristic Collapse Pressure, found from equation 2.11

p_{min} = Minimum Internal Pressure, usually taken as zero during installation

With the plastic capacities defined as:

$$S_p(t) = f_y \pi (D - t) t \quad (2.17)$$

$$M_p(t) = f_y (D - t)^2 t \quad (2.18)$$

And the flow stress parameter defined as:

$$\alpha_c = (1 - \beta) + \beta \frac{f_u}{f_y} \quad (2.19)$$

With:

f_u = Tensile strength

f_y = Yield stress

And the β factor defined as:

$$\beta = \frac{60 - D/t_2}{90} \quad (2.20)$$

3 Non-Linear Finite Element Method

The finite element method is a commonly used numerical method, used to solve problems like for instance stress analysis, diffusion, fluid flow and heat transfer problems. The focus in this chapter will be on the non-linear finite element method and the non-linearities that are present in structural analysis. This is covered in order to give the basics behind the material that the software used in this thesis, SIMLA, is built upon, namely the non-linear finite element method. This chapter will cover the basics of the method applied in SIMLA, but not give details about how this is implemented in the analysis performed in this thesis. However, this will be covered in the next chapter.

3.1 General

The finite element method is based on the same foundation as structural analysis in general, where the following principles applies for both linear and nonlinear element method:

- Equilibrium
- Kinematic compatibility
- Constitutive equations: stress-strain relationship

3.1.1 Equilibrium

Equilibrium is the first of the overall three principles that structural analysis is based on. Equilibrium of the structure is expressed by means of the Principle of Virtual Displacements, which states that the work done by the true internal stresses and external forces equals each other when the structure is exposed to a virtual displacement field that satisfies the boundary conditions. Instead of trying to find the exact solution, the principle introduce approximate functions and intends to in average fulfil the differential equation for the problem using weight functions and volume integration (Sævik; 2008). Selecting weight functions such that the appropriate boundary conditions are fulfilled, one can obtain a state where the error in average for the total volume of integration is zero. However, the differential equation is not necessarily fulfilled at an arbitrary point within the volume.

The formulation of the virtual work in SIMLA neglects volume forces, but accounts for initial stresses. The principle of virtual displacement in an arbitrary equilibrium state then reads (Sævik; 2008):

$$\int_V (\rho \mathbf{a} - \mathbf{f}) \delta \mathbf{u} dV + \int_V (\boldsymbol{\sigma} - \boldsymbol{\sigma}_0) : \delta \boldsymbol{\varepsilon} dV - \int_S \mathbf{t} \cdot \delta \mathbf{u} dS = 0 \quad (3.1)$$

Where:

- ρ is the material density.
- \mathbf{a} is the acceleration field.
- \mathbf{f} is the volume force vector.
- \mathbf{u} is the displacement vector.
- $\boldsymbol{\sigma}$ is the stress tensor of Cauchy stress.
- $\boldsymbol{\sigma}_0$ is the initial stress tensor.
- $\boldsymbol{\varepsilon}$ is the strain tensor of natural strain.
- \mathbf{t} is the surface traction.

The stresses may be expressed with reference to the deformed structure (true stresses called Eulerian or Cauchy stresses) or its initial configuration (2nd Piola-Kirchhoff stresses). 2nd Piola-Kirchhoff stress is consistent with Green strain which also refers to the initial configuration. In SIMLA, all quantities are referred to the initial configuration, C_0 , i.e. Piola-Kirchoff stress and Green strain is applied.

3.1.2 Kinematic compatibility

Compatibility requirement of a structure assures that all adjacent cross sections will get the same displacement and deformation. The material itself will remain continuous as it deforms, no cracks will occur and the strain will be finite. By describing the displacements with continuous interpolation functions and ensuring proper boundary conditions, such that the strain is finite at the element boundaries, compatibility of a beam is ensured (Moan; 2003).

In SIMLA it is assumed that Bernoulli-Euler and Kirchoff-Navier's hypothesis apply, i.e. plane sections perpendicular to the neutral axis remains plain and perpendicular to the neutral axis after loading. Hence, no shear deformations. Further, the Green strain tensor is used as strain measure when formulating the incremental equilibrium equations. The 2nd order longitudinal engineering strain is neglected according to von Karman (Sævik; 2008). However, all terms related to coupling between longitudinal strain and torsion are included (Sævik and Giertsen; 2004).

Based on the above, with u , v and w as the axial, horizontal and vertical displacement respectively and θ as the torsional rotation around the neutral axial axis (see Figure 3.1), the Green strain for elastoplastic beam elements is expressed as follows:

$$E_{xx} = u_{,x} - yv_{,xx} - zw_{,xx} + \frac{1}{2}(v_{,x}^2 + w_{,x}^2) + \theta_{,x}(yw_{,x} - zv_{,x}) + \frac{1}{2}\theta_{,x}^2(y^2 + z^2) \quad (3.2)$$

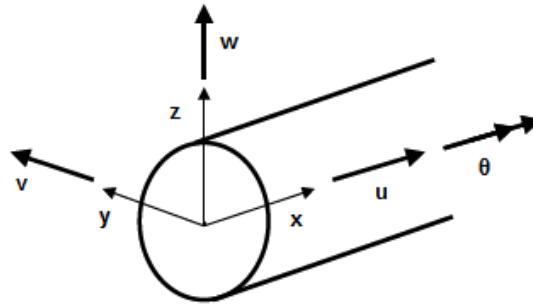


Figure 3.1: Pipe element parameters; definition of local coordinate system

3.1.3 Stress strain relationship

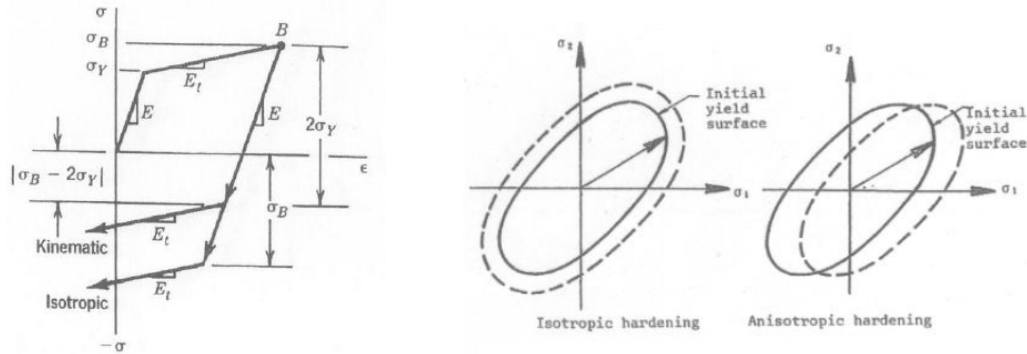
The stresses in equation 3.1 need to be related to strains. For elastic materials, this is done with Hooke's law. When the stress exceeds the proportional limit, a nonlinear relationship occur. In this case, it is necessary to apply an elasto-plastic formulation which takes into account both the stresses in the axial and the hoop directions of the pipe (Sævik; 2008). In order to form the basis for the plasticity and calculate the plastic strain, there are three major features:

1. An **initial yield condition**, i.e. the state of stress in which plastic deformation first occurs. Many yield conditions have been proposed, but experiments show that von Mises yield condition is the one best representing the material behaviour for most metals. Its simple continuous form is another advantage, especially in numerical analysis (Moan; 2003). The yield condition can generally be expressed as:

$$f(S, \kappa) = 0 \quad (3.3)$$

where f is a scalar function, κ is a strain-hardening parameter that depends upon the load history in the plastic range, and \mathbf{S} is the 2nd Piola-Kirchhoff stress tensor.

2. A **hardening rule** which describes the correction of the yield condition due to strain hardening as the plastic flow proceeds. The hardening may be described by an isotropic or kinematic model, both included in SIMLA. The features of the two material models are shown in Figure 3.2, for both an uniaxial state of stress and for a two dimensional stress-strain relationship:



(a) One-dimensional (Moan; 2003).

(b) Two-dimensional (Moan; 2003).

Figure 3.2: Isotropic and kinematic hardening.

As seen from these figures, the choice of material model especially matters when the loading is reversed or cyclic. Figure 3.2a shows that yielding always occurs after an unloading of $2\sigma_y$ in the kinematic model, whereas the material remember the hardening that has occurred in the isotropic case, i.e. the yield condition is unaltered when loading is reversed. The isotropic material model is for many metals in conflict with this hardening, as experiments has shown that the material yields at a lower stress level when loading is reversed opposed to the initial loading (Moan; 2003). This phenomenon is denoted Bauschinger effect. This effect is better captured with the Kinematic model, as the uniaxial stress state implies in Figure 3.2a, where an elastic range equals two times the yield strength preserved.

3. A **flow rule** which determines the plastic strain increment at every point in the load history. The relationship between stress and plastic strain can be obtained primarily by two different plasticity theories, namely the flow theory and the deformation theory. SIMLA is based on the flow theory, and experiments shows according to Moan (2003) that this is the better one treating problems with general loading paths, e.g. reversed and cyclic loading. Equation 3.3 defines the initial yield surface, while different values of f defines different stress states (Moan; 2003):

- $f < 0$; elastic range
- $f = 0$; plastic range
- $f > 0$; inadmissible

Further, Drucker's postulate for stable materials is assumed valid (Sævik; 2008), stating that the yield surface is convex and that the plastic strain increment is both normal to the yield surface and a linear function of the stress increment. The result is a constitutive equation which relates the total strain increment and the stress increment.

3.2 Non-linearities

Several non-linearities are present in structural analysis:

- **Geometrical non-linearities:** The equilibrium equations can for small displacements be expressed based on the initial configuration, and the loads can then be assumed to act identical on the structure throughout the analysis. For larger displacements, the geometry may change and thus the load changes through the analyses. Geometric nonlinearities will arise if the structure get deformations such that the equilibrium equations need to be expressed with respect to the deformed configuration.
- **Material non-linearities:** In short, the material behaviour becomes non-linear when the stress exceeds the yield limit. The relationship between stress and strain is in the elastic area expressed by Hooks' law as a linear relationship: $\sigma = E\varepsilon$. When the yield limit is reached, the material curve moves into the plastic area, where the stress-strain relationship varies due to change in the modulus of elasticity, and can therefore no longer be described by the linear relationship in Hooks' law.
- **Non-linearities in conjunction with boundary conditions:** Nonlinear boundary conditions may have to be taken into consideration for instance in relation to contact problems, in which two surfaces come into or out of contact (Moan; 2013). Displacements may give rise to changes in the boundary conditions if contact with other elements interferes with, and leads to changes of, the original configuration. If the analysis also includes the effect of friction, then slick-slip behaviour may occur in the contact area. This further provides an additional non-linear complexity, that commonly is dependent on the load history (Moan; 2013).

3.3 Lagrange Formulation

The Lagrangian description of motion, referring to what happens at a material particle, in contrary to the Eulerian description, which is commonly used in hydrodynamics and refers to what happens at a certain place in space, is commonly preferred in structural mechanics as the initial configuration usually is known. There are two different Lagrangian formulations that are widely used in solid mechanics, namely the Total Lagrangian and the Updated Lagrangian formulation. The difference between these is the choice of reference configuration.

Total Lagrangian is based on the initial configuration, where all static and kinematic variables used in the incremental equations are referred back to this initial configuration, C_0 , in a fixed coordinate system.

Updated Lagrangian, on the other hand, uses a curvilinear coordinate system fixed to the body and is continuously updated as the body deforms, always referring back to the last obtained equilibrium configuration, C_n .

SIMLA is based on a co-rotational formulation referring back to the initial C_0 configuration. The basic idea behind a co-rotational formulation is to separate the rigid body motions from the local or relative deformation of the element (Sævik; 2008). This is done by fixing a local coordinate system to the element and letting it continuously translate and rotate with the element as it deforms.

3.4 Solution Procedures

Analysis of both static and dynamic nature can be solved in SIMLA. In this thesis, SIMLA has been used for both purposes, studying the the curve stability of rigid pipes. Thus, a short description of the respective solution procedures will now be presented. By considering the equilibrium equations for a static and dynamic system (equation 3.4 and 3.5 respectively), it is seen that the dynamic analysis differs from the static in the way of including inertia forces and damping, and gives a time-dependent solution:

$$\mathbf{K}\mathbf{r} = \mathbf{R} \quad (3.4)$$

$$\mathbf{M}\ddot{\mathbf{r}} + \mathbf{C}\dot{\mathbf{r}} + \mathbf{K}\mathbf{r} = \mathbf{R}(t) \quad (3.5)$$

Where \mathbf{K} , \mathbf{M} and \mathbf{C} is the stiffness matrix, mass matrix and damping matrix respectively. \mathbf{R} is the external applied load vector, while \mathbf{r} , $\dot{\mathbf{r}}$ and $\ddot{\mathbf{r}}$ is respectively the displacement, velocity and acceleration vectors.

In the dynamic analysis, mass matrix is introduced in the equilibrium equations. A mass matrix that is based on the same interpolation polynomial as the stiffness matrix is called a consistent mass matrix. Concentrated/lumped mass matrix on the other hand, is a simplified method where the mass is assumed to be concentrated in the junctions. The concentrated mass matrix has multiple advantages linked to the calculation process, as it requires less storage space and a smaller number of operations in many dynamical problems (Langen and Sigbjørnsson; 1979). However, in the dynamic analyses performed in this thesis, a consistent mass matrix have been utilized. Even though this could be a more time consuming procedure, it will provide better, or at least as good, results than the concentrated mass matrix in the analyses performed.

3.4.1 Static Solution Procedure

There exist various techniques for solving static non-linear problems, such as incremental or stepwise procedures, iterative procedures and combined methods. The static solution procedure in SIMLA is based on a load control defined by the user, with Newton Raphson equilibrium iteration at each step (Sævik; 2008). This is the most frequently used iterative method for solving non-linear structural problems (Moan; 2003). The method is illustrated in Figure 3.3, and the procedure utilized in SIMLA is written as (Sævik; 2008):

$$\Delta \mathbf{r}_{k+1}^i = (\mathbf{K}_T^{-1})_{k+1}^i \Delta \mathbf{R}_{k+1}^i \quad (3.6)$$

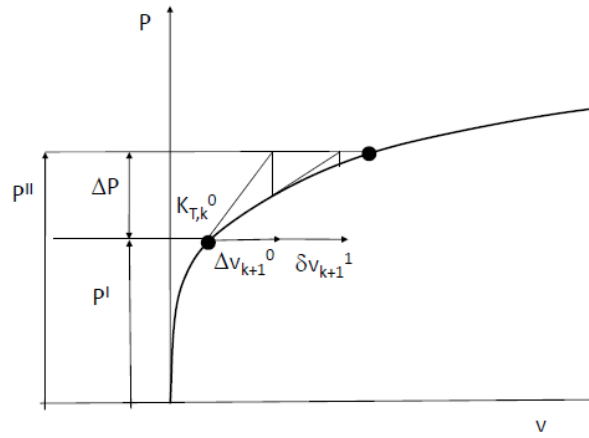


Figure 3.3: Illustration of Newton Raphson iteration (Sævik; 2008)

3.4.2 Dynamic Solution Procedure

Nonlinear dynamic problems can not be solved by modal superposition, hence, direct time integration of the equation of motion is necessary. The direct integration methods are alternatives to modal methods, and can successfully be used to treat both geometric and material non-linearities. The method can be performed by either an explicit or an implicit method.

Explicit method

The method is explicit if the displacement at the new time step, $t + \Delta t$, can be obtained based only on information about the displacements, velocity and accelerations from the current and previous time steps:

$$\mathbf{r}_{k+1} = \mathbf{f}(\mathbf{r}_k, \dot{\mathbf{r}}_k, \ddot{\mathbf{r}}_k, \mathbf{r}_{k-1}, \dot{\mathbf{r}}_{k-1}, \ddot{\mathbf{r}}_{k-1}, \mathbf{r}_{k-2}, \dots) \quad (3.7)$$

Where the subscript refers to the time step.

Explicit methods are conditionally stable and very short time steps must therefore be applied. When explicit methods are formulated in terms of lumped mass and damping matrices, i.e. a simplification where the mass and the damping are assumed to be concentrated in the nodes, it is not necessary to solve a coupled equation system in the time march (Sævik; 2008). This leads to very low computational efforts per time step. Explicit methods are therefore commonly used in explosion and impact analysis, as it is necessary to use short time steps in order to achieve sufficient accuracy in analysis of impulse type response(Sævik; 2008).

Implicit method

Implicit method is characterized in that the displacements at the new time step, $t + \Delta t$, are obtained by the velocities and accelerations at the new time step, together with the information from the previous time steps:

$$\mathbf{r}_{k+1} = \mathbf{f}(\dot{\mathbf{r}}_{k+1}, \ddot{\mathbf{r}}_{k+1}, \mathbf{r}_k, \dot{\mathbf{r}}_k, \ddot{\mathbf{r}}_k, \mathbf{r}_{k-1}, \dots) \quad (3.8)$$

Implicit methods will in general have better numerical stability than explicit methods, as information about the next step is utilized. These methods may become uneconomical if short time steps is unavoidable due to accuracy requirements. This is due to the fact that it is necessary to solve the coupled equation system at each time step (Sævik; 2008).

Various implicit methods exists and differs in the way of how the acceleration is assumed to vary within the time steps and at which time the equilibrium is fulfilled. In case of long analysis, it is beneficial to use methods where the result becomes unconditionally stable, i.e. numerical stability is provided regardless of the length of the time step. In nonlinear problems, one can not on a general basis guarantee that the solution is unconditionally stable. However, according to Langen and Sigbjørnsson (1979), experiences and analytical studies have shown that constant average acceleration between the time steps provides unconditional stable analysis in many important and practical nonlinear problems. Constant average acceleration between the time steps can be assured in SIMLA, which utilizes the HHT- α method, by setting the control parameter for the dynamic analysis $\beta = 1/4$.

3.4.3 Incremental time integration: HHT- α Method

The dynamic equilibrium equation is solved by numerical incremental time integration. The solution need to be obtained by an incremental method since the system equilibrium equation is nonlinear. In SIMLA the HHT- α method is used in the time integration scheme. The method is based upon the well known Newmark- β method, but differs in the way of introducing numerical damping by means of time averaging. The structural damping can in SIMLA be implemented as Rayleigh-damping and concentrated damping:

$$\mathbf{C} = \mathbf{C}_0 + \alpha_1 \mathbf{M} + \alpha_2 \mathbf{K} \quad (3.9)$$

It can be shown that the modes with high frequency are damped out by the stiffness proportional damping, while modes with very low frequency similarly gets damped out by the mass proportional damping. As the response of high frequency modes is of low interest in dynamic analysis, Rayleigh damping can be introduced in order to damp out these modes by means of stiffness proportional damping. However, it has been shown by Fylling et al. (1995), rendered by Sævik (2008), that introducing Rayleigh damping in the well known Newmark- β method mainly will damp out the medium modes, leaving the lower and higher modes almost unaffected. However, the higher modes can be removed by numerical damping. This will in the Newmark- β method reduce the order of accuracy from 2nd to 1st order accuracy. However, the reduced accuracy can be eliminated by applying the HHT- α method, ensuring that the high frequency modes get damped out and at the same time retain 2nd order accuracy. The modified equilibrium equation for the system used in SIMLA is from the HHT- α method, and is given as:

$$\mathbf{M}\ddot{\mathbf{r}}_{k+1} + (1 + \alpha)\mathbf{C}\dot{\mathbf{r}}_{k+1} - \alpha\mathbf{C}\dot{\mathbf{r}}_k + (1 + \alpha)\mathbf{R}_{k+1}^I - \alpha\mathbf{R}_k^I = (1 + \alpha)\mathbf{R}_{k+1}^E - \alpha\mathbf{R}_k^E \quad (3.10)$$

Where α is a parameter used in order to control the damping properties, \mathbf{R}^I is the internal force vector and \mathbf{R}^E is the external force vector. The smaller the value of α , the more damping is induced in the numerical solution. HHT- α method coincides with the Newmark- β method when $\alpha = 0$.

The equilibrium iterations used in SIMLA is formulated as a Newton-Raphson iteration scheme, where the equilibrium iterations are performed before increasing the time step. A predefined number of iterations chosen by the user will be performed. If equilibrium is not achieved, the time step will be divided before a new trial is initiated (Sævik; 2008).

4 SIMLA

SIMLA is a special purpose software for engineering analysis of offshore pipelines during design, installation and operation. SIMLA is based on the non-linear finite element method, where both static and dynamic analysis can be performed. Time domain is used to describe the load history and the analysis sequence in both cases (Sævik et al.; 2013). The numerical procedure is based on finite elements that are formulated using the Principle of Virtual Work, and is capable of simulating the structural response in terms of stresses, soil reaction forces and curve stability parameters (Sævik and Giertsen; 2004).

In this thesis, SIMLA has been used during laying, where new elements are introduced from a moving vessel. The purpose of the analysis is to implement turnpoints along the predefined route and based on the results obtained analyze the number of required turnpoints. Both static and dynamic analyses are performed in order to form the basis in the final resolution of required numbers of turnpoints. The goal is to achieve a satisfying curve stability, and at the same time preserve the structural integrity of the pipeline while ensuring that the contact force between the pipe and the turnpoints are kept below the geotechnical capacity of the turnpoints.

4.1 Building the Model

The input data used in this thesis is based on information provided by Subsea 7. The Seven Navica pipelay vessel will be used during the installation. Seven Navica allows lay angles between 20° and 90° . From an installation report provided by Nessmo (2014), the optimal lay angle was found to be 56° for the case investigated. This lay angle has therefore been adopted in this analysis.

A simple predefined route has been investigated, consisting of two straight distances with a curved section with a radius of 400 [m] in between (see Figure 4.3). This is built by utilizing MATLAB and is further written to a text-file, used as input-file in SIMLA. When the curve radius becomes as low as in this case, the pipeline will not remain stable without additional measures, and installation of turnpoints is necessary. The number of turnpoints required is analyzed in SIMLA.

In the route investigated, 10 turnpoints have originally been installed. In the process of finding the optimal number of turnpoints, it has in this thesis been conducted analyses for 3-10 turnpoints along the route. This is done in order to find out whether fewer turnpoints could have been installed or not.

The input file to SIMLA is generated in FlexEdit, a text editor tailored for use

with a variety of Marintek programs, including SIMLA. The model is built by first running an initial static configuration, assuming that the pipeline is installed at the seabed. Hence, the initial configuration is obtained by identifying seabed contact points. Both static and dynamic analysis are then carried out, where the actual lay process is simulated, and the pipeline consequently experience the operation from being fed out from the lay vessel until it rests on the seabed.

4.2 The different analyses

To clarify and later on in this chapter easier explain the difference between the analyses performed, a short description of the analyses will now be declared. More details about the analyses will be presented later. However, it was found appropriate to explain the basics now, such that a distinction between the analyses is apparent when further descriptions are given later on in this chapter.

Basically, two kinds of analyses are performed; respectively static and dynamic analysis. Both of these is subdivided into two parts, one analysis where the static configuration of the model is set up, and one main part where the static or the dynamic analysis is performed based on this configuration.

4.2.1 Initial configuration

Both the static and the dynamic analysis consist of a pre-analysis, where the static configuration of the model is achieved. In this configuration, the pipe is assumed laid on the seabed, such that the contact points along the pipeline route are obtained. The initial configuration of the model is performed in SIMLA through the AUTOSTART control command.

4.2.2 Static analysis

The static analysis consist of one analysis where the static configuration is achieved and the contact points of the route are obtained. This configuration only facilitates the feed analysis, where the pipe gets fed out and the lay process is simulated. From this feeding analysis the static results are obtained. By feeding out the pipeline, the pipe elements experience the operation from being fed out from the lay vessel, until it rests on the seabed. The feeding of the pipeline is controlled through the STATIC-FEED time control card and the analysis is performed through the TIMEINIT control card, which is based on the AUTOSTART from the initial configuration. This makes it possible to introduce history effects, such as friction, non linear seabed contact elements and non linear pipe elements.

4.2.3 Dynamic analysis

The dynamic analysis is then performed in order to find the dynamic response and how this impacts the results obtained from the static analysis. The analysis is intended to be performed at the laying stage where the dynamic impact is highest, such that a worst case scenario of the laying process is obtained. The dynamic analysis is performed as a RESTART of the initial configuration in the control card. It allows the dynamic element model to be modified compared to the static model. This is convenient as the optimal model for static and dynamic simulations may differ (Passano et al.; 2008). In this case, the number of elements in the model is adjusted to give a high resolution along the most critical areas of the curvature, i.e. near the turnpoints evaluated.

4.3 Input Data

The input data used in the analysis will be summarized in this section. The data used are based on data for the Oseberg Delta 2 field, located 8 km south-west of the Oseberg Field Centre. The analysis is performed on a 10" ID production pipeline going between two templates. The necessary information has been provided by Subsea 7. The pipeline is installed by the reeling method from the Seven Navica pipelay vessel (see Figure 4.1 and Figure 4.2).

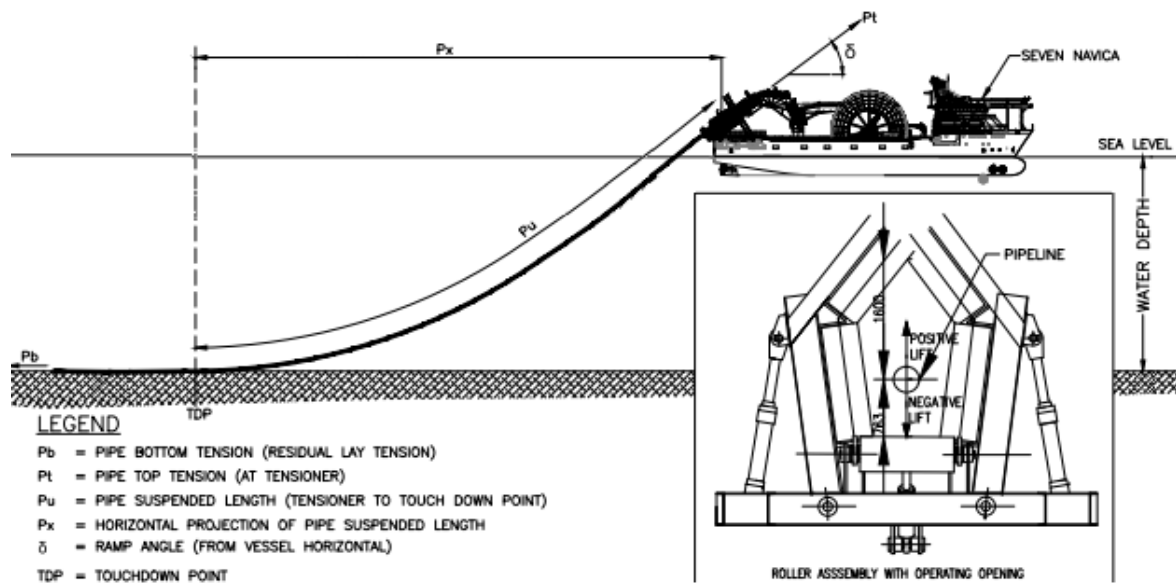


Figure 4.1: Seven Navica - Lay Configuration (from Nessmo (2014))



Figure 4.2: Seven Navica (from Nessmo (2014))

4.3.1 Route

MATLAB has been used in order to make a input file defining the pipeline route. The nodes of the pipeline route are defined for every meter and are written to the file *Route_Data_PL.txt*. This is done in the Matlab script *Simla_Route_Input_Calculations.m* which can be found in appendix C.1.

The entire route is assumed to have a constant water depth, in other words no curvature in the vertical direction, only along the sea floor. The coordinates from the input text-file is read in SIMLA, and the pipeline is laid based on the description obtained from this file. The route investigated can be seen from Figure 4.3 below:

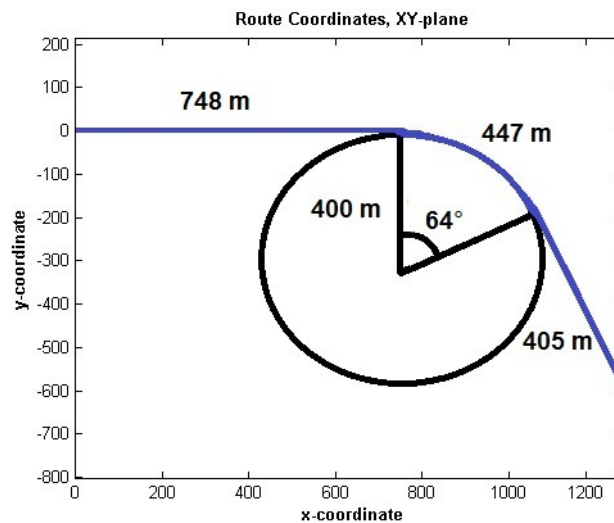


Figure 4.3: Pipeline Route in the xy-plane

4.3.2 Pipe Properties

The pipeline dimensions used in the analysis can be found in Table 4.1:

Table 4.1: Pipeline Dimensions

Description	Value [mm]
Inner Diameter	254
Steel Outer Diameter	305
Nominal Steel Wall Thickness	25.5
Coating Thickness	80.4
Total Outer Diameter	465.8

The steel material used is according to DNV SMLS 450 (DNV; 2012). The material properties used can be found in the following table:

Table 4.2: Steel Properties

Description	Value	Unit
Steel Density	7850	kg/m ³
Young's Modulus	207	GPa
Poisson's Ratio	0.3	[-]
SMYS	450	MPa
SMTS	535	MPa

The pipe is also provided with coating consisting of a seven layer polypropylene system (7 LPP), with the following properties:

Table 4.3: Coating Properties

Coating Layer		Thickness [mm]	Density [kg/m ³]
1	FBE	0.3	1300
2	Adhesive	0.3	900
3	Solid PP	9.4	900
4	PP Foam	34.4	740
5	Solid PP	3.0	900
6	PP Foam	29.0	740
7	Solid PP	4.0	900
Total Thickness:		80.4	

In SIMLA, the PIPE31 element is used in the analysis. This element is a 3D, two-noded beam element with linear material properties for elastic pipe elements.

4.3.3 Environmental Conditions

When it comes to the input of environmental conditions, an even seabed with constant water depth of 110 [m] is assumed. The simplification was decided in consultation with professor Svein Sævik and Trond Ståle Nessmo in Subsea 7. This was found appropriate, with insignificant influence on the results, due to the small range of variation of the water depth in the case investigated.

Waves/Sea State

The waves are modelled in SIMLA by use of the Jonswap spectrum to describe a irregular sea state. The wave elevation is expressed as:

$$\zeta(x, y, t) = \sum_{k=1}^{N_\omega} \zeta_{Ak} \sin(\omega_k t + \phi_k^p + \phi_k) \quad (4.1)$$

Where ϕ_k is the random phase angle, while ϕ_k^p is the position dependent phase angle, both uniformly distributed between $[-\pi, \pi]$. N_ω is the number of wave components and ζ_{Ak} is the wave amplitude of component k, with the corresponding wave frequency ω_k . The wave amplitude is further defined as:

$$\zeta_{Ak} = \sqrt{2S(\omega_k)\Delta\omega} \quad (4.2)$$

Where S is the wave spectrum, with the three parameter JONSWAP wave spectrum defined as follows: (Sævik; 2008):

$$S(\omega) = \alpha \frac{g^2}{\omega^5} e^{-\beta \left(\frac{\omega_p}{\omega}\right)^4} \gamma^e \left[-\frac{1}{2} \left(\frac{\omega - \omega_p}{\sigma \omega_p}\right)^2 \right] \quad (4.3)$$

With:

$$\alpha = 1.2905 \left(\frac{H_s}{T_z}\right)^2 \quad (4.4)$$

$$\beta = \begin{cases} 1.205, & \text{if } T_p < 5\sqrt{H_s} \\ 1, & \text{if } T_p \geq 5\sqrt{H_s}. \end{cases} \quad (\text{North Sea Conditions}). \quad (4.5)$$

$$\gamma = \begin{cases} e^{5.75-1.15\frac{T_p}{\sqrt{H_s}}}, & \text{if } T_p \geq 3.6\sqrt{H_s}. \\ 5, & \text{if } T_p < 3.6\sqrt{H_s}. \end{cases} \quad (4.6)$$

$$\sigma = \begin{cases} 0.07, & \text{for } \omega \leq \omega_p. \\ 0.09, & \text{for } \omega > \omega_p. \end{cases} \quad (4.7)$$

$$\frac{T_p}{T_z} = 1.407(1 - 0.287 \ln \gamma)^{1/4} \quad (4.8)$$

Where:

H_s is the significant wave height.

T_z is the zero-up crossing frequency.

T_p is the peak period.

ω_p is the peak frequency.

The analyses are performed with a 3 hour duration of the sea state, with a significant wave height (H_s) of 2.5 [m], and different spectrum peak periods (T_P). A significant wave height of 2.5 [m] was chosen as it is desirable to perform installation in wave height up to this level (Nessmo; 2014). Three wave period cases are investigated with $T_P = 7$ [s], $T_P = 11$ [s] and $T_P = 15$ [s]. When the period that gives the highest loads on the pipe and turnpoints is found, the worst case wave direction has been investigated. This parameter study was carried out with only a 10 minutes sea state and with 3 turnpoints along the route. Based on what is found to be the worst wave period and direction, the dynamic analyses are carried out.

Transfer function

The vessel motion data is based on the lay vessel Seven Navica and the response amplitude operator (RAO) -data was provided by Subsea 7 on a Riflex format. However, the READTRF card in SIMLA is able to read the transfer functions on other formats, including the Riflex-format.

Current

Current effects have been taken into consideration based on a one year extreme current, with the following current profile:

Table 4.4: Current Profile

Depth [m]	1-Year Extreme Current [m/s]
Surface	1.05
25	0.9
50	0.9
75	0.8
107	0.6
Seabed	0.0

A parameter study, investigating which current direction that results in the worst load impact on the turnpoints and the pipe, has been carried out. 4 directions have been tested; upstream, downstream and transverse current pushing the pipe either away from or towards the turnpoint.

4.3.4 Soil

The soil condition is taken as hard sand, where the friction utilized is based on DNV (2010) for sand. The friction factor of $\mu=0.6$ is used in the SIMLA analysis in both lateral and axial direction.

Representation of the pipe/soil interaction becomes more and more vital as offshore pipelines are required to operate at higher pressures and temperatures. From this, uncontrolled lateral buckling and global axial displacement may occur. In order to assess this, it is of high importance to model the pipe/soil properties as correct and realistic as possible. In SIMLA, the seabed has been modelled by use of the CONT126 contact element, except for the initial configuration carried out before the static analysis, where the CONT125 contact element is used instead. The difference is that the CONT125 element measure transverse displacement relative to the route described on the seabed profile. Whereas CONT126 measures friction transverse displacement from the position where the last contact was obtained (Sævik et al.; 2013).

The contact interface between the pipe and the seabed is further defined by the CONTINT card. The contact elements are attached to all nodal points along the pipeline. The contact force in the vertical direction is defined by linear stiff springs that are attached vertically to the pipeline. This is implemented in SIMLA by defining a hyperelastic material behaviour with a force-displacement curve of constant slope, as described in Figure 4.4. The HYCURVE model is based on a nonlinear elastic behaviour of the material, with the basic principle that the resultant quantity is a one to one function of the associated deformation without hysteresis (Sævik; 2008).

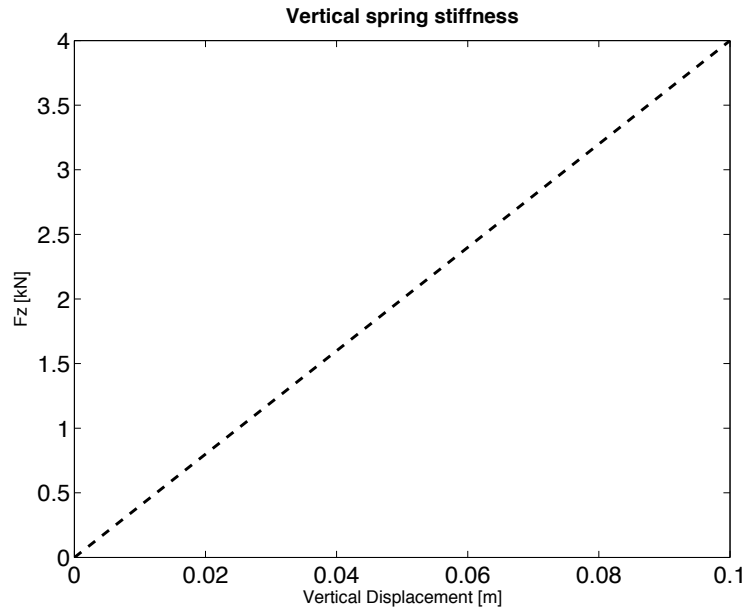
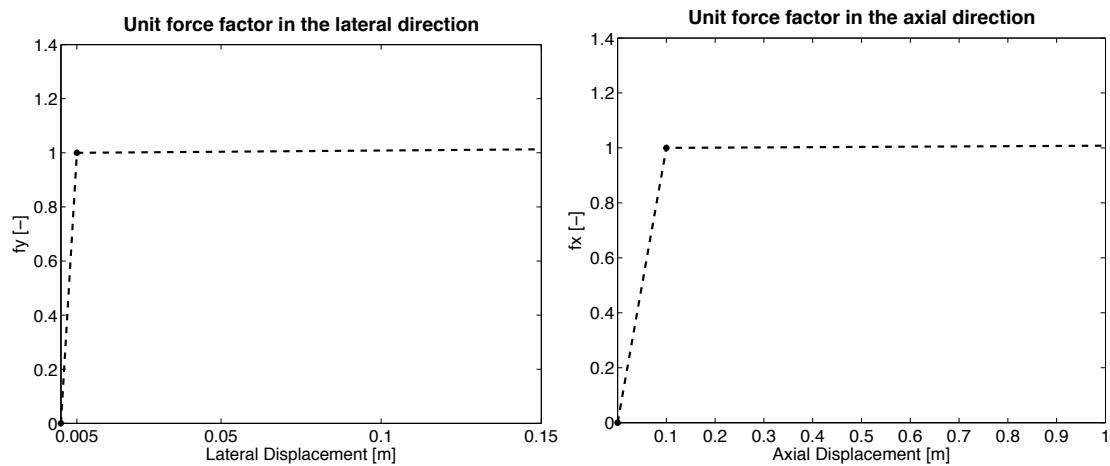


Figure 4.4: Vertical spring stiffness

The material curves in the horizontal plane are defined by the EPCURVE parameter in SIMLA, in order to implement an elastoplastic material behaviour with kinematic hardening. Further, the friction coefficients are scaled by a unit force factor with the mobilization length of 0.005 [m] and 0.1 [m] in the axial and lateral direction respectively:



(a) Unit force factor in lateral direction

(b) Unit force factor in axial direction

Figure 4.5: Unit force factors

In order to ensure a correct pipeline route configuration, sliding of the pipeline is deactivated when the initial configuration is set up. This is done by implementing a high unit force factor, such that the pipeline follows the specified route configuration without any sliding. In the feeding and dynamic analyses, the sliding of the pipe is then activated. This is done by changing the unit force factor in the soil material defined in SIMLA. During laying, the axial friction is turned off. The reason for neglecting this is to obtain a more accurate distribution of the axial force in the pipeline. Hence, soil interaction forces will only be introduced if the pipe moves transverse relative to the planned route (Sævik and Giertsen; 2004).

4.3.5 Turnpoints

The same MATLAB script as used to define the route coordinates, is used in order to determine and define the positions of the turnpoints. These positions are not written directly, but are manually copied into the SIMLA-files. The positions are calculated based on simple geometry considerations, and are changed in Matlab by changing the desirable number of turnpoints.

The turnpoints are modelled in SIMLA by use of the CONT164 roller contact element, with a chosen diameter of 2 [m]. To define the positions of the turnpoints, it is modelled a dummy beam, from where the turnpoints are allocated an eccentricity from. This is done in the ELECC card in SIMLA. By using the CONTINT card, the contact interfaces between the pipe and the turnpoints are defined.

The turnpoints are typically installed with a certain turnpoint tolerance. The tolerance utilized in this thesis is a tolerance of 0.5 [m] in the lateral direction and 3.0 [m] in the longitudinal direction. A modification has been done to the MATLAB script used to find turnpoints positions, in order to include the tolerance in the analysis. This is done in order to be able to evaluate the worst case positions. As the longitudinal tolerance of 3 [m] has been assumed to be of insignificant order compared to the distance between the turnpoints, only the lateral tolerance has been applied. Figure 4.6 shows the ideal turnpoint position (represented by black dots), and the worst case positions, i.e. placed 0.5 [m] lateral to the ideal position (represented by the red dots):

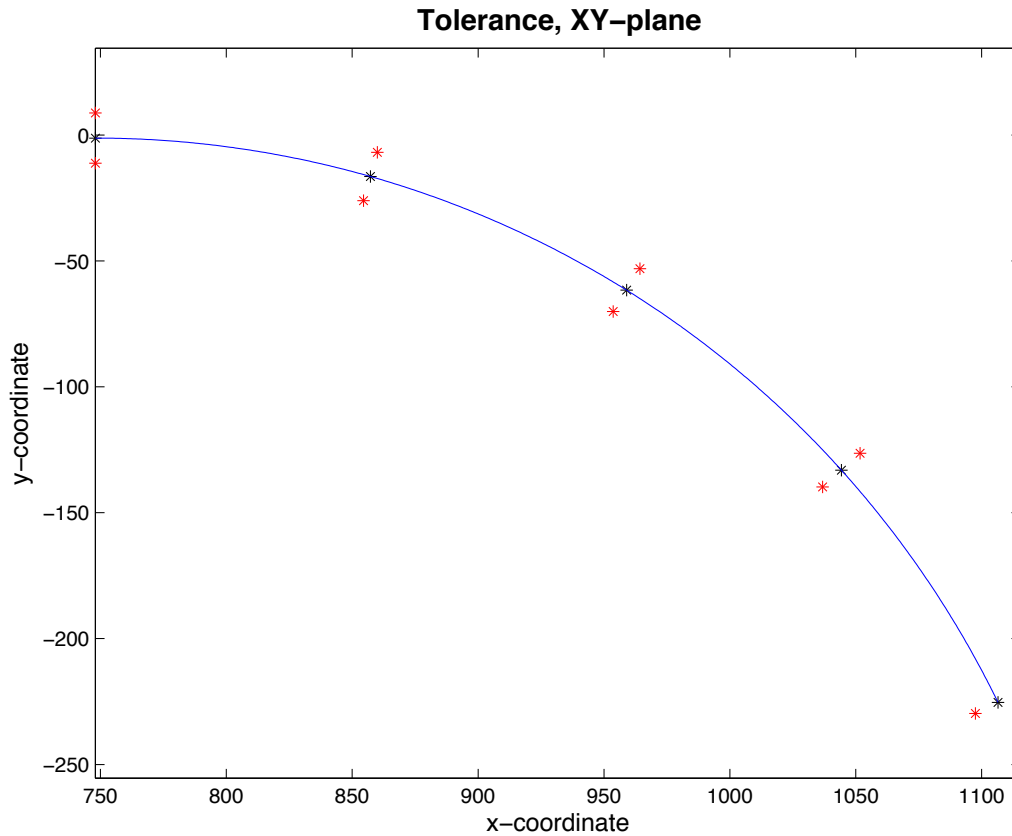


Figure 4.6: Turnpoint tolerance calculated from Matlab

For the case investigated, each turnpoints has a geotechnical capacity of 80 [kN]. When assessing the results, this capacity has to be considered. It will also be assessed whether this is a reasonable capacity or whether an increased or decreased capacity of the turnpoints could be applied or not. By example, if it is seen that the pipe fulfils the local buckling criteria, but not the turnpoint capacity, a consideration of increasing this capacity must be done.

4.4 Running the Analyses

The static analyses are mainly just run through a short-cut key in FlexEdit, where the analyses have been set up. This could not be done for the dynamic analyses, as they proved to be far too demanding of being run this way. The dynamic analyses had to be run through Cyqwin, a command interface that enables the possibility of specifying the desirable amount of memory that should be allocated to the analysis.

Late in the work, it became evident that the most critical response would occur at the same time during a sea state with the same seed number, i.e. the same waves generated. One analysis, with a 3 hour sea state was therefore run in order to obtain the most critical response. Then, all other dynamic analyses were set up with a short time-interval around this critical time-period. This proved to be a significant efficiency-gain and was essential in order to get results produced in due time.

Running the analyses through Cygwin allows for carrying out multiple analyses simultaneously. By using a shell/go script, it was also possible to run several analyses in sequence, without being dependent of starting the analyses manually when another was completed. By example, this has been applied during the process of setting up the different parameter studies, in order to allow for multiple analyses with different input parameters in SIMLA.

5 Turnpoints Calculations

Pipeline installation along a prescribed pipeline route would generally involve curved sections in the horizontal plane, due to existing subsea infrastructure or natural seabed characteristics. With respect to route optimization in confined areas, this often leads to several horizontal curves along the pipeline route. The curve radius is commonly so large that the bending resistance of the pipe can be omitted. However, the tension induced in the pipeline throughout laying tends to straighten the curvature, unless it is kept in place due to the soil resistance. If the lateral soil friction is insufficient, it might be necessary to establish lateral supports to guide the pipeline, ensuring that the desired pipeline curvature is achieved (Braestrup et al.; 2005). Rigid pipelines are commonly stable during pipe laying by weight for curve radius of 1000 [m] or greater. At a smaller curve radius, additional actions like lateral supports, so called turnpoints, may be required.

5.1 Background

As outlined in the scope of work, current project experience shows that the calculations of required number of turnpoints, based on both structural integrity of the pipe and turnpoint capacity to withstand horizontal contact force, is conservative compared to what seen offshore. It is believed that an improved method of calculating contact force from pipeline on turnpoints would reduce the number of turnpoints installed offshore. This could possibly reduce the installation costs with a great amount, as less turnpoints will give lower production costs, as well as reduced installation time and hence installation costs.

5.2 Horizontal curve stability

An important routing and installation criteria is the minimum horizontal curvature radius that can be obtained by the friction from the seabed. As outlined above, if the friction from the seabed itself is not sufficient to provide curve stability of the pipeline, turnpoints can be installed in order to assist this. The minimum horizontal radius that can be obtained only by the seabed friction, can be found from simple transverse equilibrium consideration in the horizontal plane (Sævik; 2012):

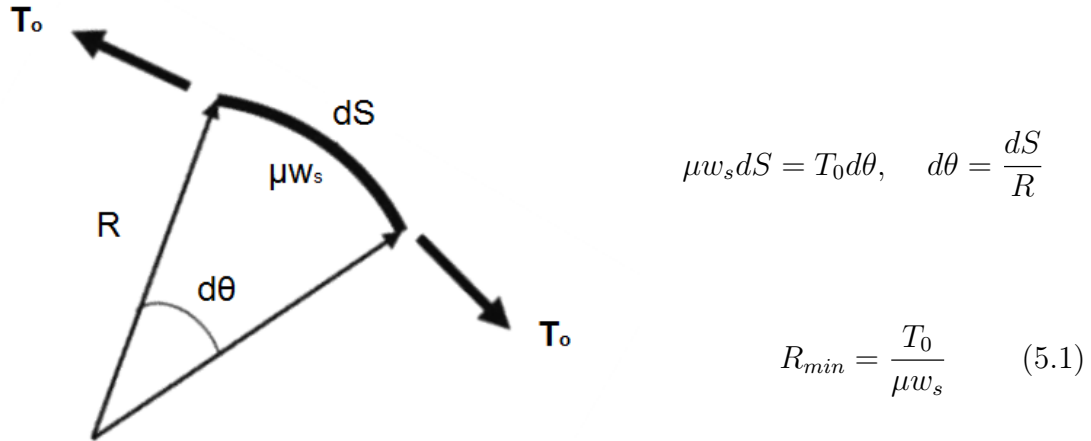


Figure 5.1: Minimum horizontal radius

Where:

μ is the soil friction.

T_0 is the bottom tension in the pipeline

w_s is the submerged weight of the pipeline.

R_{min} is the minimum horizontal curve radius.

5.3 Current method

The methodology for turnpoint calculations used in Subsea 7 will now be presented. This is implemented in order to gain an understanding of the problem and see the difference with the method applied in this thesis. The method is rendered from information provided by Subsea 7 through Nessmo (2014).

The methodology for calculating bending moment and corresponding pipe stresses are based on:

- Pipe bending moment due to initial curvature.
- Bending moment due to turnpoint positioning tolerance based on simplified beam theory.
- Turnpoint bending moment due to pipeline tension.

The arc length of the curve between turnpoints that gives an pipeline utilisation ratio of unity, is considered to be optimum distance between the turnpoints. The

utilisation is calculated as ratio of the bending moment in the curve, as sum of all components described above, to plastic bending moment capacity of the pipeline.

The force acting at the turnpoint, due to interaction between pipeline and turnpoint, is calculated assuming that the force is smeared over the arc length of the pipeline between the turnpoints. The pipeline establishes contact with all turnpoints and the load at each turnpoint is identical to the idealised pipeline with constant bottom tension and uniform lateral frictional resistance. Part of the resistance to withstand the maximum bottom tension will be provided by lateral frictional resistance of the pipeline. The turning points are required to be designed to provide the shortfall, in order to keep the pipeline follow the tight curvature.

5.4 Method applied

In this thesis, SIMLA has been used in order to determine the number of required turnpoints along the pipeline route. Both a static and a dynamic analysis have been performed in order to control the curve stability and the load effect on the pipeline and the turnpoints. The pipe is being fed out in the static analysis, such that the pipe experience the process from being fed out from the lay vessel until it rests on the seabed. A dynamic analysis is then performed at what is found to be the most critical position along the route. This is done in order to find the dynamic response and how this impacts the results obtained from the static analysis.

The fact that the pipeline in SIMLA could be laid with the curvature of the case that is investigated, is something that differs from the method used by Subsea 7 today (Nessmo; 2014), where the bottom tension is found based on laying analysis at a straight distance in Orcaflex. This tension is then utilized as input in the method described in the previous section.

Several parameter studies have been performed during the dynamic analysis in order to determine the overall worst case in terms of the structural integrity of the pipeline. Determinations of the most critical wave period, wave direction and current direction have been performed. The most critical touchdown-position along the pipeline route has also been investigated in order to find the position at which the dynamic imposed loads are at their maximum.

To control the results and find an optimal number of turnpoints along the pipeline curvature, a control check against local buckling has been performed. By utilizing DNV's formula for a load controlled design criteria against local buckling (DNV;

2012), see Section 2.8.5, the number of turnpoints are evaluated.

The control performed is based on a Ultimate Limit state. The load effect is performed as a local check, since system effects are not present, i.e. major parts of the pipeline are exposed to the same functional loads. With a condition load effect factor based on a pipeline resting on an uneven seabed, the following load effect factors and condition loads factor applies: $\gamma_F = 1.1$, $\gamma_E = 1.3$ and $\gamma_c = 1.07$.

Hence, the design effective axial force and the design moment, then becomes (from Equation 2.1):

$$M_{Sd} = 1.1 \cdot 1.07 \cdot M_F + 1.3 \cdot M_E \quad (5.2a)$$

$$S_{Sd} = 1.1 \cdot 1.07 \cdot S_F + 1.3 \cdot S_E \quad (5.2b)$$

The moment applied in the equation above is the equivalent moment, i.e. $M_{eq} = \sqrt{M_y^2 + M_z^2}$, with the following definitions:

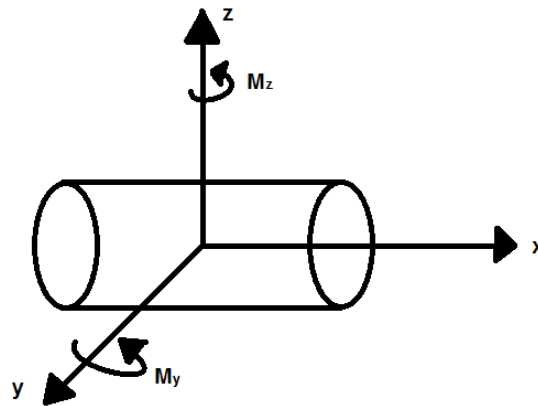


Figure 5.2: Coordinate system, moments definition

6 Results

To post-process the results, Simpost is used in order to extract the results suitable for plotting, and MatrixPlot is used to plot the results. Further, a Matlab script has been made in order to plot, among other, the tension and the equivalent moment along the route. Xpost, a 3D visualization program, has also been used in order to verify the results.

6.1 Parameter study

To obtain the worst case results, several parameters have been studied in order to ensure that the pipeline structural integrity and stability along the seabed is preserved. Changing different parameters, and observing the consequence when varying these, is done in order to find when the dynamic impact is at its highest. This is necessary in order to be able to ensure that a solution with an appropriate number of turnpoints along the route is obtained. When deciding which case is the worst, equivalent moment along the route, tension in the pipeline and the contact force between the pipe and the turnpoint has been evaluated and studied.

6.1.1 Current Direction

The first parameter that has been investigated is the current direction. Four cases of the current direction have been investigated, namely upstream, downstream and transverse current from both sides (see Figure 6.1a). The current direction was investigated with 3 turnpoints along the route. The current is applied relative to the touchdown position. As the worst touchdown position along the route was not yet determined, a touchdown position at the last turnpoint was utilized.

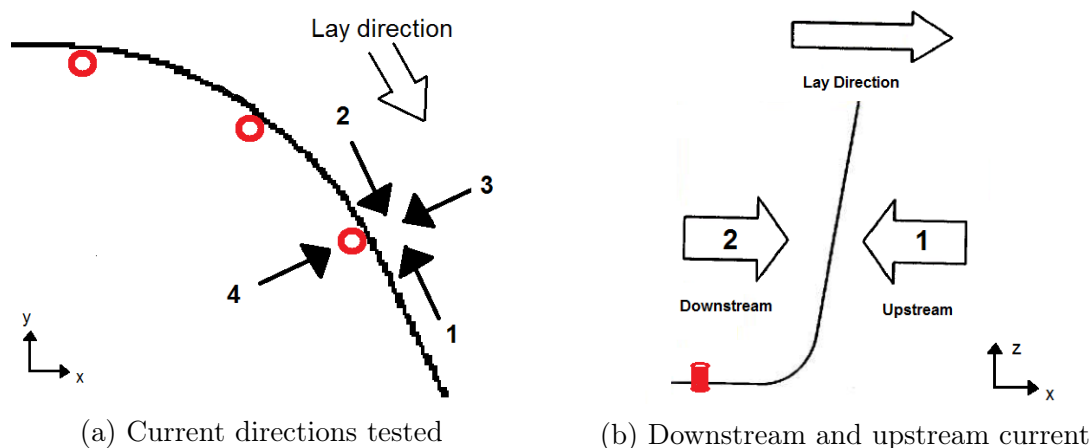


Figure 6.1: Current Cases

The results from the current parameter study clearly showed that Case 3, namely a transverse current pushing the pipe towards the turnpoint, was the most critical. This gave a bit lower axial force in the pipeline than for instance the downstream case, but a substantial higher moment and contact force between turnpoint and pipeline. The fact that the downstream case gave highest tension is consistent with what to expect. By considering Figure 6.1b, it becomes evident that the downstream case will tend to increase the tension and reduce the risk of over-bending, while upstream will reduce the tension and increase the risk of over-bending. However, the overall worst case scenario was when the current pushed the pipeline against the turnpoint.

6.1.2 Touchdown position

In the static analysis the pipe is being fed out from the laying vessel, such that the pipeline experience the whole laying process. In the dynamic analysis, only one point along the laying process is investigated. In order to obtain the solution representing the worst laying position along the route, a parameter study changing the touchdown-position of the pipe has been carried out. As for rest of the parameter studies, this was carried out with three turnpoints along the route. In total, five scenarios were tested:

1. Touchdown position: At the mid turnpoint (KP=972)
2. Touchdown position: Right after the mid turnpoint (KP=973)
3. Touchdown position: Right before the last turnpoint (KP=1145)
4. Touchdown position: At the last turnpoint (KP=1195)
5. Touchdown position: Right after the last turnpoint (KP=1197)

See Figure 6.2 for further explanation.

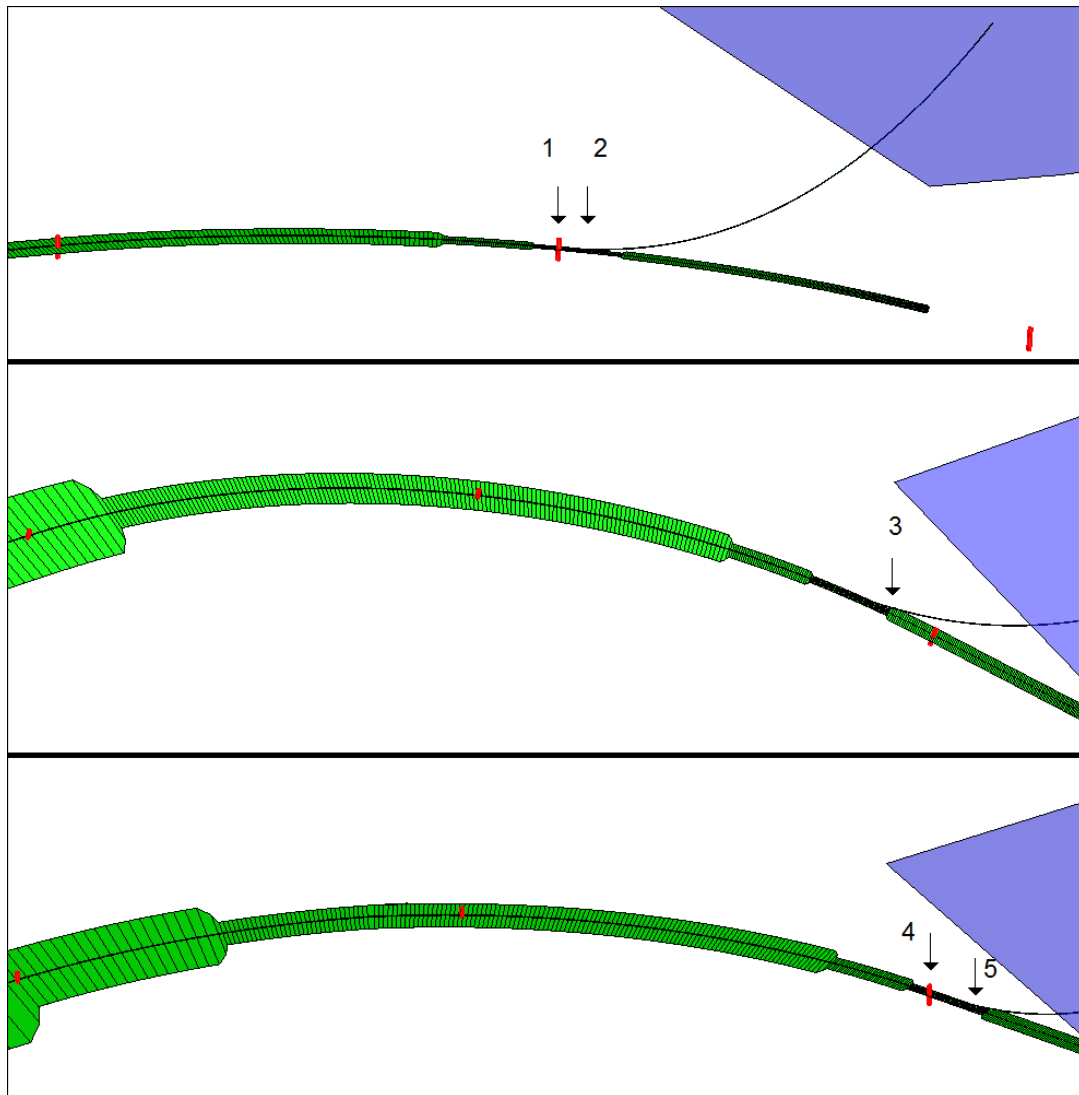


Figure 6.2: Touchdown positions investigated

It is assumed that one of these five scenarios will give the highest dynamic response along the route. The positions were chosen at, or close to, the turnpoints as it is expected that this provides the highest response and contact force between the turnpoint and the pipeline. Position 4 and 5 were chosen as the entire pipeline curvature is laid. Position 1 and 2 were chosen to see whether there was a difference at the mid turnpoint and the last turnpoint, or whether symmetry of the problem applies. Position 3, right before the last turnpoint was chosen in order to investigate the response at a position furthest away from a turnpoint-support. When the worst of these was found, the touchdown position was further moved a small distance forward and backward, in order to control how much impact a incremental change of the touchdown position influenced the result.

The results from changing the touchdown positions showed that a touchdown position right after the mid and the last turnpoint gave almost the same results. Touchdown-point at the last turnpoint gave the greatest contact force between the turnpoint and the pipe. However, the difference was minor compared to a touchdown-position right after the mid turnpoint (Case 2), which gave the highest equivalent moment. However, the difference was minor here as well. It was found appropriate and reasonable to run all the analyses with a touchdown-position just after the last turnpoint. Choosing a fixed touchdown position, equal for all the analyses, regardless of the number of turnpoints, eased the setup of the analyses and the comparison of the results. Choosing the mid turnpoint would have introduced a situation where the touchdown position in case of even number of turnpoints differs from both each other and for odd number of turnpoints.

As an incremental change of touchdown position after the last turnpoint gave insignificant impact of the results, the touchdown position was set 2 [m] after the last turnpoint.

The fact that the response at the mid and the last turnpoint provided essentially equal results, symmetry of the problem could probably be applied. In other words, it would most likely be sufficient to run the analysis only for the first two turnpoints, as the distance between the turnpoints decreases with a increased number of turnpoints installed. This would reduce the computational time required for running the analysis, because fewer elements would be introduced. However, this was not applied. If more time had been available, this could have been further examined.

6.1.3 Wave period

In order to get an idea of which wave period that will cause the highest loads on the pipeline and the turnpoints, three wave periods have been tested, namely $T_P = 7$ [s], $T_P = 11$ [s] and $T_P = 15$ [s]. It was found that a short wave period represented the worst case scenario. Hence, a wave period of $T_P = 7$ [s] have been applied in the further analyses.

6.1.4 Wave Direction

In order to find which wave direction that gives the highest load impact during the installation, 5 different wave directions have been tested. The wave directions are considered symmetrical about the longitudinal axis of the vessel. 0° is defined as following sea (Case 1), 90° is beam sea (Case 3) and 180° is head sea (Case 5), see Figure 6.3

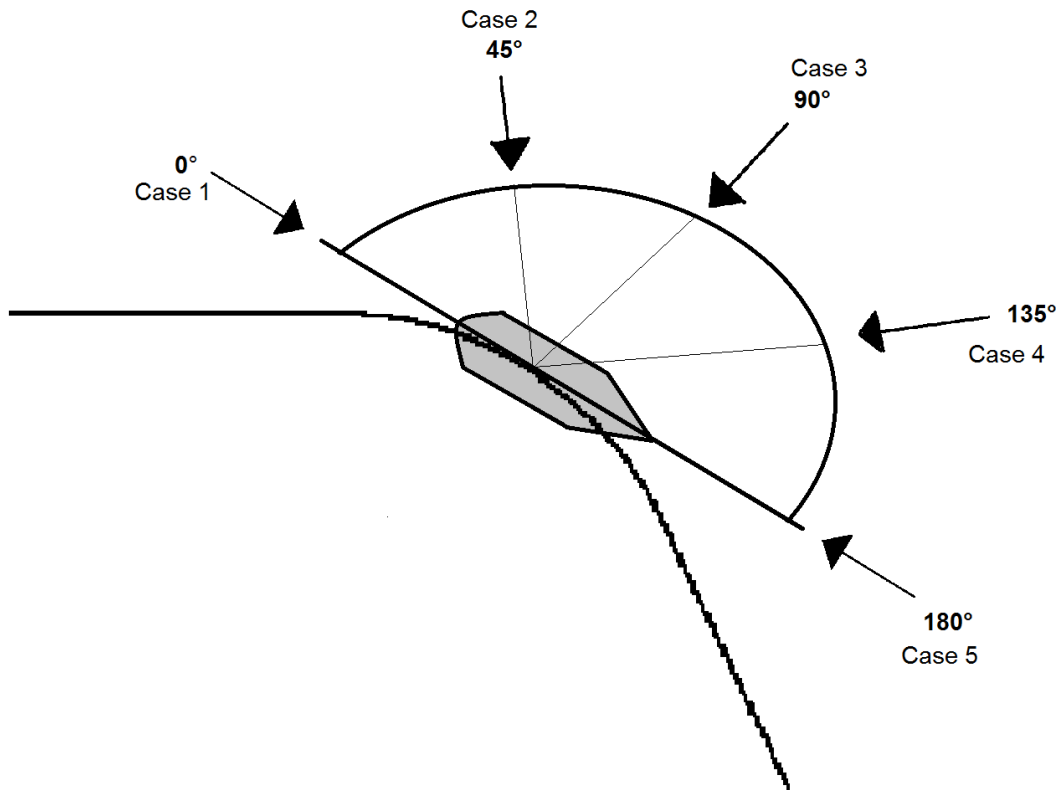


Figure 6.3: Wave directions

Case 2, i.e. a wave heading of 45° , introducing both roll and pitch motion of the vessel, gave the most critical case. A more detailed study of the wave direction, to find the ultimate worst case wave direction could have been performed, but since the purpose in this thesis is to study turnpoints interaction, not details in the vessel response, a wave heading of 45° has been utilized.

6.1.5 Summary of the parameter study

From the parameter study, the following parameters have been applied in the final analyses:

Table 6.1: Parameters applied

Parameter:	Value:	Details:
Current direction:	90°	See Figure 6.1
Touchdown position:	1197 [m]	See Figure 6.2
Wave direction:	45°	See Figure 6.3
Wave Period, T_P :	7 [s]	

6.2 Static analysis

In the static analysis the pipe is being fed out from the laying vessel and laid along a predefined route. Numerous analyses have been performed in order to see how the number of turnpoint supports along the route affects the results. The laying is carried out approximately from where the curvature starts, through the curve, and slightly past the end of the curvature. The laying process itself is carried out during 500 steps, where the results from every 50 of these were saved. Figure 6.4 below shows the final step of the laying process. The grey area is the seabed where the pipe already has been laid before the feeding analysis starts, while the green area is the seabed on which the pipe is being fed onto.

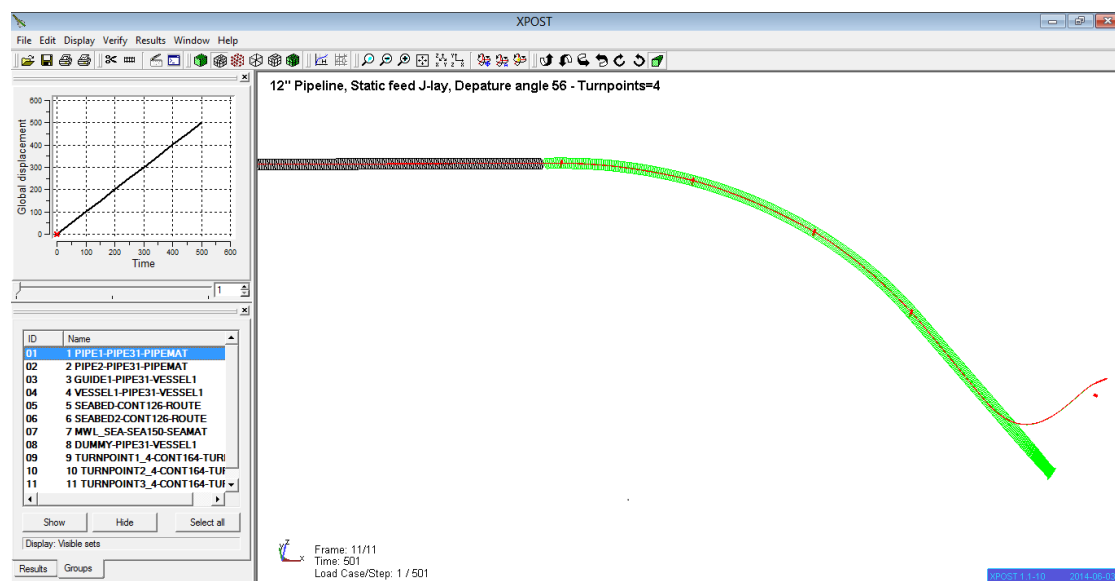


Figure 6.4: Feed analysis

6.2.1 Configuration of axial friction

The static analysis was first carried out with axial friction activated during laying. However, as the axial force distribution changed considerably with the number of turnpoints along the route (see Figure 6.5), this was assessed more carefully.

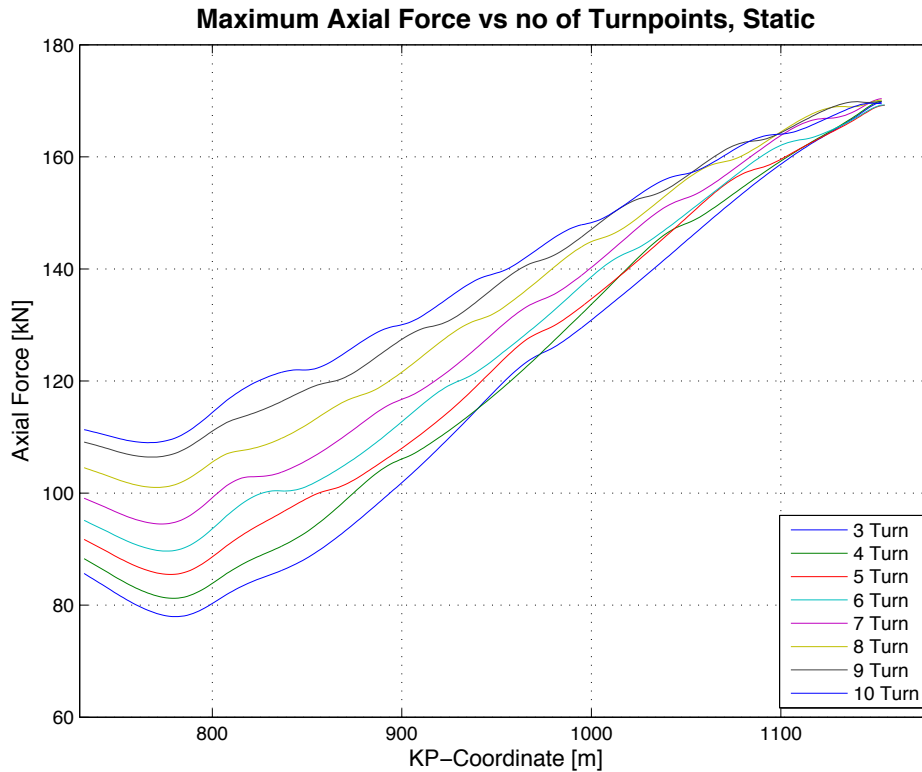
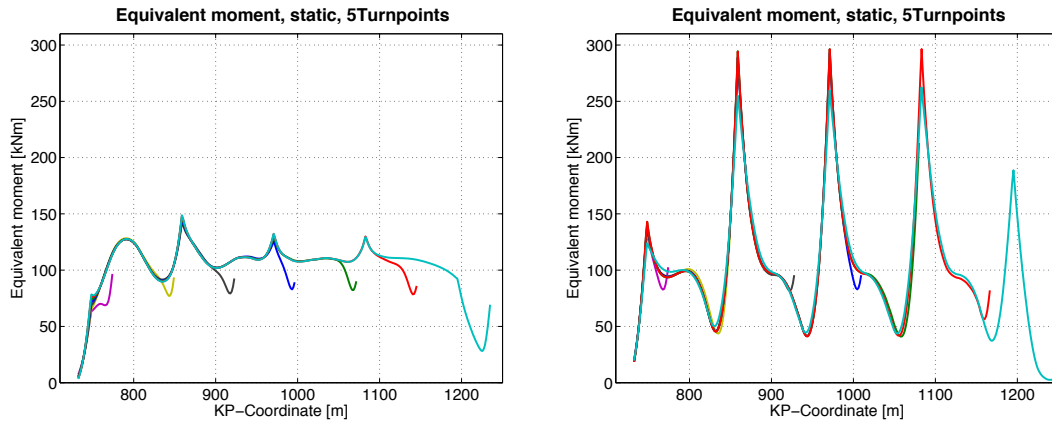


Figure 6.5: Axial force in the pipeline - with axial friction activated

The findings indicating that the axial friction increases with the number of turnpoints was considered unrealistic. Hence, the analysis was performed deactivating the axial friction during laying. This gave a more or less constant axial force in the pipe regardless of the number of turnpoints installed, which seems more realistic and physically correct. As the pipe is laid at a constant water depth, it is assumed that the departure angle and thus the tension in the pipe remains more or less unchanged during laying. Thus, deactivating axial friction is considered as a reasonable assumption.



(a) Axial friction activated (5 Turnpoints) (b) Axial friction deactivated (5 Turnpoints)

Figure 6.6: Static moment distributions with and without axial friction activated

By comparing the results with and without axial friction against each other, substantial differences is found. First, it is seen from Figure 6.5 and Figure 6.7, presented in the beginning of the next section (section 6.2.2), that the maximum tension in the pipe obviously is higher when the axial friction is activated. Then, as seen from Figure 6.6 above, the moment in the pipeline is considerably higher when axial friction is deactivated. This is due to the fact that the axial friction increases the tension in the pipeline and hence gives lower moment peaks around the turnpoints. Axial friction has therefore been turned of during laying. The reason for neglecting this is to obtain a more accurate distribution of the axial force in the pipeline. Hence, soil interaction forces will only be introduced if the pipe moves transverse relative to the planned route (Sævik and Giertsen; 2004).

6.2.2 Axial force

From the reasoning above, the static analysis has been carried out with the axial friction turned off. Feeding out the pipe from the lay vessel and laying of the pipe along the predefined route, gives an approximately constant axial force distribution in the pipe. The tension is also almost unaffected by the number of turnpoints, see Figure 6.7:

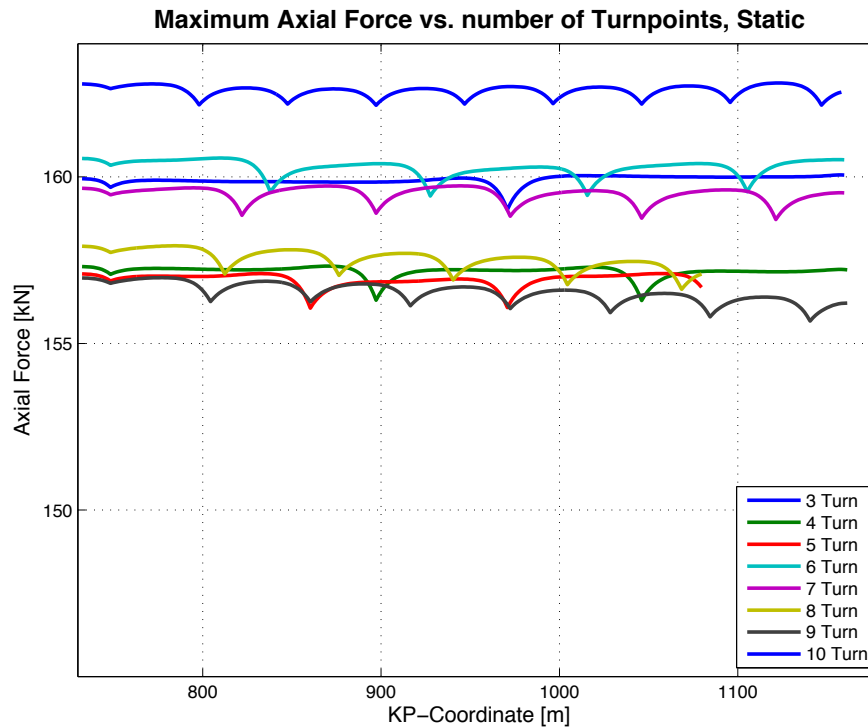


Figure 6.7: Axial force in the pipeline vs number of turnpoints, Static results

The above given plot represents the tension in the pipe at the seabed, in the curved pipeline-section. The plot represents the maximal tension obtained in the pipe during the laying of the pipeline, which is the reason why every curve does not have the same length. The figure shows that the tension in the pipeline is more or less the same, regardless of the number of turnpoints along the route. This seems reasonable as there is no friction activated in the axial direction, which again is based on the approximation that the pipe is laid at a constant water depth.

6.2.3 Moments

When it comes to the equivalent moment along the curved section, the static results (see Figure 6.8) show that the maximum moment gets reduced with the number of turnpoints along the route. The graphs show that the moments are flattening out as number of turnpoints increase, which seems reasonable as the distances between the supports are reduced. The reason why the graphs are multi-colored, is that the results from laying the pipeline in curve has been displayed in 11 steps, where every step is included in the plots below.

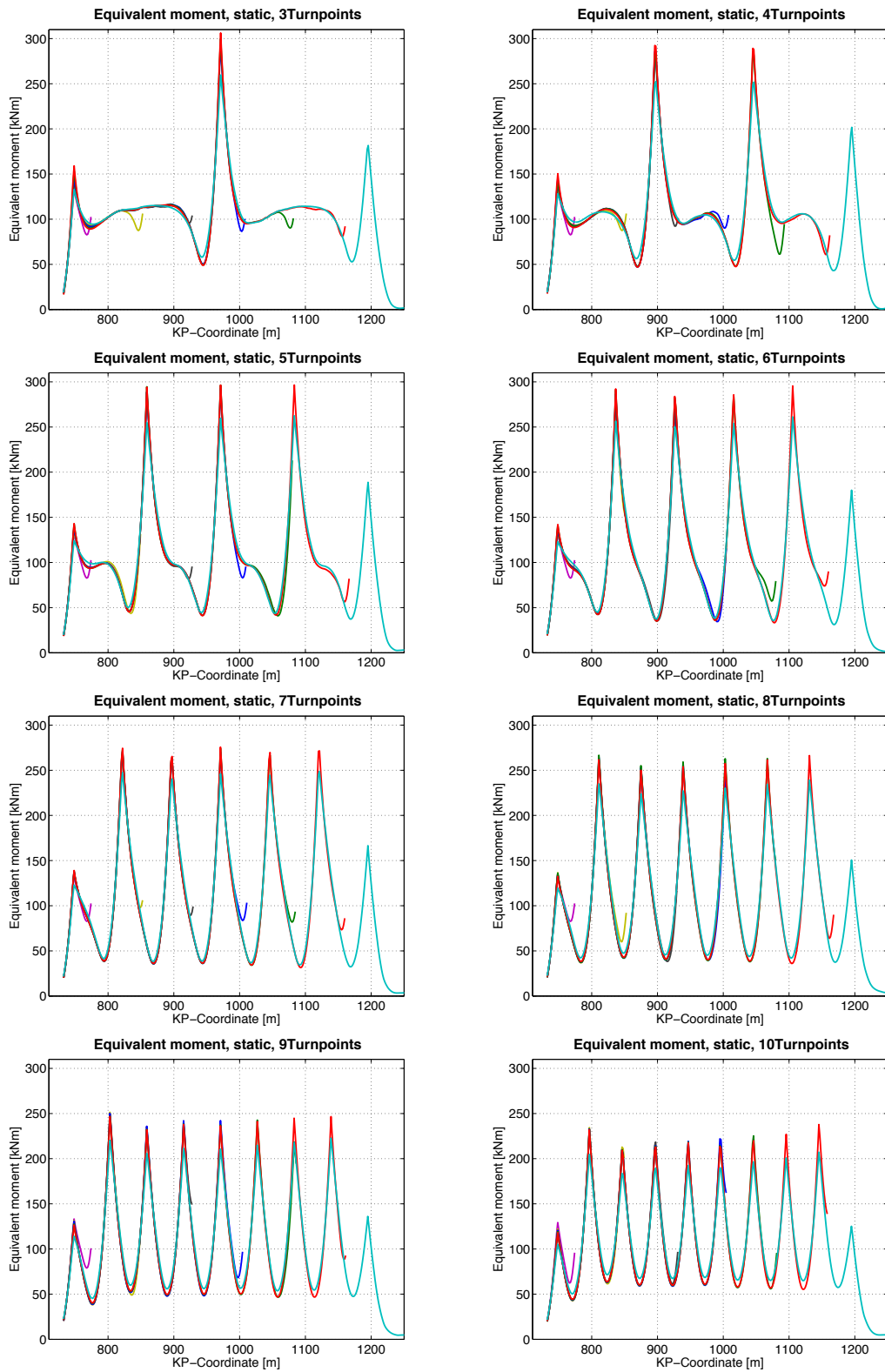


Figure 6.8: Equivalent moment in pipeline vs number of turnpoints, Static results

6.2.4 Contact force

When it comes to the contact force between the turnpoints and the pipeline, it can be seen from Figure 6.9 below that the contact force decreases as more turnpoints are installed. This is of course explained by the fact that more supports can resist the forces acting on the pipeline.

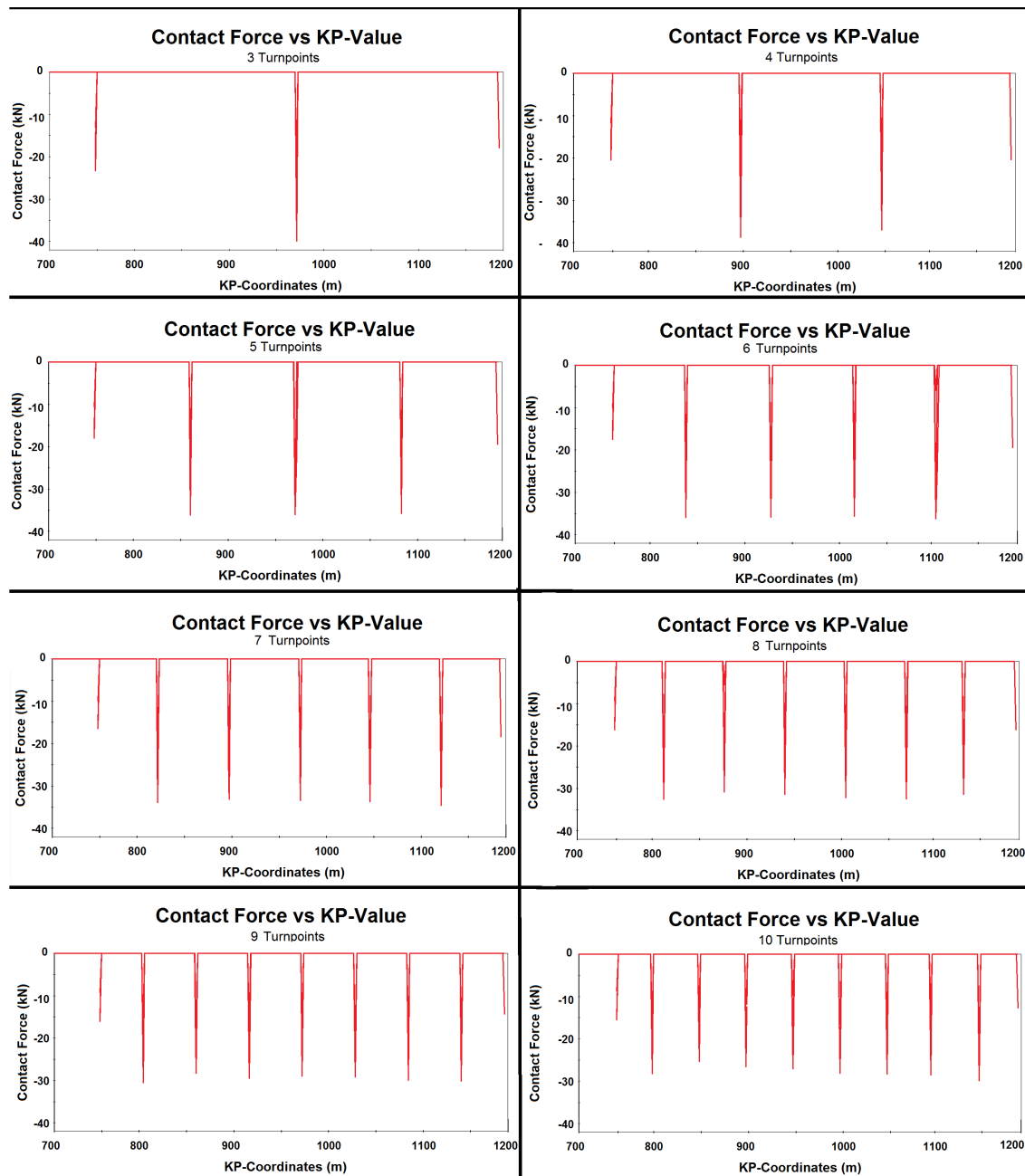


Figure 6.9: Contact force vs number of turnpoints, Static results

It is noted that the contact force is symmetrically distributed over the pipeline route. Based on this, symmetry of the problem could thereby be exploited, in order to reduce the size of the model. The assumption made in the method for turnpoint calculations applied by Subsea 7 today, corresponds to what is found here. The assumption states that the contact force can be calculated by assuming that the force acting between the turnpoints is smeared over the arc length. As the results from Figure 6.9 indicates, the contact force at the end turnpoints is about half the size of the force acting at the turnpoints in between, which is in accordance with the assumption made. This may indicate that the end turnpoints can be installed with lower geotechnical capacity than for the rest of the turnpoints.

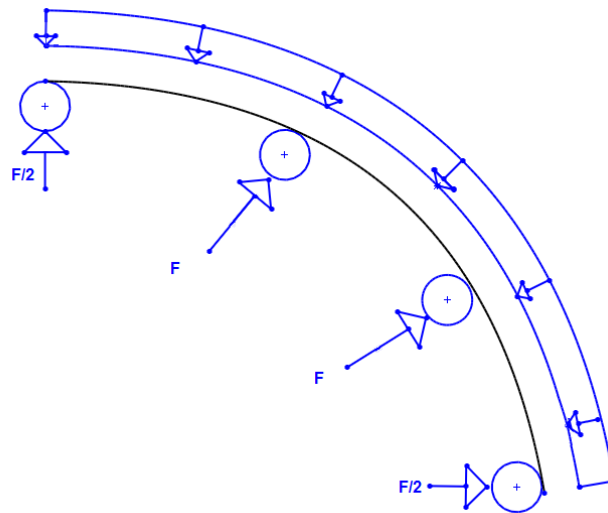


Figure 6.10: Assumed model applied by Subsea 7 - uniformly distributed load between the turnpoints

Table 6.2: Static results

Turnpoints:	Max Axial force: [kN]	Max Moment: [kNm]	Max Contact force: [kN]
3	160.0	306.2	40.1
4	157.3	292.4	38.9
5	157.1	296.5	36.3
6	160.6	295.4	36.4
7	159.7	275.7	34.7
8	157.9	266.6	32.7
9	157.1	251.3	30.7
10	162.8	237.8	30.0

Table 6.2 summarize the static results. It shows that the tension in the pipeline remains more or less unaffected by the number of turnpoints installed. The contact force decreases with the number of turnpoints, as the force gets distributed over more supports. However, since the contact force is of a much higher order when the dynamics are applied to the system, not much focus has been directed to the contact force from the static analysis. When it comes to the equivalent moments obtained, it is seen from the Table 6.2, as in Figure 6.8, that the moments are flattening out as the number of turnpoints increase.

6.3 Dynamic analysis

In the dynamic analysis, a 3 hour sea state described by the Jonswap spectrum with a significant wave height of 2.5 [m] has been carried out. The waves and the current have been applied 45° from behind and 90° from the side respectively, in accordance with the findings from the parameter studies. In addition, the wave period utilized has a peak period of 7 [s], and the touchdown position of the pipeline is right behind the last turnpoint.

6.3.1 Representation of the sea state

Since the dynamic analyses were really time consuming, only one dynamic analysis with a complete 3-hour sea state has been carried out. This was carried out with 3 turnpoints along the route. In fact, to spare even more time, the 3-hour sea state was split into three 1-hour analyses that overlapped each other. From these analyses, the most critical time during the three hour sea state was obtained. Then, all the other analyses were set up with a short time-interval around that critical time-period. This was done because the most critical response would occur at the same time during a sea state with the same seed number.

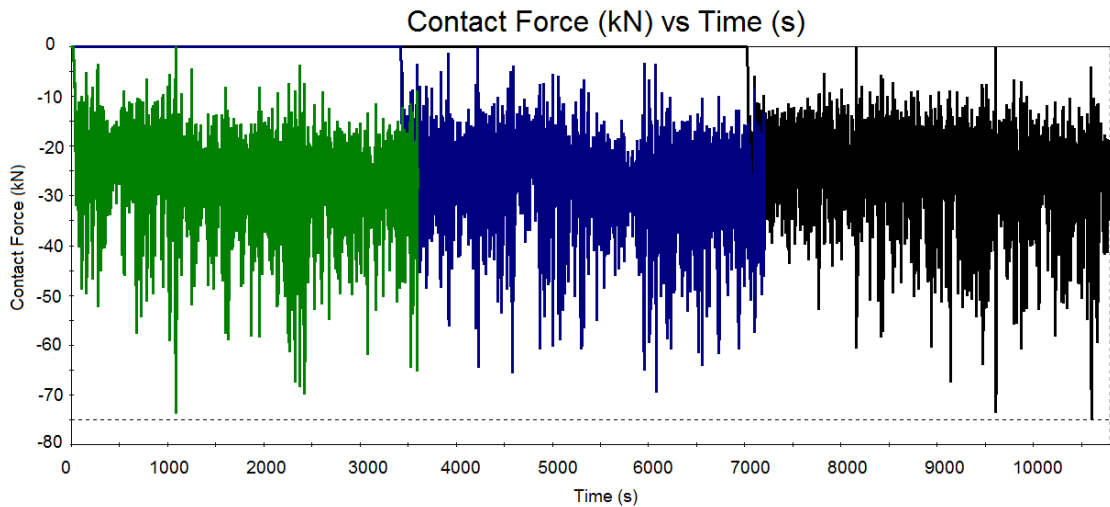


Figure 6.11: Response during a 3 hour sea state

From Figure 6.11 it should have been found that the most critical time occurred after about 10600 [s]. However, as there was an error in the first run of the third hour sea state, it was assumed that the worst case occurred at the peak around 1080 [s]. Therefore, a time interval between 900 [s] and 1200 [s] has been applied in the other analyses. As all analyses were run in this interval before discovering that an even worse response occurs after 10600 [s], this was not changed. However, the difference is not of a significant magnitude and since the main goal in this thesis is to compare the effect of turnpoints installed, the error introduced was accepted.

During the process of running the dynamic analyses it was suggested to only run all the dynamic analyses with a one hour sea state, due to the computational time of these analyses. When it was discovered that a short time interval could represent the entire sea state, it was decided to test for a complete 3 hour sea state instead. The short interval was then set up around the most critical time period of the 3 hour sea state. However, in the end it may appear that the results in fact are based on a bit less than a 3 hour sea state, due to the error described above.

To control that it is sufficient to only run the analyses in the interval of [900s, 1200s], the results obtained from the short analysis is plotted and compared against the full analysis, within the same time interval:

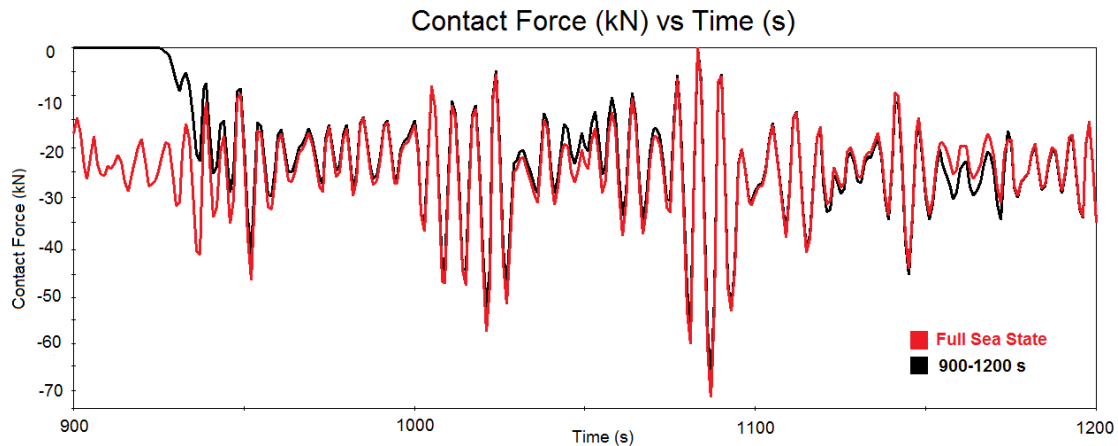


Figure 6.12: Comparison of full vs a short interval representing the same sea state

The results clearly show that the short interval represents the full analysis after a short initial start-up phase. The reason why it takes some time before the graphs overlap is that it takes some time to include the waves and the currents. The pressure and gravity in the system is first included, then waves and current are gradually introduced. However, when reaching the critical time, the results seem to be consistent with each other, but perhaps with a slightly smaller response in the short interval representing the full analysis. However, the difference is considered insignificant. Based on this reasoning, a time interval between [900s, 1200s] has been applied for all the dynamic analyses, in order to represent the full 3 hour sea state.

6.3.2 Axial force

When the representation of the 3-hour sea state had been established, the analysis comparing the dynamic results against the number of turnpoints was carried out. The results from the maximum axial force obtained in the pipeline during the sea state is plotted in Figure 6.13 against the KP-value of the pipeline. The different curves represents different numbers of turnpoints installed along the route:

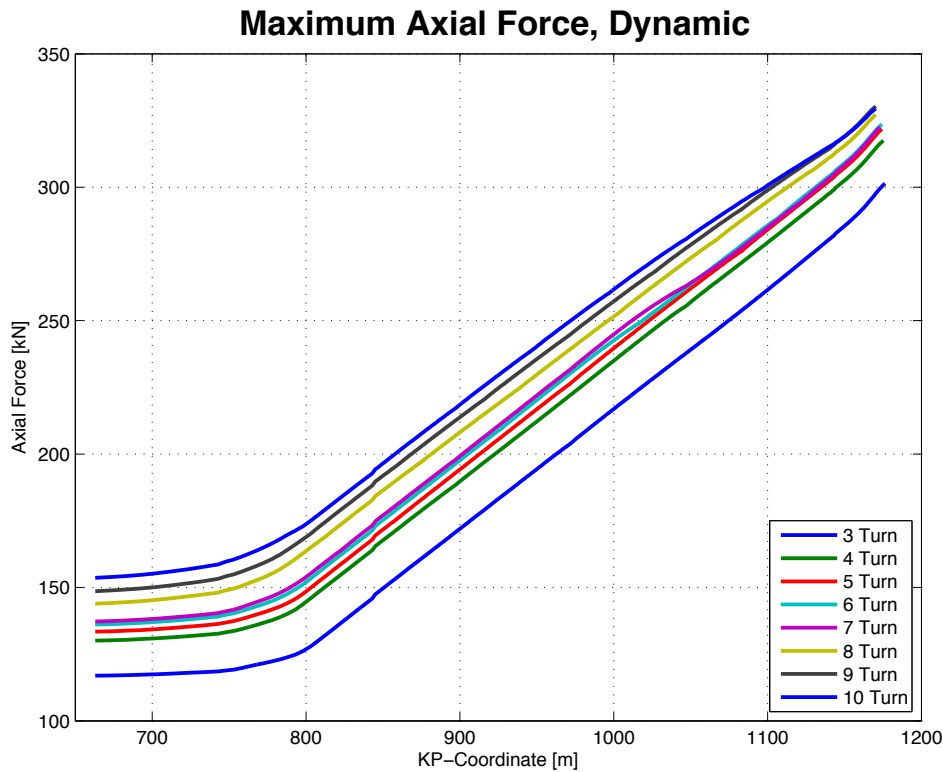


Figure 6.13: Axial force in the pipeline vs number of turnpoints, Dynamic results

It can be seen from the plot that the turnpoints increase the tension in the pipe, i.e. the pipe gets stiffer. When few turnpoints are installed along the curvature, it can be seen from the pipeline configuration that the pipe is stretched and straighten between the turnpoints. As the number of supports increase, this effect is reduced and the curve becomes more smooth. This implies that the resistance against movement in the touchdown-position becomes larger and less pipe is pulled out of the curve, which leads to an increase in the dynamic tension. In other words, the system gets stiffer. From this reasoning, the results seem to be reasonable.

6.3.3 Moments

The results of the equivalent moments obtained in the dynamic analyses correspond to findings from the static results, namely that the moments are reduced as the number of turnpoints along the route increases. The results presented in Figure 6.14 below represent the maximum moment obtained during the 3-hour sea state:

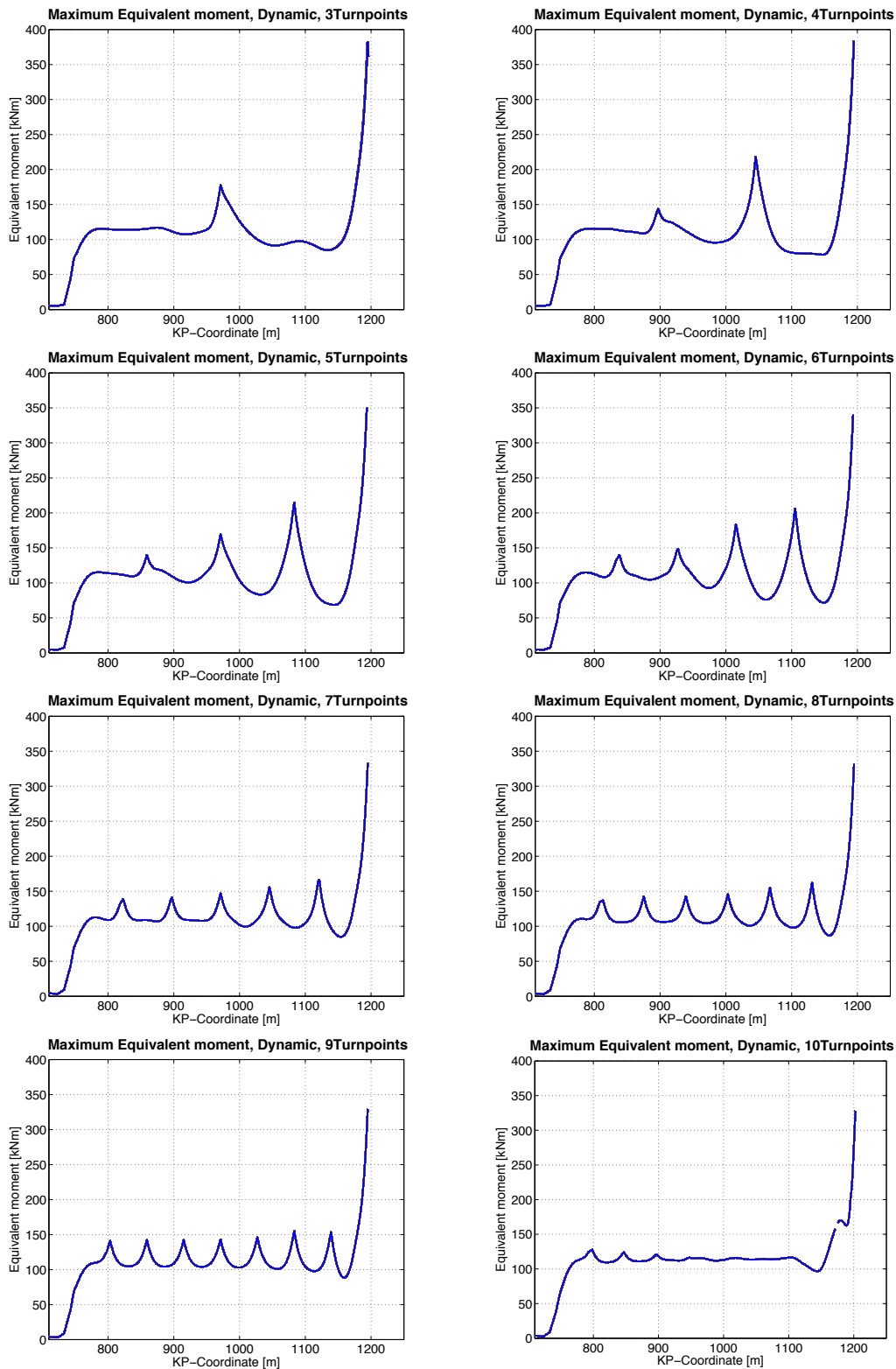


Figure 6.14: Equivalent moment in pipeline vs number of turnpoints, Dynamic results

6.3.4 Contact force

The contact force between the pipeline and the turnpoints is essentially unchanged, regardless of the number of turnpoints along the route. This can be seen from Figure 6.15. The figure illustrates the contact force between the pipeline and the last turnpoint at the most critical time period during the 3 hour sea state. The contact force will be highest in this turnpoint due to the chosen touchdown position investigated.

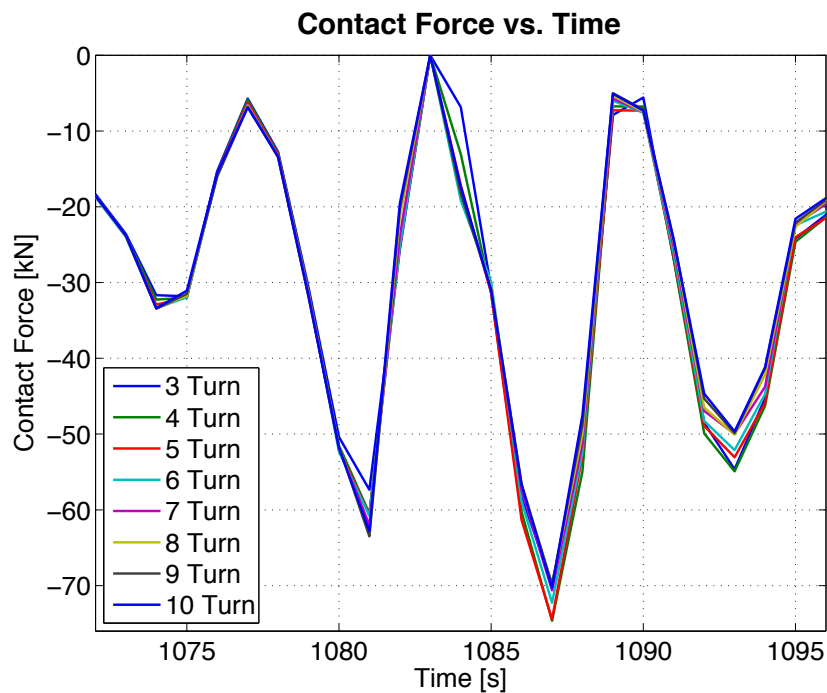


Figure 6.15: Contact force at the last turnpoint, Dynamic results, 3-10 turnpoints

From Figure 6.15 above, it can be seen that the greatest contact force will occur after 1087 [s]. From the investigation of deciding which time interval to run the dynamic analysis, in order to represent the full 3-hour sea state, the same was found to be the time at which the response would be at its highest. As the most significant contact force is found after 1087 [s] into the analysis, the contact forces have been plotted at this time against the KP-value of the pipe in Figure 6.16 below. This is done in order to easier see how the contact force varies against the number of turnpoints installed:

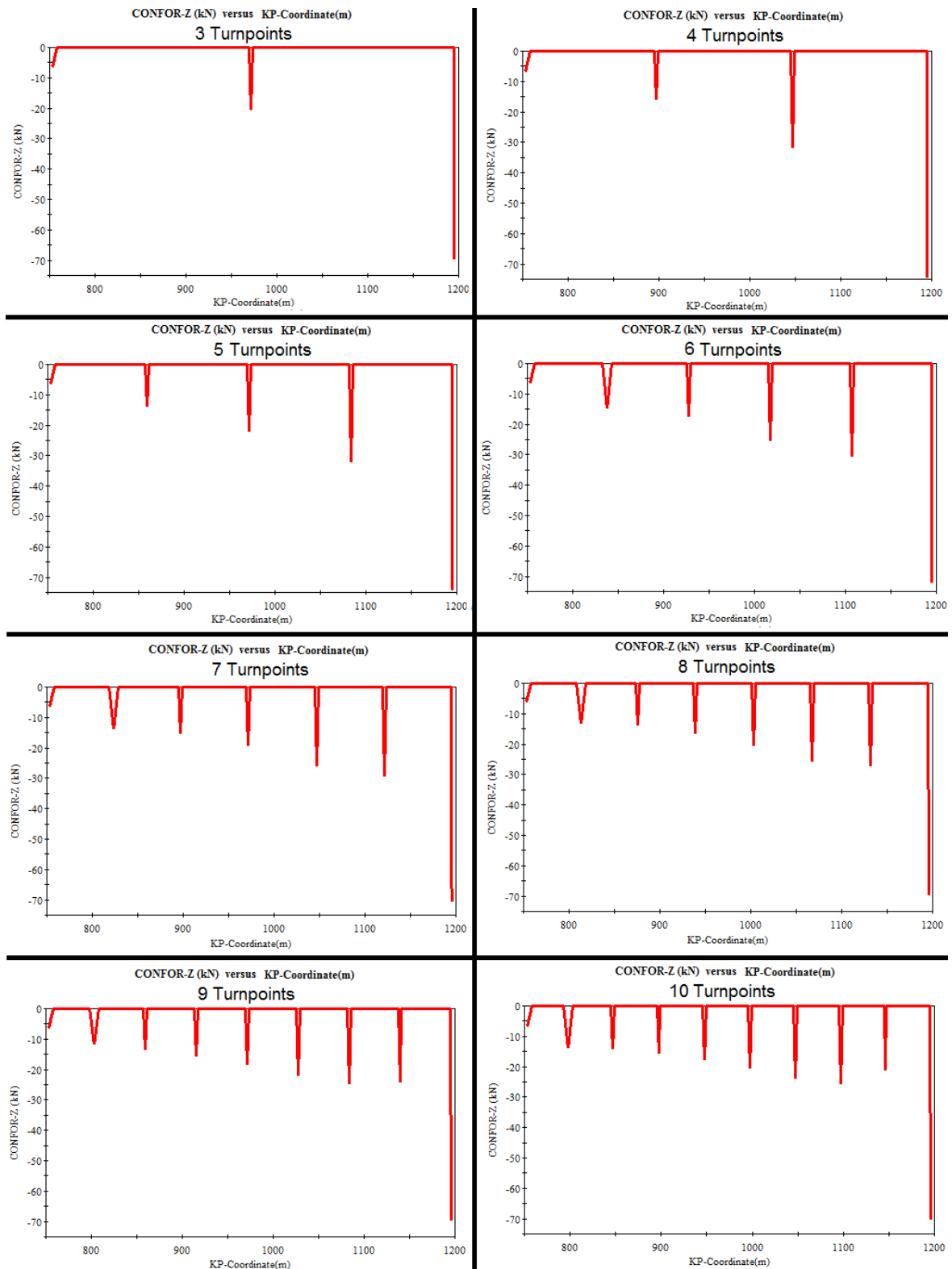


Figure 6.16: Contact force against KP-value at $t=1087$ s, for 3-10 turnpoints

As it may be difficult to see the results clearly from the plots above, a table summarizing the dynamic results is included below:

Table 6.3: Dynamic results

Turnpoints:	Max Axial force: [kN]	Max Moment: [kNm]	Max Contact force: [kN]
3	301.4	382.5	69.7
4	317.5	383.9	74.6
5	321.8	350.1	74.4
6	323.6	340.0	72.3
7	322.5	333.0	70.6
8	327.2	332.1	69.9
9	330.3	329.4	69.9
10	329.5	328.1	70.3

The results presented in Table 6.2 show that the equivalent moments obtained from the dynamic analyses decrease with more supports installed along the pipeline route. As expected, this corresponds to what was found in the static results. The dynamic tension in the pipeline, on the other hand, increases with an increased number of turnpoints installed. In other words, the system gets stiffer as more turnpoints are included. When it comes to the contact force between the turnpoints and the pipeline, the lowest interaction is actually obtained when only 3 turnpoints are installed. In case of installing 4 or 5 turnpoints, the interaction forces are considerably higher, while the force becomes somewhat lower when the number of turnpoints exceeds this amount.

The fact that only three turnpoints along the route provides the lowest contact force seem odd. The most intuitive thought is that more turnpoints would give lower contact force at each turnpoint, as the force is more distributed and can be absorbed by additional supports, which was the case in the static analyses. However, by considering the dynamic tension in the pipeline, an explanation might be found. As mentioned, more turnpoints results in higher dynamic tension in the pipeline, which can be seen from both the table above and Figure 6.13. Hence, as the stiffness of the system increases, the dynamic response will increase. From this reasoning, the increase in contact force can be explained. However, as the contact force decreases when 4 or more turnpoints are installed, the effect of installing additional supports becomes superior to the increase in tension.

6.4 Local Buckling check

Based on the dynamic and static results, a local buckling control must be performed. The results obtained are included in Table 6.4:

Table 6.4: Control of Local Buckling

Turnpoints:	Max Axial force: [kN]		Max Moment: [kNm]		Local Buckling Utilization*: [-]
	Static	Dynamic	Static	Dynamic	
3	160.0	301.4	306.2	382.5	1.1016
4	157.3	317.5	292.4	383.9	1.0655
5	157.1	321.8	296.5	350.1	0.9695
6	160.6	323.6	295.4	340.0	0.9354
7	159.7	322.5	275.7	333.0	0.8608
8	157.9	327.2	266.6	332.1	0.8343
9	157.1	330.3	251.3	329.4	0.7871
10	162.8	329.5	237.8	328.1	0.1235

* Calculated from equation 2.16, in accordance with DNV (2012).

The results in Table 6.4 show that installing 3 or 4 turnpoints along the route will not satisfy the local buckling criteria in DNV (2012), described in Equation 2.16. The criteria states that the local buckling utilization calculated, based on the functional and environmental tensions and moments in the pipeline, is not allowed to exceed 1.0. This criteria is not satisfied until 5 or more turnpoints are installed. However, before any conclusions can be made, the effect of turnpoint tolerance must be considered.

Changing the static analyses from activating to deactivating the axial friction during laying, actually led to the difference in case of accepting to discard 3 and 4 turnpoints along the route. The fact that the static tension in the pipe was lowered when ignoring the axial friction, gave rise to an increase in the static moment. The substantial increase of moment amounted the difference from meeting the requirement to not fulfil the local buckling criteria for 3 and 4 turnpoints. This shows the importance of assessing the results before accepting them.

6.5 Turnpoint tolerance

The turnpoints are installed with a certain turnpoint tolerance, both longitudinal and perpendicular to the route. The turnpoints are assumed to be installed with a lateral tolerance of 0.5 [m] and 3.0 [m] in the longitudinal direction, in accordance with information provided by Nessmo (2014). In order to include the turnpoint tolerance in the installation considerations, separate analyses have been carried out. However, the longitudinal tolerance of 3 [m] has been neglected, as it has been assumed that this distance is insignificant compared to the distance between the turnpoints.

Analyses of the turnpoint tolerance have been conducted by implementing 5, 6 and 7 turnpoints along the route. Four cases have been carried out, as they are believed to be potential worst case scenarios. The cases tested are illustrated in Figure 6.17 below:

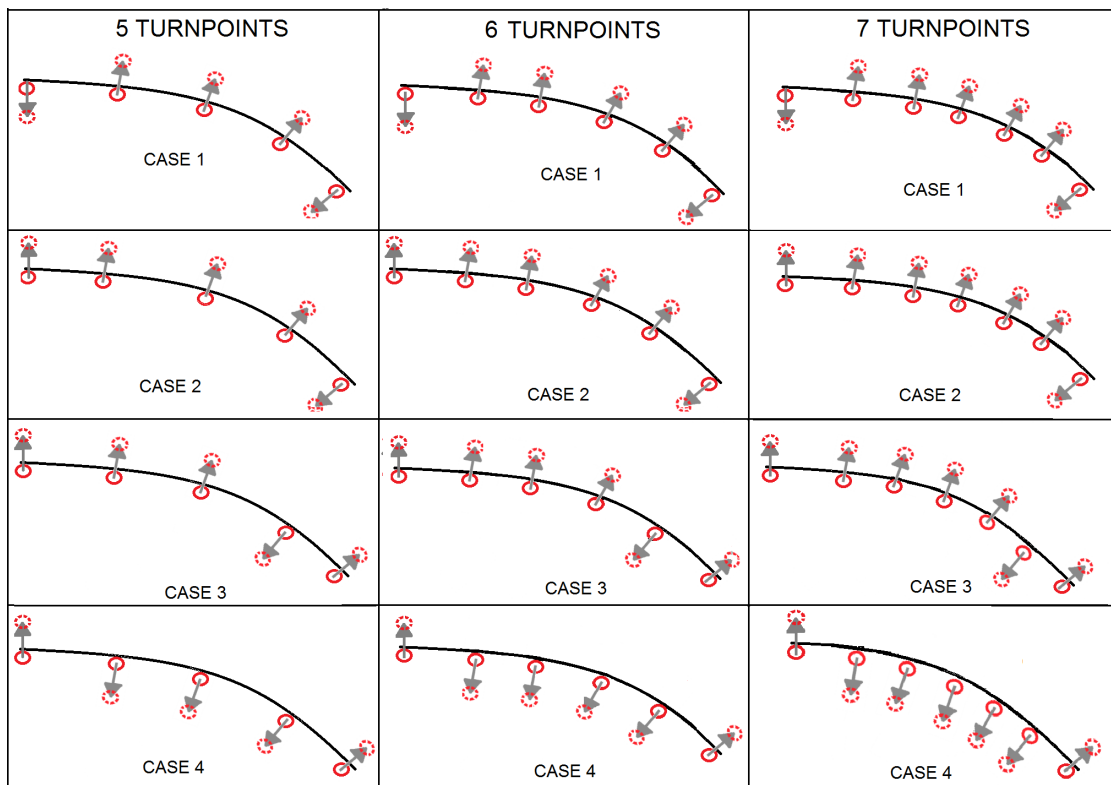
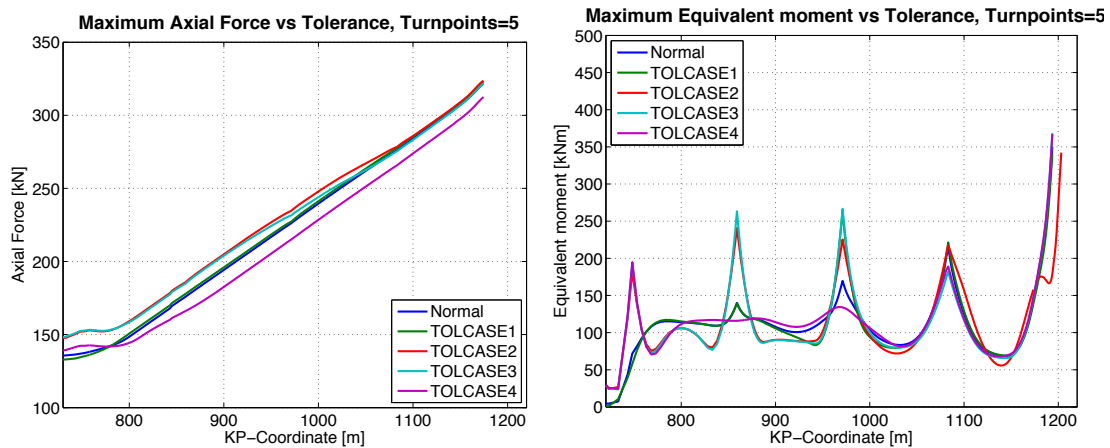


Figure 6.17: Turnpoint tolerance cases investigated, 5, 6 and 7 Turnpoints

The arrows in Figure 6.17 represents the worst case positions, i.e. the turnpoints are moved 0.5 [m] compared to the ideal position, in the lateral direction, indi-

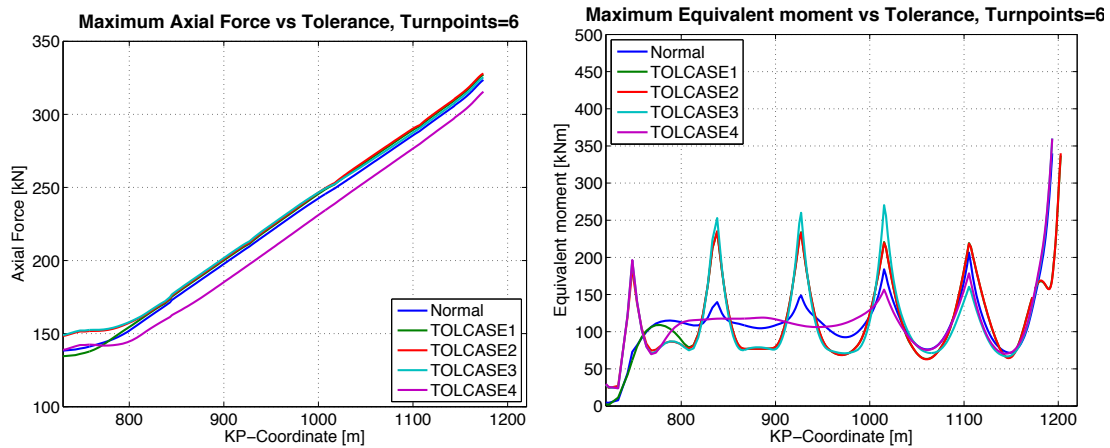
cated by the arrows. Case 1 represents a scenario where the overall curvature gets greater, i.e. the curve radius becomes even lower. In Case 2, there will be an abrupt curve change between the second last and the last turnpoint. Case 3 was chosen since this case is believed to entail a loss of one turnpoint, i.e. no contact between the pipe and the second last turnpoint. Case 4 is somewhat the opposite scenario of Case 1 and the pipe is here allowed to move inwards in the middle, such that the pipe gets more straightened out.

Below, the results obtained for 5 and 6 turnpoints are presented in Figure 6.18, Figure 6.19 and Table 6.5:



(a) Axial force vs tolerance cases (b) Equivalent moment vs. tolerance cases

Figure 6.18: Impact from different tolerance cases, 5 turnpoints



(a) Axial force vs tolerance cases (b) Equivalent moment vs. tolerance cases

Figure 6.19: Impact from different tolerance cases, 6 turnpoints

Table 6.5: Results from the worst case turnpoint positions

Turnpoints:	Contact Force [kN]			
	Case 1	Case 2	Case 3	Case 4
5	72.5	72.5	79.8	76.7
6	69.3	69.6	78.1	75.7

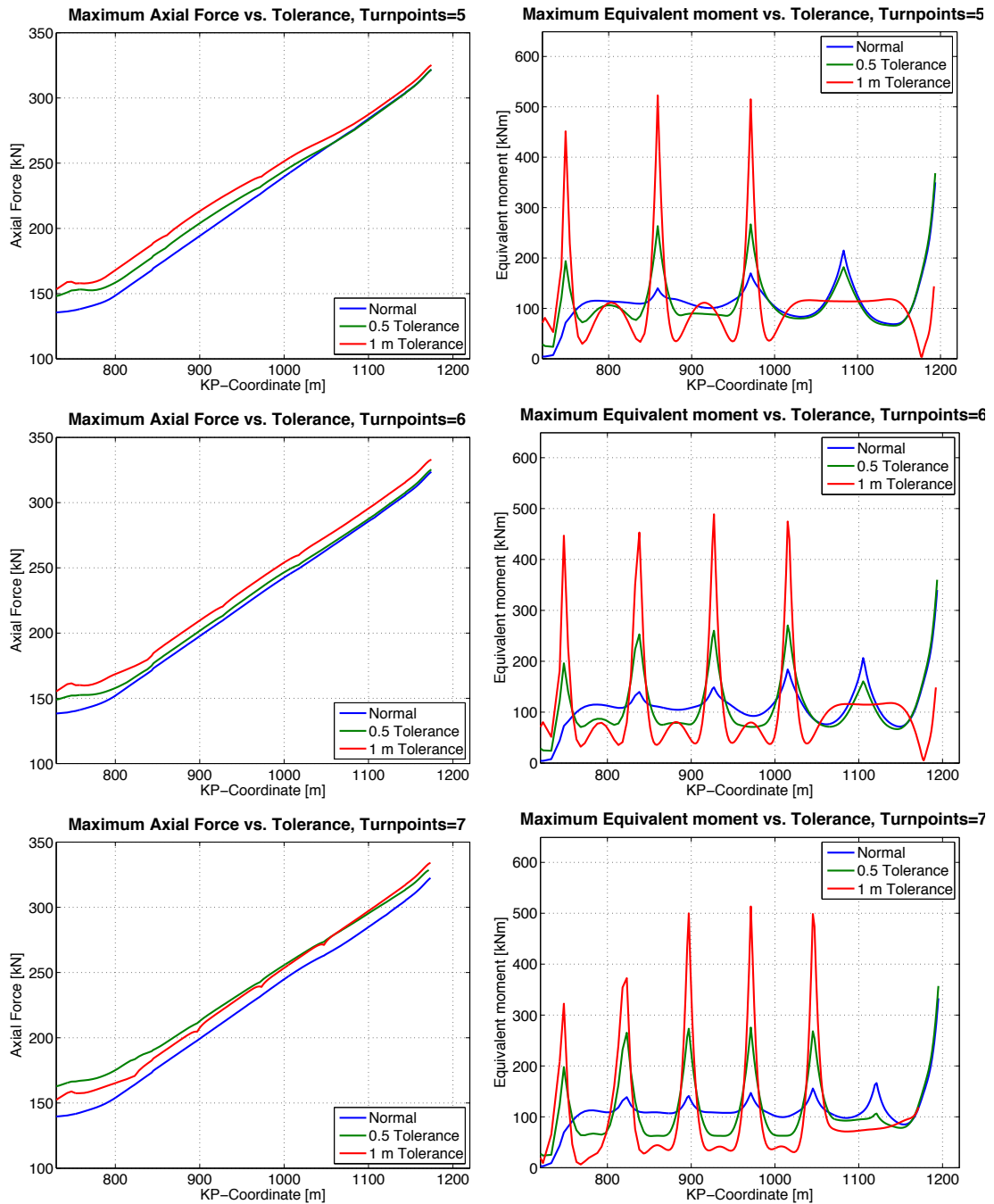
The results obtained clearly indicates that it is Case 3 that represent the worst case. This case gives both the highest moment and the greatest contact force between the turnpoints and the pipe. Here, all turnpoints are placed 0.5 [m] outwards, except the second last one, which is placed 0.5 [m] inwards. This results in a "loss" of the second last turnpoint, i.e. no contact between the pipeline and this turnpoint. Based on this, only Case 3 has been tested when 7 turnpoints are installed along the route. The results obtained from the worst case turnpoints positions (Case 3) are summarized and compared against the number of turnpoints in Table 6.6 below:

Table 6.6: Results from the worst case turnpoint position

Turnpoints:	Max Axial force: [kN]	Max Moment: [kNm]	Max Contact force: [kN]	Local Buckling Utilization [-]
5	321.7	368.3	79.8	1.0268
6	325.3	360.1	78.1	0.9981
7	328.5	357.1	78.0	0.9333

It can be seen that when considering a worst case scenario for 5 turnpoints installed with a 0.5 [m] turnpoint tolerance, the local buckling criteria is not fulfilled. This implies that 6 or more turnpoints has to be installed, as 6 turnpoints barely satisfies the local buckling criteria. The turnpoint tolerance is hence decisive in the manner that an additional turnpoint has to be installed in order to preserve the structural integrity of the pipe, in terms of local buckling. The contact force between the pipe and the turnpoints is also affected and increased as the turnpoints are installed with the above mentioned tolerance. However, the contact force never exceeds 80 [kN], which is the turnpoint capacity. In other words, it is the local buckling criteria that is the restrictive factor.

In order to get an idea of how the turnpoint tolerance affects the results, analyses where the lateral tolerance have been increased to 1 [m] has been conducted. The following results are obtained:



(a) Axial force vs turnpoint tolerance

(b) Moment vs. turnpoint tolerance

Figure 6.20: Effect of turnpoint tolerance

These results show that the impact on the pipe is more significant when the tolerance is increased to 1 [m] in the lateral direction. There are considerable changes in the moments, when the turnpoint tolerance is taken into account. When no tolerance is applied, it is apparent that the pipe experiences the greatest moment around the last turnpoint. However, when turnpoint tolerance is included, there are less differences in the moment peaks around the last and the other turnpoints. Actually, with a high tolerance, it is found that the greatest moment does not occur near the last turnpoint. From this, since the decision of how many turnpoints to be installed eventually needs to take tolerance into consideration, symmetry of the problem should not be utilized, as the most critical moment can be overlooked.

The tension in the pipe is barely affected. However, the equivalent moment is considerably higher. From this, a graph has been plotted to illustrate how the local buckling utilization is changed with the turnpoint tolerance:

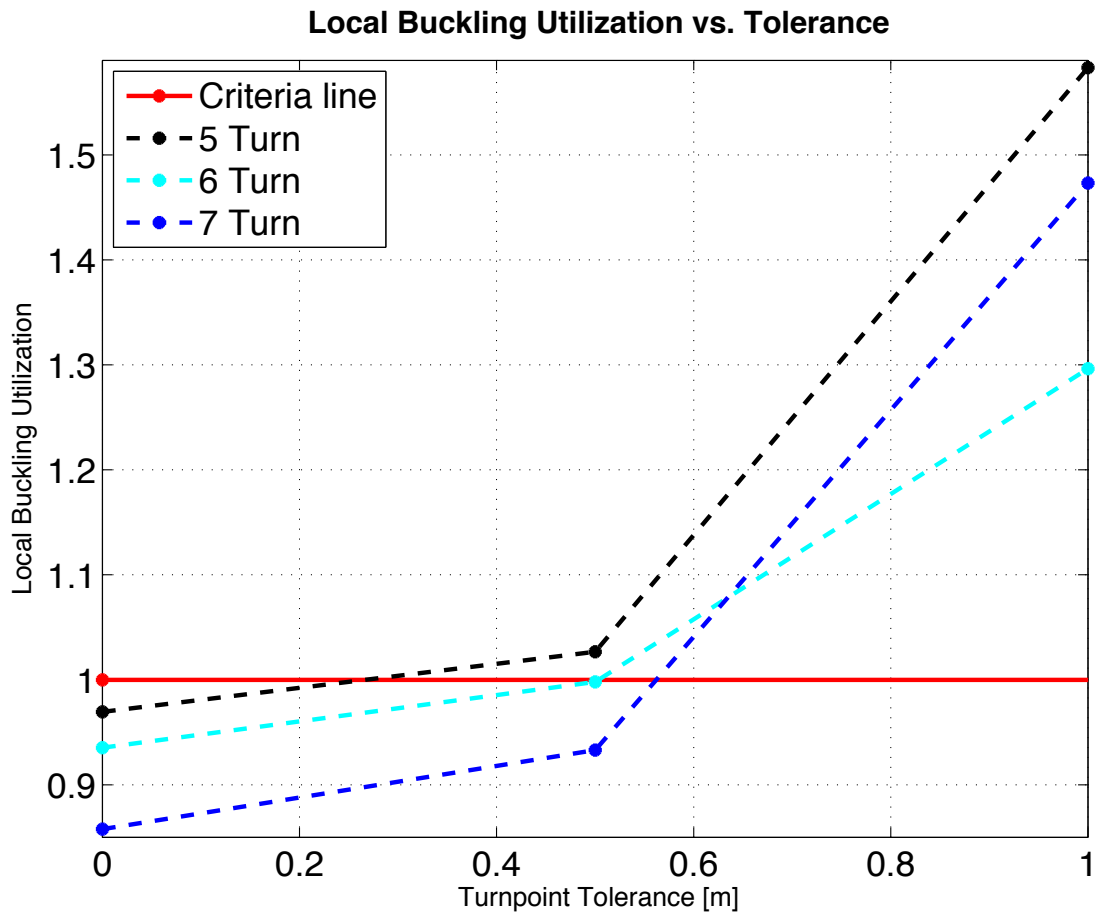


Figure 6.21: Local buckling utilization as a function of turnpoint tolerance

Figure 6.21 is based upon the local buckling utilization calculated when the turnpoints are installed with 0, 0.5 [m] and 1 [m] lateral tolerance. From this, it can be seen that not even 7 turnpoints along the route can assure that the local buckling criteria gets fulfilled when the lateral tolerance is as high as 1 [m]. It is noted that the utilization-line for 7 turnpoints actually intersects the utilization line for 6 turnpoints when the tolerance exceeds 0.5 [m]. This is somewhat puzzling, given that it differ from the other results. However, it may indicate that increased tolerance gives higher impact when many turnpoints are installed. One possible explanation could be that installing many turnpoints provides less flexibility in the system. Hence, the tolerance effects get an increased local influence. With fewer turnpoints installed, the effect of the installation tolerance gets distributed over longer sections, as there are a smaller number of turnpoints defining the geometry.

When it comes to the maximum contact force obtained between the pipe and the turnpoints, the following has been obtained:

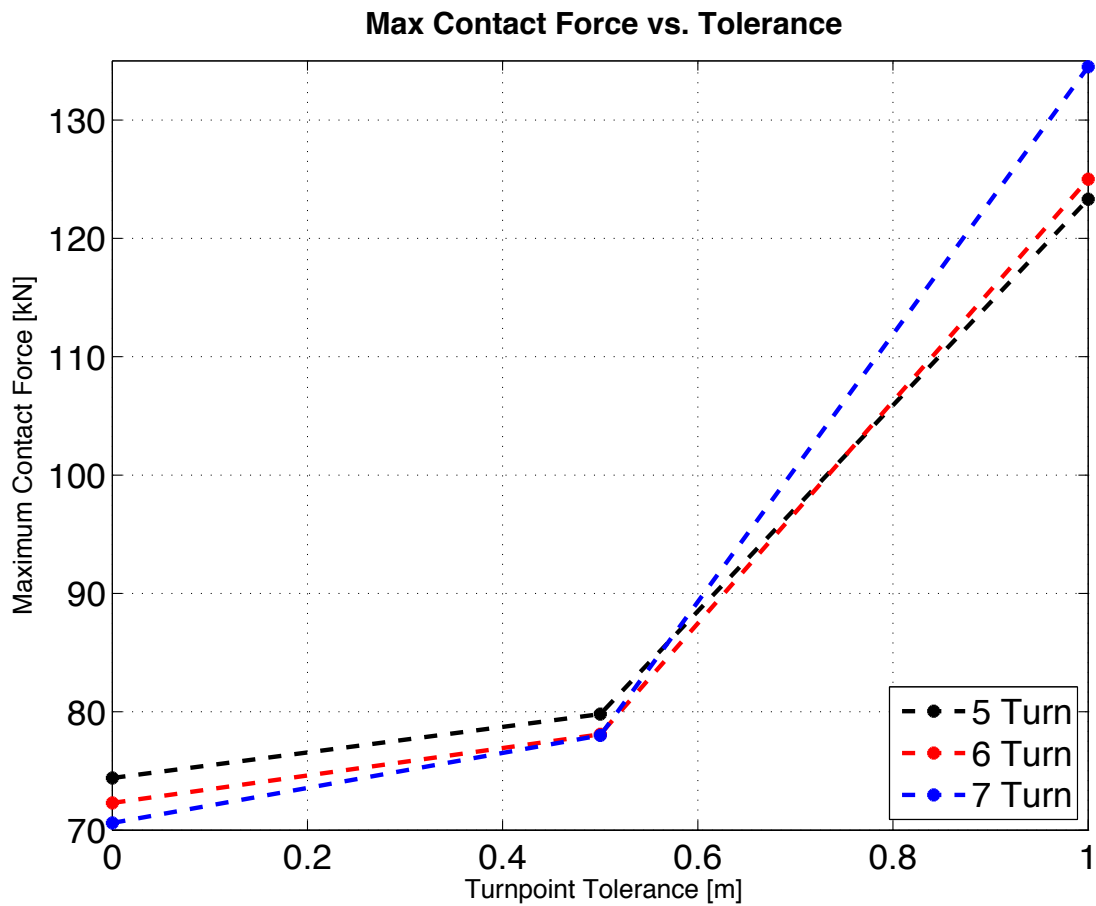


Figure 6.22: Contact force as a function of turnpoint tolerance

Figure 6.22 above can be explained by considering the axial force in the pipeline in Figure 6.20a. When the turnpoints are installed with 0.5 [m] tolerance, the max tension in the pipe is almost identical for the cases of 5 and 6 turnpoints installed. Whereas for the case of 7 turnpoints, it can be seen that the tension has been further increased. As pointed out earlier, increased tension will lead to a stiffer system and hence a greater dynamic response. The contact force for 7 turnpoints is therefore more increased than for 5 and 6 turnpoints, between 0 and 0.5 [m] tolerance. Furthermore, comparing the axial force for 5 and 6 turnpoints in case of 0.5 [m] and 1.0 [m] tolerance, it can be seen that the difference in tension is more extensive for 6 turnpoints, than for 5 turnpoints. Hence, the increase of contact force is greater for 6 turnpoints than for 5 turnpoints in the range of 0.5 [m] to 1.0 [m] tolerance.

7 Conclusion

Based on the knowledge gained during the thesis work, several interesting discoveries have been made. The static analysis has been conducted without considering the axial friction. The results obtained with axial friction activated gave less credible results, as the static axial distribution was changed with increased number of turnpoints. As the pipe is laid in a constant water depth, deactivating the axial friction can be justified. The reason is that the constant water depth leads to a stable departure angle, and thus an approximately constant tension in the pipe during laying. The results obtained by deactivating the axial friction during laying gave plausible results with a more logical axial force distribution.

From the static results, it was evident that the tension in the pipeline remains essentially unchanged, regardless of the number of turnpoints installed (see Figure 6.7). This is reasonable, considering that the model was set up with no axial friction activated during the laying. The equivalent moment obtained from the different analyses, showed that introducing more turnpoints along the route resulted in a flattening of the moment-curve (see Figure 6.8). This is reasonable as the distance between the turnpoints is reduced. In the same manner, the contact force between the turnpoints and the pipeline was reduced, as the force gets distributed between a higher number of supports. It can further be noted that both the contact force and the moment is quite symmetrically distributed over the pipeline curvature. Based on this, symmetry of the problem could thus be exploited in the static analysis, and thereby reducing the size of the model.

In the current method utilized by Subsea 7, the contact force acting at the turnpoint, due to interaction with the pipeline, is calculated by assuming that the force is smeared over the arc length between the turnpoints. By comparing this assumption against the results obtained in this thesis, it is found from the static analysis that the contact force is symmetrically distributed. The contact force in the first and the last turnpoint is about half the size of the force acting on the turnpoints in between. Hence, from the static analysis, this seems to be a good assumption. This may indicate that the end turnpoints can be installed with a lower geotechnical capacity than for the turnpoints in the middle of the curve. However, based on the findings in the dynamic analysis, this does not apply.

The dynamic tension in the pipeline increases as more turnpoints are installed (see Figure 6.13), i.e. the system gets stiffer. As the system gets stiffer with more turnpoints, the contact force between the turnpoint and the pipeline is actually at its lowest when only 3 turnpoints are installed. This is explained by the increase of tension in the pipeline. A stiffer system results in a larger dynamic response. Hence, the contact force is at its lowest when only 3 turnpoints are installed. As more supports are installed beyond this, the effect of the turnpoints is superior to

the increase in tension. Hence, the contact force starts to decrease when more than 4 turnpoints are installed. However, it never falls below the contact force obtained for 3 turnpoints in the cases investigated in this thesis (up to 10 turnpoints). However, the requirement on the geotechnical capacity of the turnpoints remains more or less the same, regardless the number of turnpoints installed, as the contact force is barely affected by the different number of turnpoints are installed.

By comparing the results obtained, with the current turnpoint method utilized by Subsea 7, it has been found that the axial force in the system increases when more turnpoints are installed. This is as of today not accounted for in the current method utilized by Subsea 7. As the increase in tension provides higher dynamic response, this should be accounted for in the turnpoint calculations.

The local buckling criteria dictates that neither 3 nor 4 turnpoints along the route satisfies the DNV standard. Hence, 5 or more turnpoints must be installed.

By studying the tolerance effect, it became evident that an increased turnpoint tolerance leads to an approximately exponential increase in contact force, moment and hence the local buckling criteria. Exceeding 0.5 [m] lateral tolerance, gave significant impacts on the results. It is evident that the turnpoint tolerance is of high importance. Keeping the tolerance as low as possible is essential in order to install as few turnpoints as possible. It also became evident that the maximum moment does not necessarily occur at the last turnpoint. Hence, this indicates that symmetry of the problem should not be utilized in the analyses that include the turnpoint tolerance, as the most critical moment can be overlooked.

From the analyses where turnpoint tolerances of 0.5 [m] in lateral direction are included, it has been found that 5 turnpoints along the curvature does not fulfil the local buckling criteria. Hence, installation of 6 turnpoints is proposed. This is lower than the originally 10 turnpoints that have been installed for the case investigated. Hence, the method utilized by Subsea 7 is found to be over-conservative, as expected and seen from offshore experiences.

In the method utilized by Subsea 7, it is assumed that one turnpoint is losing completely contact with the pipe, when turnpoint tolerance is considered. However, the method applied in this thesis is modelling a more realistic event, and captures the fact that the contact between the turnpoint and the pipe is not completely lost when the tolerance is kept low. This could be an explanation for why the method utilized by Subsea 7 seems to be conservative. In an offshore operation, it is desirable to have the highest possible tolerance, as the installation could be performed faster. However, since it also is desirable to install as few turnpoints as possible, this interaction has to be considered. By acquiring more knowledge of the tolerance effect, a more well-considered and controlled decision can be made.

8 Recommendations for Further Work

Based on the experience gained throughout this thesis work, some remarks have been noted and found worth taking a closer look at. First of all; as pointed out in the conclusion, it could possibly be sufficient to only consider the first two turnpoints in the route, as it appears that symmetry of the problem applies when not including the turnpoint tolerance. Unfortunately, this has not been further investigated during this thesis, due to limited time available. From the results obtained in this thesis, it definitely seems that this system property could be utilized, but there has not been conducted any final analysis confirming this. However, if this hypothesis could be proved, a significant amount of time will be saved in running the analysis, because fewer elements would need to be included.

A more extensive study of the parameters applied in the dynamic analyses, should probably be performed before a certain number of turnpoints along the route can be established. By example, the wave direction in this thesis was set equal to 45° from behind of the vessel, as the wave direction was investigated for every 45° . A more critical wave direction could most likely have been determined, resulting in higher response of the Seven Navica lay vessel. Hence, the results obtained in this thesis are possibly underestimating the impact on the pipe to some extent. This would possibly result in a recommendation of more turnpoints installed. However, as the intention of this thesis primarily was to increase the understanding of calculating the required number of turnpoints, not to find the optimal number of turnpoints only in the case investigated, this has not been done. Nevertheless, in order to use the method applied in this thesis to establish the required number of turnpoints in other analyses, more extensive parameter studies should be performed.

A more detailed study of the turnpoint tolerance is found useful, as the findings show that the turnpoint tolerance has a strong influence on the results. In an offshore operation, it is desirable to have the highest possible tolerance, as the installation could be performed faster. However, it is also desirable to install as few turnpoints as possible. By acquiring more knowledge of the tolerance effect, a more well-considered and controlled decision can be made, since the interaction between fast installation and few turnpoints has to be considered. In this thesis, the turnpoint tolerance has been tested for 5-7 turnpoints installed, and with 0, 0.5 [m] and 1.0 [m] lateral tolerance. As the results for 1 [m] tolerance are considerably higher than the ones obtained for 0 and 0.5 [m], keeping the tolerance as low as possible is obviously of high importance. However, as the results were limited in scope, mostly speculations of the turnpoint tolerance have been made. Not enough data has been collected in order to ascertain the trends found in the results. In this thesis, a tentative explanation of the phenomenon that high tolerance gave

greater impact on the structure in case of 7, rather than 5 or 6, turnpoints has been proposed. The explanation is based on the fact that more turnpoints provides less flexibility in the pipe. Taking into consideration that the effect of turnpoint tolerance gets distributed over longer sections when less turnpoints defines the geometry of the pipe, the effect of turnpoint tolerance is worse for many, than for few turnpoints. It would have been interesting to examine whether this explanation is trustworthy or not. However, since this only has been tested for three different number of turnpoints installed, and with limited tests of tolerance, there is not sufficient grounds to ascertain the proposed explanation. A more extensive study of the turnpoint tolerance is therefore proposed.

Bibliography

- Aamlid, O., Collberg, L. and Slater, S. (2011). Collapse capacity of uoe deep-water linepipe, *Proceedings of the ASME 2011 30th International Conference on Ocean, Offshore and Artic Engineering*, OMAE2011-49570, Rotterdam, The Netherlands.
- Bai, Y. and Bai, Q. (2005). *Subsea Pipelines and Risers*, Elsevier Science Ltd, Amsterdam.
- Bai, Y. and Bai, Q. (2012). *Subsea Engineering Handbook*, Gulf Professional Publishing.
- Braestrup, M. W., Andersen, J. B. and Andersen (2005). *Design and Installation of Marine Pipelines*, Blackwell Publishing, Oxford, UK.
- DNV (2006a). DNV-RP-F105, Recommended Practice: Free Spanning Pipelines.
- DNV (2006b). DNV-RP-F108, Recommended Practice: Fracture Control for Pipeline Installation Methods Introducing Cyclic Plastic Strain.
- DNV (2007). DNV-RP-F110, Recommended Practice: Global Buckling of Submarine Pipelines.
- DNV (2010). DNV-RP-F109, Recommended Practice: On-Bottom Stability Design of Submarine Pipelines.
- DNV (2012). DNV-OS-F101, Offshore Standard for Submarine Pipeline Systems.
- Fylling, I., Larsen, C., Sødahl, N., Ormberg, H., Engseth, A., Passano, E. and Holthe, K. (1995). Riflex theory manual, *SINTEF report no. STF70 F 95219*.
- Fyrileiv, O., Aamlid, O., Venås, A. et al. (1996). Analysis of expansion curves for subsea pipelines, *The Sixth International Offshore and Polar Engineering Conference*, International Society of Offshore and Polar Engineers.
- Fyrileiv, O., Mørk, K. and Chezian, M. (2005). Experiences Using DNV-RP-F105 in Assessment of Free Spanning Pipelines, *ASME 2005 24th International Conference on Offshore Mechanics and Arctic Engineering*, OMAE2005-67453, Halkidiki, Greece.
- Guo, B. (2014). *Offshore pipelines: design, installation, and maintenance*, Elsevier/Gulf Professional, Amsterdam. 2nd ed.
- Hobbs, R. (1981). Pipeline buckling caused by axial loads, *Journal of Constructional Steel Research* **1**(2): 2–10.

- Langen, I. and Sigbjørnsson (1979). Dynamisk Analyse av Konstruksjoner.
- Marley, E., Aamlid, O. and Collberg, L. (2012). Assessment of Recent Experimental Data on Collapse Capacity of UOE Pipeline, *Proceedings of the 2012 9th International Pipeline Conference*, IPC2012-90698, Calgary, Alberta, Canada.
- Moan, T. (2003). Finitie Element Modelling and Analysis of Marine Structures. TMR 4190, Department of Marine Technology, NTNU.
- Moan, T. (2013). Lecture Notes in Advanced Structural Analysis, Chapter 12 - Nonlinear Analysis. TMR4305, Department of Marine Technology, NTNU.
- Mohitpour, M., Golshan, H. and Murray, M. A. (2007). *Pipeline Design & Construction: A Practical Approach*, ASME press New York. Third Edition, Chapter 3.
- Murphy, C. E. and Langner, C. G. (1985). Ultimate Pipe Strength under Bending, Collapse and Fatigue, *Proceedings of the 4th International Conference on Offshore Mechanics and Arctic Engineering*, Vol. 1, pp. 467–477.
- Nessmo, T. S. (2014). Personal communication, Mail during master thesis work. Subsea 7.
- Palmer, A. C. and King, R. A. (2008). *Subsea pipeline engineering (2nd Edition)*, PennWell. Chapter 10.
- Palmer, A., Ellinas, C., Richards, D., Guijt, J. et al. (1989). Submarine Pipeline On-Bottom Stability: Recent AGA Research,, *Offshore Technology Conference*, OTC 6055, Houston, Texas, USA.
- Palmer, A., Ellinas, C., Richards, D., Guijt, J. et al. (1990). Design of Submarine Pipelines Against Upheaval Buckling, *Offshore Technology Conference*, OTC 6335, Houston, Texas, USA.
- Passano, E., Gjøsteen, J. K. Ø. and Sævik, S. (2008). Onboard Screening of Forecast Weather During Installation, *ASME 2008 27th International Conference on Offshore Mechanics and Arctic Engineering*, OMAE2008-57435, American Society of Mechanical Engineers, Estoril, Portugal.
- Sævik, S. (2008). *SIMLA - Theory Manual*, MARINTEK, Trondheim, Norway.
- Sævik, S. (2012). Lecture Notes in Offshore Pipeline Technology.
- Sævik, S. and Giertsen, E. (2004). Advances in design and installation analysis of pipelines in congested areas with rough seabed topography, *Proc. of OMAE'2004*, OMAE 2004-51344, ISBN: 0-7918-3745-9, Vancouver, Canada.

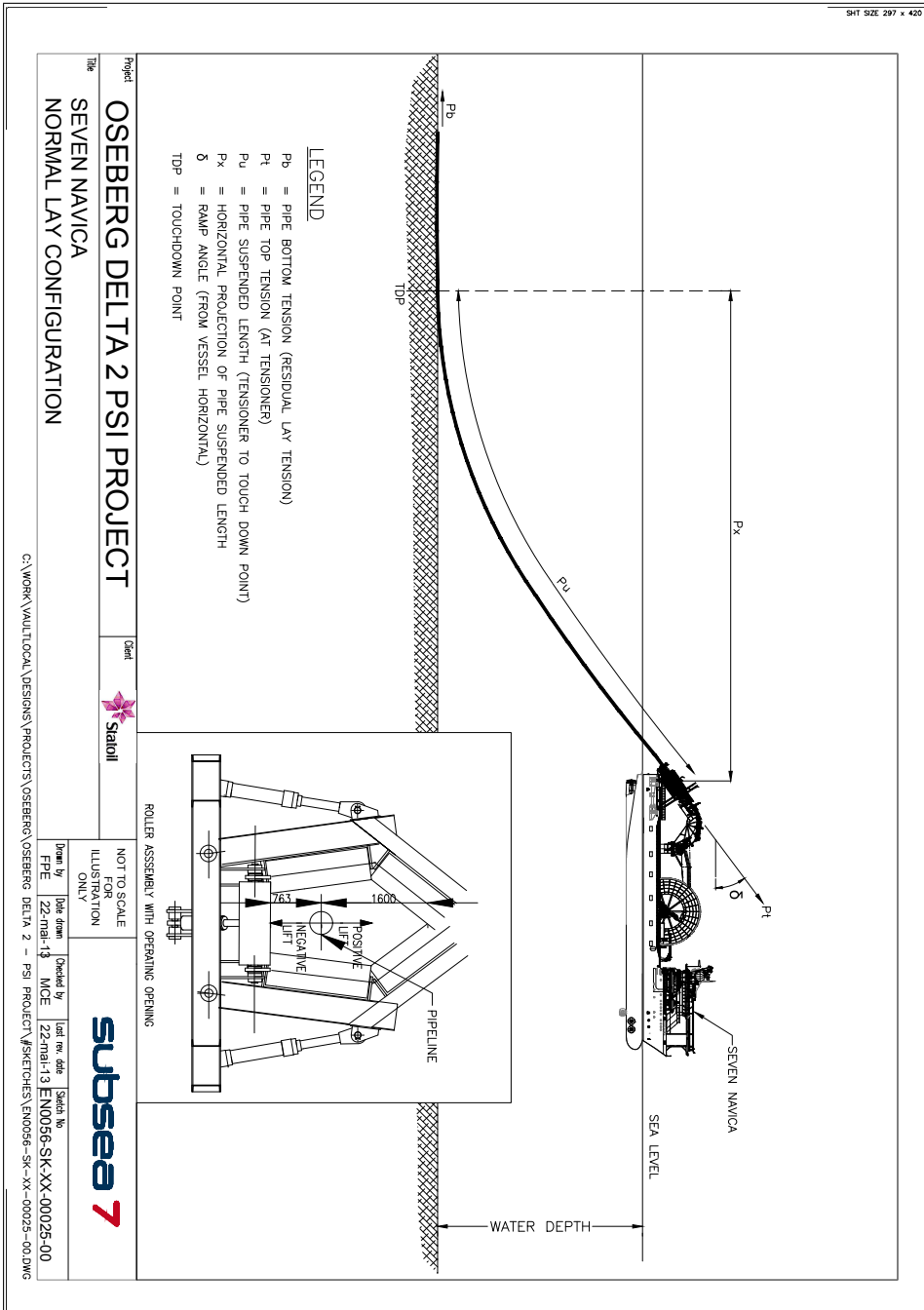
Sævik, S. and Levold, E. (1995). High temperature snaking behaviour of pipelines, *The Fifth International Offshore and Polar Engineering Conference*, International Society of Offshore and Polar Engineers.

Sævik, S., Økland, O. D., Baarholm, G. S. and Gjørsteen, J. K. (2013). *SIMLA Version 3.15.12 - User Manual*, MARINTEK, Trondheim, Norway.

Torselletti, E., Vitali, L., Bruschi, R. and Colleberg, L. (2003). Minimum Wall Thickness Requirements For Ultra Deep-Water Pipelines, *Proceedings of OMAE03: 22nd International Conference on Offshore Mechanics and Arctic Engineering*, OMAE2003-37219, Cancun, Mexico.

Appendices

A Lay Configuration



B SIMLA Input Files

All the SIMLA input files are included in a zip-folder. Below, one example of a static and a dynamic analysis are included.

B.1 J-Feed_3Turn.sif

```
1 HEAD 12" Pipeline , Static feed J-lay , Depature angle 56 - Turnpoints=3
2 #
3 #
4 # J-Feed_3Turn.sif
5 #
6 #
7 # Description of the analysis:
8 # - Static analysis; feeding out the pipeline.
9 # - Starts up from 20 seconds into the inital configuration (J-LayT.sif),
10 # i.e. right before starting laying in the curvature.
11 # - Feed elements introduced from the laying vessel.
12 # - 3 Turnpoints along the curvature are introduced.
13 # - Dummy beam introduced, in order place the turnpoints by allocating an
14 # eccentricity from this.
15 # - More realistic unit force applied in order to activate friction.
16 # However, lateral friction is deactivated in order to get a more accurate#
17 # tension distribution in the pipe.
18 # - Current gets activated over the first 10 steps. Constant force
19 #
20 #
21 # Control data:
22 #
23 #
24 # MAXIT NDIM ISOLVR NPOINT IPRINT CONR GAC ISTRES
25 CONTROL 500 3 2 8 1 1e-5 9.81 TIMEINIT
26 #
27 # IFILE TIME PIPEGRP VESSELGRP
28 "J-LayT/J-LayT_OsebergDelta2" 20 pipe1 vessel1
29 #
30 # SEAGRP TENSIONERGRP TCONGRP
31 MWL_sea guidel none
32 #
33 #
34 #
35 # Defining visualization parameters:
36 #
37 # Visual presentation in X-POST:
38 # MODE FACTOR RESULT
39 VISRES INTEGRATION 1 sigma-xx
40 #
41 #
42 #
43 # Units used (for correct display in plots):
44 # This analysis is done in kg, m, s
45 #
46 # mass length time
47 UNITS 1.0 1.0 1.0
48 #
49 #
50 #
51 # Analysis time control:
52 #
```

```

52 # First a step is done using the Autostart routine (defined in the Control #
53 # card), afterwards load steps defined by the SIMLA card is carried out. #
54 # The accuracy for the second load step sequence is also defined here. #
55 # #
56 # T DT DTVI DIDY DT0 TYPE HLAFLAG #
57 TIMECO 1.0 1.0 1.0 1.0 2.0 STATIC NOHLA #
58 TIMECO 501.0 1.0 50.0 1.0 50.0 STATIC-FEED NOHLA #
59 # TEPTYPE ITERCO ITCRIT MAXIT MAXDIV CONR #
60 AUTO GO-ON ALL 100 5 1e-5 #
61 # #
62 # #
63 # #
64 # #
65 # Building the model: #
66 # #
67 # #
68 # Node input: #
69 # #
70 # TYPE NODE XCOR YCOR ZCOR #
71 # PIPE NODES: #
72 NOCOOR COORDINATES 1 -1000.0 0.0 14.30 #
73 1001 600.0 0.0 14.30 #
74 # #
75 # FEED PIPE: #
76 # TYPE NODE XCOR YCOR ZCOR #
77 NOCOOR COORDINATES 15001 600.0 0.0 14.30 #
78 16500 600.0 0.0 14.30 #
79 NOCOOR COORDINATES 25001 601.6 0.0 14.30 #
80 26500 601.6 0.0 14.30 #
81 # #
82 # GUIDE ELEMENT: #
83 # TYPE NODE XCOR YCOR ZCOR #
84 NOCOOR COORDINATES 6011 601.6 0.0 1.0 #
85 NOCOOR COORDINATES 6012 603.6 0.0 1.0 #
86 # #
87 # VESSEL: #
88 # TYPE NODE XCOR YCOR ZCOR #
89 NOCOOR COORDINATES 7001 600.0 0.0 0.0 #
90 NOCOOR COORDINATES 7002 603.6 0.0 0.0 #
91 # #
92 # SEA NODES #
93 # TYPE NODE XCOR YCOR ZCOR #
94 NOCOOR COORDINATES 2001 150.0 -150.0 0.0 #
95 2002 -150.0 -150.0 0.0 #
96 2003 -150.0 150.0 0.0 #
97 2004 150.0 150.0 0.0 #
98 # #
99 # Beam needed to define the turnpoints: #
100 NOCOOR COORDINATES 29001 0 0.0 -110 #
101 29002 1 0.0 -110 #
102 # #
103 # #
104 # #
105 # Element connectivity input: #
106 # Building up the connectivity matrix. #
107 # #
108 # PIPE: #
109 # ELGR ELTY MATNAME ELID NODE1 NODE2 #
110 ELCON pipe1 pipe31 pipemat 1 1 2 #
111 # N NELINC NODINC #
112 REPEAT 1000 1 1 #
113 # #
114 # PIPE JOINTS TO BE FED OUT: #
115 # ELGR ELTY MATNAME ELID NODE1 NODE2 #

```

```

116 ELCON   pipe2   pipe31  pipemat   15001   15001   25001
117 #      N      NELINC  NODINC
118 REPEAT  1500    1      1
119 #-----#
120 # PIPE GUIDE:
121 #      ELGR   ELTY   MATNAME   ELID   NODE1   NODE2
122 ELCON   guide1  pipe31  vessel1   6011   6011   6012
123 #-----#
124 # VESSEL:
125 #      ELGR   ELTY   MATNAME   ELID   NODE1   NODE2
126 ELCON   vessel1 pipe31  vessel1   7001   7001   7002
127 #-----#
128 # SEABED FOR PIPE FROM STATIC SIMLA GROUP:
129 #      ELGR   ELTY   MATNAME   ELID   NODE1
130 ELCON   seabed  cont126 route    2101   1
131 #      N      NELINC  NODINC
132 REPEAT  1000    1      1
133 #-----#
134 # SEABED FOR FEED PIPE:
135 #      ELGR   ELTY   MATNAME   ELID   NODE1
136 ELCON   seabed2 cont126 route    4001   15001
137 #      N      NELINC  NODINC
138 REPEAT  1500    1      1
139 #-----#
140 # SEA:
141 #      ELGR   ELTY   MATNAME   ELID   NODE1   NODE2   NODE3   NODE4
142 ELCON   MWL_sea sea150  seamat    2001   2001   2002   2003   2004
143 #-----#
144 #-----#
145 #-----#
146 # Beam needed to define the turnpoints:
147 #      ELGR   ELTY   MATNAME   ELID   NODE1
148 ELCON   dummy   pipe31  vessel1   29001  29001   29002
149 #-----#
150 # TURNPOINTS:
151 #      ELGR   ELTY   MATNAME   ELID   NODE1
152 ELCON   turnpoint1_3 cont164  turnpoints 9001   29001
153 ELCON   turnpoint2_3 cont164  turnpoints 9002   29001
154 ELCON   turnpoint3_3 cont164  turnpoints 9003   29001
155 #-----#
156 #-----#
157 #-----#
158 # Orient Input (Giving element normals):
159 #-----#
160 #      TYPE          NO          X          Y          Z
161 # PIPE NODES:
162 ELORIENT          COORDINATES  1          -1000.0    1.0        14.30
163                   1000          600.0      1.0        14.30
164 #-----#
165 # FEED PIPE:
166 ELORIENT          COORDINATES  15001      600.0      1.0        14.30
167                   16500      600.0      1.0        14.30
168 #-----#
169 # GUIDE:
170 ELORIENT          COORDINATES  6011        601.6      1.0        1.0
171 #-----#
172 # VESSEL:
173 ELORIENT          COORDINATES  7001        603.6      1.0        0.0
174 #-----#
175 # SEABED FOR ORIGINAL PIPE:
176 ELORIENT          EULERANGLES  2101        0          0          0
177 REPEAT  1000 1 0 0 0
178 #-----#
179 # SEABED FOR FEED PIPE:

```

```

180 ELORIENT      EULERANGLES      4001      0      0      0
181 REPEAT      1500 1 0 0 0
182 #
183 # Beam needed to define the turnpoints:
184 # DUMMY:      TYPE      NO      X      Y      Z
185 ELORIENT      COORDINATES      29001      1      1.0      -110
186 #
187 # TURNPOINTS:
188 ELORIENT      EULERANGLES      9001      0      0      0
189 REPEAT      3 1 0 0 0
190 #
191 #-----#
192 #-----#
193 # ELEMENT ECCENTRICITY:
194 #-----#
195 # TURNPOINTS:
196 #      ELTYP      ELID      ELEND      XECC      YECC      ZECC      ANG
197 ELECC      STINGER      9001      1      748      -1.2329      0      0
198 #      DX1      DY1      DZ1      DX2      DY2      DZ2
199 #      0      0      -5      0      0      5
200 #
201 #      ELTYP      ELID      ELEND      XECC      YECC      ZECC      ANG
202 ELECC      STINGER      9002      1      958.9743      -61.6140      0      0
203 #      DX1      DY1      DZ1      DX2      DY2      DZ2
204 #      0      0      -5      0      0      5
205 #
206 #      ELTYP      ELID      ELEND      XECC      YECC      ZECC      ANG
207 ELECC      STINGER      9003      1      1106.4950      -225.3674      0      0
208 #      DX1      DY1      DZ1      DX2      DY2      DZ2
209 #      0      0      -5      0      0      5
210 #
211 #-----#
212 # Element Property Input:
213 #-----#
214 # PIPE:
215 #      ELGRP      PIPE      RADIUS      THICKNESS      CD_R      CD_T      CM_R
216 ELPROP      pipe1      pipe      0.13975      0.0255      1.0      0.1      2.0
217 #      CM_T      Dry_Mass      Submerged_Mass      ODP      ODW      RKS
218 #      1.2      251.03      76.20      0.4658      0.4658      0.5
219 #
220 #      ELGRP      PIPE      RADIUS      THICKNESS      CD_R      CD_T      CM_R
221 ELPROP      pipe2      pipe      0.13975      0.0255      1.0      0.1      2.0
222 #      CM_T      Dry_Mass      Submerged_Mass      ODP      ODW      RKS
223 #      1.2      251.03      76.20      0.4658      0.4658      0.5
224 #-----#
225 # VESSEL:
226 #      ELGRP      PIPE      RADIUS      THICKNESS      CD_R      CD_T      CM_R
227 ELPROP      vessel1      pipe      1.0      0.1      0.8      0.1      2.0
228 #      CM_T      Dry_Mass      Submerged_Mass      ODP      ODW      RKS
229 #      1.2      41.4e-3      15.6e-3      0.1783      0.1783      0.5
230 #
231 #-----#
232 # GUIDE:
233 #      ELGRP      PIPE      RADIUS      THICKNESS      CD_R      CD_T      CM_R
234 ELPROP      guide1      pipe      0.5      0.02      1.0      0.1      2.0
235 #      CM_T      Dry_Mass      Submerged_Mass      ODP      ODW      RKS
236 #      1.1      1.00e-3      1.00e-3      0.508      1.00      0.5
237 #
238 #-----#
239 # Beam needed to define the turnpoints:
240 #      ELGRP      PIPE      RADIUS      THICKNESS      CD_R      CD_T      CM_R
241 ELPROP      dummy      pipe      1.0      0.1      0.8      0.1      2.0
242 #      CM_T      Dry_Mass      Submerged_Mass      ODP      ODW      RKS
243 #      1.2      41.4e-3      15.6e-3      0.1783      0.1783      0.5

```

```

244 # #
245 # #
246 # TURNPOINTS: #
247 # ELGRP TYPE DIAMETER #
248 ELPROP turnpoint1_3 ROLLER 2
249 ELPROP turnpoint2_3 ROLLER 2
250 ELPROP turnpoint3_3 ROLLER 2
251 # #
252 # #
253 # #
254 # Defining the bottom properties: #
255 # #
256 # #
257 # Contact surface properties: #
258 # #
259 # CONAME COFILE NLINES KP0 #
260 COSURFPR route "../Route_Data_PL.txt" 1 0.0
261 # XSTART YSTART ANGSTART MLINEID #
262 0.0 0.0 0.0 100
263 # #
264 # #
265 # #
266 # Soil description: #
267 # #
268 # MLINEID KP1 KP2 MATERIAL_NAME #
269 COSUPR 100 -1000 400 soil1
270 400 100000 soil2
271 # #
272 # #
273 # Contact Interfaces: #
274 # #
275 # SEABED: #
276 # GRPNAME MASTERNAME SLAVENAME IS1 ISN TX TY #
277 CONTINT seabed pipe1 route 1 1000 1000.0 0.0
278 # TZ MAXIT IGAP #
279 0.0 10 1
280 # #
281 # GRPNAME MASTERNAME SLAVENAME IS1 ISN TX TY #
282 CONTINT seabed2 pipe2 route 15001 16500 1000.0 0.0
283 # TZ MAXIT IGAP #
284 0.0 10 1
285 # #
286 # SEA: #
287 # GRPNAME MASTERNAME SLAVENAME #
288 CONTINT MWL_sea MWL_sea pipe1 #
289 # #
290 # GRPNAME MASTERNAME SLAVENAME #
291 CONTINT MWL_sea MWL_sea pipe2 #
292 # #
293 # TURNPOINTS: #
294 # -feed: #
295 # GRPNAME MASTERNAME SLAVENAME IS1 ISN #
296 CONTINT turnpoint1_3 turnpoint1_3 pipe2 15001 16500 #
297 # TX TY TZ MAXIT IGAP #
298 10000.0 10000.0 0.0 40 1
299 # #
300 # GRPNAME MASTERNAME SLAVENAME IS1 ISN #
301 CONTINT turnpoint2_3 turnpoint2_3 pipe2 15001 16500 #
302 # TX TY TZ MAXIT IGAP #
303 10000.0 10000.0 0.0 40 1
304 # #
305 # GRPNAME MASTERNAME SLAVENAME IS1 ISN #
306 CONTINT turnpoint3_3 turnpoint3_3 pipe2 15001 16500 #
307 # TX TY TZ MAXIT IGAP #

```

```

308          10000.0          10000.0          0.0          40          1
309 #
310 #
311 #
312 #
313 #          CONSTRAINT INPUT
314 #
315 #
316 # Pipe bottom end:
317 #
318 # Prescribed displacement      TYPE      NODE      DOF      AMPL      THIST
319 CONSTR PDISP                  LOCAL      1      1      0.0      200
320 CONSTR PDISP                  LOCAL      1      2      0.0      200
321 CONSTR PDISP                  LOCAL      1      3      0.0      200
322 CONSTR PDISP                  LOCAL      1      4      0.0      200
323 CONSTR PDISP                  LOCAL      1      5      0.0      200
324 CONSTR PDISP                  LOCAL      1      6      0.0      200
325 #
326 #
327 # Vessel Node, COG:
328 #
329 # Prescribed displacement      TYPE      NODE      DOF      AMPL      THIST
330 CONSTR PDISP                  GLOBAL     7002      1      0.0      200
331 CONSTR PDISP                  GLOBAL     7002      2      0.0      200
332 CONSTR PDISP                  GLOBAL     7002      3      0.0      200
333 CONSTR PDISP                  GLOBAL     7002      4      0.0      200
334 CONSTR PDISP                  GLOBAL     7002      5      0.0      200
335 CONSTR PDISP                  GLOBAL     7002      6      0.0      200
336 #
337 #
338 # Guide:
339 #
340 # Constraint equation          TYPE      SNODE      DOF      C0      MNODE      DOF      C1
341 CONSTR CONEQ                  GLOBAL     6012      1      0.0      7001      1      1.0
342 CONSTR CONEQ                  GLOBAL     6012      2      0.0      7001      2      1.0
343 CONSTR CONEQ                  GLOBAL     6012      3      0.0      7001      3      1.0
344 CONSTR CONEQ                  GLOBAL     6012      4      0.0      7001      4      1.0
345 CONSTR CONEQ                  GLOBAL     6012      5      0.0      7001      5      1.0
346 CONSTR CONEQ                  GLOBAL     6012      6      0.0      7001      6      1.0
347 #
348 #
349 # Constraint between SIMLA-pipe and FEED-pipe:
350 #
351 # Constraint equation          TYPE      SNODE      DOF      C0      MNODE      DOF      C1
352 CONSTR CONEQ                  LOCAL     1001      1      0.0      15001     1      1.0
353 CONSTR CONEQ                  LOCAL     1001      2      0.0      15001     2      1.0
354 CONSTR CONEQ                  LOCAL     1001      3      0.0      15001     3      1.0
355 CONSTR CONEQ                  LOCAL     1001      4      0.0      15001     4      1.0
356 CONSTR CONEQ                  LOCAL     1001      5      0.0      15001     5      1.0
357 CONSTR CONEQ                  LOCAL     1001      6      0.0      15001     6      1.0
358 #
359 #
360 # FEED-pipe upper end:
361 #
362 # Constraint equation          TYPE      SNODE      DOF      C0      MNODE      DOF      C1
363 CONSTR CONEQ                  LOCAL     26500     1      0.0      6011      1      1.0
364 CONSTR CONEQ                  LOCAL     26500     2      0.0      6011      2      1.0
365 CONSTR CONEQ                  LOCAL     26500     3      0.0      6011      3      1.0
366 CONSTR CONEQ                  LOCAL     26500     4      0.0      6011      4      1.0
367 CONSTR CONEQ                  LOCAL     26500     5      0.0      6011      5      1.0
368 CONSTR CONEQ                  LOCAL     26500     6      0.0      6011      6      1.0
369 #
370 #
371 # FEED-group:

```



```

372 # _____#
373 # Constraint equation          SNODE  MNODE1  MNODE2  MNODE3          #
374 CONSTR FEEDCONEQ            25001   6011   15002   6011          #
375 #       N   SLAVINC MASTINC          #
376 REPEAT  1499    1     1          #
377 # _____#
378 # _____#
379 # _____#
380 # Beam needed to define the turnpoints:          #
381 # _____#
382 # Prescribed displacement      TYPE   NODE  DOF   AMPL  THIST          #
383 CONSTR PDISP                  GLOBAL 29001  1     0.0   200          #
384 CONSTR PDISP                  GLOBAL 29001  2     0.0   200          #
385 CONSTR PDISP                  GLOBAL 29001  3     0.0   200          #
386 CONSTR PDISP                  GLOBAL 29001  4     0.0   200          #
387 CONSTR PDISP                  GLOBAL 29001  5     0.0   200          #
388 CONSTR PDISP                  GLOBAL 29001  6     0.0   200          #
389 # _____#
390 # _____#
391 #                               BOUNDARY CONDITIONS          #
392 # _____#
393 # _____#
394 # Sea surface:          #
395 # _____#
396 #       TYPE   NODID  DOF          #
397 BONCON GLOBAL  2001   1          #
398 REPEAT 4 1          #
399 BONCON GLOBAL  2001   2          #
400 REPEAT 4 1          #
401 BONCON GLOBAL  2001   3          #
402 REPEAT 4 1          #
403 # _____#
404 # _____#
405 # _____#
406 # _____#
407 #                               LOADS:          #
408 # _____#
409 # _____#
410 # Current Loading:          #
411 # _____#
412 #       NO     TYPE     DEPTH  CURR  PHI          #
413 CURLOAD   100   global    0     1.05  3.5949          #
414           -25   0.9     3.5949          #
415           -50   0.9     3.5949          #
416           -75   0.8     3.5949          #
417           -107  0.6     3.5949          #
418           -110  0.0     3.5949          #
419 # _____#
420 # _____#
421 # _____#
422 # Seaload Spesifications:          #
423 # _____#
424 #       SEAGR    X1     Y1     X2     Y2     CURRNO  THIST          #
425 SEALO  MWL_sea  -100000 -100000 100000 100000  100     400          #
426 # _____#
427 # _____#
428 # _____#
429 # External Pressure & Gravity Load:          #
430 # _____#
431 #       PRESHIST  GRAVHIST          #
432 PELOAD  100     100          #
433 # _____#
434 # _____#
435 # _____#

```

```

436 #
437 # LAY SIMULATION DATA
438 #
439 #
440 # VesselID npipe ID_pipe ID_sbd
441 SIMLA 7002 2 pipe1 seabed
442 # pipe2 seabed2
443 # FILE NODES
444 # "soil_reaction_forces_TDP-static.txt" 5
445 # SMYS UTIL TYPE NELPST TowerL DIST TOL
446 # 450e6 1.0 T 1 24.0 0.0 0.1
447 #
448 #
449 #
450 #
451 # FEED COMMAND
452 #
453 #
454 # Tels Simla to feed out elements in the analysis.
455 #
456 # GRPNAME TIME IOP C0[rad/m] C1[rad/kNm]
457 FEED pipe2 1.0 1 0.0 0.0
458 #
459 #
460 #
461 #
462 # Joint property input:
463 #
464 # JOINTABNAME ELGRP1
465 JOINTPR_APPLY route pipe1
466 #
467 # NAME TYPE KP1 KP2 RADIUS THICKNESS
468 JOINTPR_DEFINE route pipe -1000 100000 0.13975 0.0255
469 # CDR CDT CMR CMT Dry_Mass Submerged_Mass
470 # 1.0 0.1 2.0 1.2 251.03 76.20
471 # ODP ODW RKS LABEL
472 # 0.4658 0.4658 0.5 "FBE/PP"
473 #
474 #
475 #
476 #
477 # History data:
478 #
479 #
480 # EXTERNAL PRESSURE & GRAVITY:
481 # NO TIME Load_Factor
482 THIST 100 0.0 1.00
483 # 100.0 1.00
484 #
485 # VESSEL MOTION:
486 # NO TIME Load_Factor
487 THIST 200 0.0 0.00
488 # 100.0 0.00
489 #
490 # CURRENT:
491 # NO TIME Load_Factor
492 THIST 400 0.0 0.00
493 # 10.0 1.00
494 # 100.0 1.00
495 #
496 #
497 #
498 #
499 # MATERIAL DATA

```

```

500 #
501 #
502 # PIPE from static Simla J-lay:
503 #
504 #          MNAME  LINEAR  POISS  TALFA  TECOND  HEATC  BETA
505 MATERIAL  pipemat linear  0.3    1.17e-5  50    800    0
506 #   EA      EIY      EIZ      GIT      E      G
507   4.6349e9  4.5637e7  4.5637e7  3.5105e7  207e9  79.6e9
508 #
509 #
510 #
511 # VESSEL:
512 #
513 #          MNAME  LINEAR  POISS  TALFA  TECOND  HEATC  BETA
514 MATERIAL  vessel1 linear  0.3    1.17e-5  50    800    0
515 #   EA      EIY      EIZ      GIT      E      G
516   1.034e13  3.25e16  3.25e16  1.16e16  210e9  80.8e9
517 #
518 #
519 #
520 # FEED pipe:
521 #
522 #          MNAME  TYPE          IHARD  POISS  RHO  TALFA  TECOND
523 MATERIAL  pipemat2  elastoplastic  1.0    0.3    0.0  1.17e-5  0.0
524 #          HEATC          EPS          SIGMA
525          0.0              0.0000      0.0
526          0.0018          367.0e6
527          0.0023          409.0e6
528          0.0052          451.0e6
529          0.0291          493.0e6
530          0.2000          535.0e6
531 #
532 #
533 #
534 # SEA:
535 #
536 #          MNAME  MTYPE  RHO
537 MATERIAL  seamat  sea    1026
538 #
539 #
540 #
541 # BEAM NEEDED TO DEFINE THE TURNPOINTS:
542 #
543 #          MNAME  LINEAR  POISS  TALFA  TECOND  HEATC  BETA
544 MATERIAL  dummy  linear  0.3    1.17e-5  50    800    0
545 #   EA      EIY      EIZ      GIT      E      G
546   1e13    3e13    3e13    1e13    210e9  79.6e9
547 #
548 #
549 # ROLLER:
550 #
551 #          MNAME          MTYPE          MUX  MUY  XNAME  YNAME  ZNAME
552 MATERIAL  turnpoints  contact      0.3  0.3  turnx  turny  turnz
553 #
554 # Properties for friction in x direction (turned off in contint card):
555 #          MNAME  HYCURVE          EPS          SIGMA
556 MATERIAL  turnx  HYCURVE      -10000      -2000000e3
557          10000      2000000e3
558 #
559 # Properties for friction in y direction (turned off in contint card):
560 #          MNAME  HYCURVE          EPS          SIGMA
561 MATERIAL  turny  HYCURVE      -10000      -2000000e3
562          10000      2000000e3
563 #

```

```

564 # Stiffness of rollers #
565 # MNAME HYCURVE EPS SIGMA #
566 MATERIAL turnz HYCURVE -10000 -15000000e3 #
567 10000 15000000e3 #
568 #-----#
569 #-----#
570 #-----#
571 # SOIL PROPERTIES #
572 #-----#
573 #-----#
574 # Properties of the already laid pipe: #
575 # MNAME CONTACT MUX MUY XNAME YNAME ZNAME #
576 MATERIAL soil1 contact 0.6 0.6 soilx soily soilz #
577 #-----#
578 #-----#
579 # Properties for the newly laid pipe: #
580 # MNAME CONTACT MUX MUY XNAME YNAME ZNAME #
581 MATERIAL soil2 contact 0.6 0.6 soilx soil2y soilz #
582 #-----#
583 #-----#
584 # AXIAL-DIRECTION: MNAME EPCURVE IHARD EPS SIGMA #
585 MATERIAL soilx epcurve 1 0.0 0.0 #
586 0.005 1.0 #
587 100.0 10.0 #
588 #-----#
589 # LATERAL-DIRECTION: MNAME EPCURVE IHARD EPS SIGMA #
590 #-----#
591 # Already laid pipe: #
592 MATERIAL soily epcurve 1 0.0 0.0 #
593 0.1 1.0 #
594 1000.0 10.0 #
595 #-----#
596 # Newly laid pipe: #
597 MATERIAL soil2y epcurve 1 0.0 0.0 #
598 0.1 1.0 #
599 1000.0 10.0 #
600 #-----#
601 # Z-DIRECTION: MNAME HYCURVE EPS SIGMA #
602 MATERIAL soilz hycurve -10000.0 -400000.0e3 #
603 10000.0 400000.0e3 #
604 #-----#
605 #-----#

```

B.2 Dynamic_Restart_3Turn.spi

```

1 HEAD 12" Pipeline , Dynamic Restart , Depature angle 56 – Turnpoints = 3
2 #-----#
3 #-----#
4 # Dynamic_restart_3Turn.sif #
5 #-----#
6 #-----#
7 # Description of the analysis: #
8 # – Dynamic analysis carried out at what is believed will provide highest #
9 # dynamic response in the system during the laying stage. #
10 # – Consistent Mass matrix applied. #
11 # – More realistic unit force applied in order to activate friction. #
12 # – Touchdown-position = 1197 – right after the last turnpoint. #
13 # – 500 pipe-elements. Higher resolution near the turnpoints. #

```

```

14 # – Vessel modeled as a spring element in order to implement the vessel #
15 # motion. #
16 # – Interval [900, 1200]s #
17 # – First time step to activate pressure and gravity linearly. #
18 # – From 910s to 940s, activating current and waves gradually by the use #
19 # of the RAMPCOS-function. #
20 # – Pipe restrained at the end, representing the one template. #
21 # #
22 # #
23 # #
24 # Control data: #
25 # #
26 # #
27 # MAXIT NDIM ISOLVR NPOINT IPRINT CONR GAC ISTRES No #
28 CONTROL 500 3 2 8 1 1e-5 9.81 RESTART 1 #
29 # #
30 # #
31 # Control Parameters for dynamic analysis: #
32 # #
33 # MSTAT ALPHA1 ALPHA2 ALPHA #
34 DYNCONT 2 0.0 0.095 -0.05 #
35 # #
36 # #
37 # Visual presentation in X-POST: #
38 # #
39 # MODE FACTOR RESULT #
40 VISRES INTEGRATION 1 sigma-xx #
41 # #
42 # #
43 # Dynamic (Nodal) results: #
44 # #
45 # TYPE NODEID DOF #
46 DYNRES_N 1 5001 1 #
47 DYNRES_N 1 5001 2 #
48 DYNRES_N 1 5001 3 #
49 DYNRES_N 1 5001 4 #
50 DYNRES_N 1 5001 5 #
51 DYNRES_N 1 5001 6 #
52 # #
53 # #
54 # Dynamic (Element) Results: #
55 # #
56 # (ELEMENT) FORCES EL1 ELNOD DOF #
57 DYNRES_E 2 9001 1 3 #
58 DYNRES_E 2 9002 1 3 #
59 DYNRES_E 2 9003 1 3 #
60 # #
61 # #
62 # Envelope Results: #
63 # #
64 # PIPE: #
65 # (NODAL) DISPL NODE1 NODE2 DOF LOAD_STEP #
66 ENVRES_N 1 1 501 1 1 #
67 ENVRES_N 1 1 501 2 1 #
68 ENVRES_N 1 1 501 3 1 #
69 # #
70 # TURNPOINTS: #
71 # (ELEMENT) FORCES EL1 EL2 ELNOD DOF TIME0 #
72 ENVRES_E 2 9001 9003 1 3 1 #
73 # #
74 # SEABED: #
75 # (ELEMENT) FORCES EL1 EL2 ELNOD DOF TIME0 #
76 ENVRES_E 2 3001 3501 1 1 1 #
77 ENVRES_E 2 3001 3501 1 2 1 #

```

```

78 ENVRES_E      2      3001      3501      1      3      1
79 #
80 # PIPE:
81 # (ELEMENT) FORCES EL1      EL2      ELNOD      DOF      TIME0
82 ENVRES_E      2      1      500      2      1      1
83 ENVRES_E      2      1      500      2      4      1
84 ENVRES_E      2      1      500      2      5      1
85 ENVRES_E      2      1      500      2      6      1
86 # (ELEMENT) TORSION EL1      EL2      ELNOD      DOF      TIME0
87 ENVRES_E      3      1      500      1      2      1
88 #
89 #
90 # Units used (for correct display in plots):
91 # This analysis is done in kg, m, s
92 #
93 #      Mass      Length      Time
94 UNITS      1.0      1.0      1.0
95 #
96 #
97 #
98 # Analysis time control:
99 # First a step is done using the Autostart routine (defined in the Control
100 # card), afterwards load steps defined by the SIMLA card is carried out.
101 # The accuracy for the second load step sequence is also defined here.
102 #
103 #      T      DT      DTVI      DTDY      DT0      TYPE      HLAFLAG
104 TIMECO      1.0      1.0      1.0      1.0      210.0      STATIC      NOHLA
105 TIMECO      901.0      900.0      100.0      100.0      210.0      STATIC      NOHLA
106 TIMECO      1201.0      0.1      1.0      1.0      210.0      DYNAMIC      NOHLA
107 #      TEPTYPE ITERCO      ITCRIT      MAXIT      MAXDIV      CONR
108      AUTO      GO-ON      ALL      20      5      1e-4
109 #
110 #
111 #
112 #              Building the model:
113 #
114 #
115 # Node input:
116 #
117 # PIPE NODES
118 #      TYPE      NODE      XCOR      YCOR      ZCOR
119 NOCOOR      COORDINATES      1      -220.0      0.0      10.0
120      11      -120.0      0.0      10.0
121      31      -20.0      0.0      10.0
122      181      280.0      0.0      10.0
123      221      320.0      0.0      10.0
124      301      360.0      0.0      10.0
125      501      560.0      0.0      10.0
126 #
127 # VESSEL NODE
128 #      TYPE      NODE      XCOR      YCOR      ZCOR
129 NOCOOR      COORDINATES      5001      600.0      0.0      5.0
130 #
131 #
132 # SEA NODES
133 #      TYPE      NODE      XCOR      YCOR      ZCOR
134 NOCOOR      COORDINATES      2001      150.0      -150.0      0.0
135      2002      -150.0      -150.0      0.0
136      2003      -150.0      150.0      0.0
137      2004      150.0      150.0      0.0
138 #
139 #
140 # Beam needed to define the turnpoints:
141 #      TYPE      NODE      XCOR      YCOR      ZCOR

```

```

142 NOCOOR      COORDINATES      29001      0      0.0      -110
143           29002      1      0.0      -110
144 #
145 #
146 #
147 # Element connectivity input:
148 # Building up the connectivity matrix.
149 #
150 # PIPE:
151 #      ELGR      ELTY      MATNAME      ELID      NODE1      NODE2
152 ELCON      pipe1      pipe31      pipemat      1      1      2
153 #      N      NELINC      NODINC
154 REPEAT      500      1      1
155 #
156 #
157 # VESSEL:
158 #      ELGR      ELTY      MATNAME      ELID      NODE1      NODE2
159 ELCON      vessel1      spring137      vessel1      5001      5001      501
160 #
161 #
162 # SEABED:
163 #      ELGR      ELTY      MATNAME      ELID      NODE1
164 ELCON      seabed      cont126      route      3001      1
165 #      N      NELINC      NODINC
166 REPEAT      500      1      1
167 #
168 #
169 # SEA:
170 #      ELGR      ELTY      MATNAME      ELID      NODE1      NODE2      NODE3      NODE4
171 ELCON      sea1      sea150      seamat      2001      2001      2002      2003      2004
172 #
173 #
174 # Beam needed to define the turnpoints:
175 #      ELGR      ELTY      MATNAME      ELID      NODE1
176 ELCON      dummy      pipe31      dummy      29001      29001      29002
177 #
178 #
179 # TURNPOINTS:
180 #      ELGR      ELTY      MATNAME      ELID      NODE1
181 ELCON      turnpoint1_3      cont164      turnpoints      9001      29001
182 ELCON      turnpoint2_3      cont164      turnpoints      9002      29001
183 ELCON      turnpoint3_3      cont164      turnpoints      9003      29001
184 #
185 #
186 #
187 # ELEMENT ECCENTRICITY:
188 #
189 # Vessel:
190 #      ELTYP      ELID      ELEND      XECC      YECC      ZECC
191 ELECC      beam      5001      1      -40      0      4.999
192 #
193 #
194 # TURNPOINTS:
195 #      ELTYP      ELID      ELEND      XECC      YECC      ZECC      ANG
196 ELECC      STINGER      9001      1      748      -1.2329      0      0
197 #      DX1      DY1      DZ1      DX2      DY2      DZ2
198 #      0      0      -5      0      0      5
199 #
200 #      ELTYP      ELID      ELEND      XECC      YECC      ZECC      ANG
201 ELECC      STINGER      9002      1      958.9743      -61.6140      0      0
202 #      DX1      DY1      DZ1      DX2      DY2      DZ2
203 #      0      0      -5      0      0      5
204 #
205 #      ELTYP      ELID      ELEND      XECC      YECC      ZECC      ANG

```

```

206 ELECC STINGER 9003 1 1106.4950 -225.3674 0 0
207 # DX1 DY1 DZ1 DX2 DY2 DZ2 #
208 0 0 -5 0 0 5 #
209 # #
210 # #
211 # #
212 # Orient Input (Giving element normals): #
213 # #
214 # PIPE: TYPE NO X Y Z #
215 ELORIENT COORDINATES 1 -220.0 1.0 10.0 #
216 500 560.0 1.0 10.0 #
217 # #
218 # #
219 # VESSEL: TYPE NO X Y Z #
220 ELORIENT EULERANGLES 5001 0 0 0 #
221 # #
222 # #
223 # SEABED: TYPE NO X Y Z #
224 ELORIENT EULERANGLES 3001 0 0 0 #
225 # N INC XINC YINC ZINC #
226 REPEAT 500 1 0 0 0 #
227 # #
228 # #
229 # Beam needed to define the turnpoints: #
230 # DUMMY: TYPE NO X Y Z #
231 ELORIENT COORDINATES 29001 0 1.0 -110 #
232 # #
233 # #
234 # TURNPOINTS: NO X Y Z #
235 ELORIENT EULERANGLES 9001 0 0 0 #
236 REPEAT 3 1 0 0 0 #
237 # #
238 # #
239 # #
240 # Element Property Input: #
241 # #
242 # PIPE: #
243 # ELGRP PIPE RADIUS THICKNESS CD_R CD_T CM_R #
244 ELPROP pipe1 pipe 0.13975 0.0255 1.0 0.1 2.0 #
245 # CM_T Dry_Mass Submerged_Mass ODP ODW RKS #
246 1.2 251.03 76.20 0.4658 0.4658 0.5 #
247 # #
248 # #
249 # VESSEL: #
250 # ELGRP PIPE TX TY TZ RX RY RZ #
251 ELPROP vessel1 genspring 1 1 1 1 1 1 #
252 # #
253 # #
254 # Beam needed to define the turnpoints: #
255 # ELGRP PIPE RADIUS THICKNESS CD_R CD_T CM_R #
256 ELPROP dummy pipe 1.0 0.1 0.8 0.1 2.0 #
257 # CM_T Dry_Mass Submerged_Mass ODP ODW RKS #
258 1.2 41.4e-3 15.6e-3 0.1783 0.1783 0.5 #
259 # #
260 # #
261 # TURNPOINTS: #
262 # ELGRP TYPE DIAMETER #
263 ELPROP turnpoint1_3 ROLLER 2 #
264 ELPROP turnpoint2_3 ROLLER 2 #
265 ELPROP turnpoint3_3 ROLLER 2 #
266 # #
267 # #
268 # #
269 # #

```



```

270 #                               Defining the bottom properties :                               #
271 #                                                                                               #
272 #                                                                                               #
273 # Contact surface properties :                                                                 #
274 #                                                                                               #
275 #           CONAME  COFILE                               NLINES  KP0                               #
276 COSURFPR  route   "../Route_Data_PL.txt"             1         0.0                               #
277 #   XSTART  YSTART  ANGSTART  MLINEID                               #
278 #     0.0    0.0    0.0       100                               #
279 #                                                                                               #
280 #                                                                                               #
281 #                                                                                               #
282 # Soil description :                                                                           #
283 #                                                                                               #
284 #           MLINEID  KP1    KP2    MATERIAL_NAME                               #
285 COSUPR  100        -1000000  1000000  soil1                               #
286 #                                                                                               #
287 #                                                                                               #
288 #                                                                                               #
289 # Contact Interfaces :                                                                           #
290 #                                                                                               #
291 # SEABED:                                                                                       #
292 #           GRPNAME  MASTERSNAME  SLAVENAME  IS1    ISN    TX    TY #
293 CONTINT  seabed    pipel        route     1      500   3    0  #
294 #           TZ      MAXIT        IGAP                               #
295 #           0       5           1                               #
296 #                                                                                               #
297 #                                                                                               #
298 # SEA:                                                                                           #
299 #           GRPNAME  MASTERSNAME  SLAVENAME                               #
300 CONTINT  seal     seal         pipel                               #
301 #                                                                                               #
302 #                                                                                               #
303 # TURNPOINTS:                                                                                 #
304 #           GRPNAME  MASTERSNAME  SLAVENAME  IS1    ISN    TX    TY #
305 CONTINT  turnpoint1_3  turnpoint1_3  pipel    1      500  100000 #
306 #           TY      TZ      MAXIT        IGAP                               #
307 #           100000  0       40           1                               #
308 #                                                                                               #
309 #           GRPNAME  MASTERSNAME  SLAVENAME  IS1    ISN    TX    TY #
310 CONTINT  turnpoint2_3  turnpoint2_3  pipel    1      500  100000 #
311 #           TY      TZ      MAXIT        IGAP                               #
312 #           100000  0       40           1                               #
313 #                                                                                               #
314 #           GRPNAME  MASTERSNAME  SLAVENAME  IS1    ISN    TX    TY #
315 CONTINT  turnpoint3_3  turnpoint3_3  pipel    1      500  100000 #
316 #           TY      TZ      MAXIT        IGAP                               #
317 #           100000  0       40           1                               #
318 #                                                                                               #
319 #                                                                                               #
320 #                                                                                               #
321 #                                                                                               #
322 #                               LOADS:                                                       #
323 #                                                                                               #
324 #                                                                                               #
325 # Current Loading: 1 year extreme current                                                    #
326 #                                                                                               #
327 #           NO      TYPE      DEPTH  CURR    PHI                               #
328 CURLOAD  100     global     0      1.05   3.5949 #
329 #           -25     0.9      3.5949 #
330 #           -50     0.9      3.5949 #
331 #           -75     0.8      3.5949 #
332 #           -107    0.6      3.5949 #
333 #           -110    0.0      3.5949 #

```

```

334 # #
335 # #
336 # #
337 # Sealoading Specifications: #
338 # #
339 # SEAGR X1 Y1 X2 Y2 CURRNO THIST #
340 SEALO seal -100000 -100000 100000 100000 100 400 #
341 # #
342 # #
343 # #
344 # External Pressure & Gravity Load: #
345 # #
346 # PRESHIST GRAVHIST #
347 PELOAD 100 100 #
348 # #
349 # #
350 # #
351 # Wave Load: #
352 # #
353 # ELGRP IRREGULAR WAVENO WAVEHIST X0 Y0 ANG #
354 WAVELO seal IRREGULAR 100 250 0.0 0.0 4.3803 #
355 # Tp Hs WaterDepth Dt Duration T0 #
356 7 2.5 110 0.25 10800 1.1 #
357 # KinWaterDepth SEED TYPE #
358 110 0 1 #
359 # #
360 # #
361 # History data: #
362 # #
363 # #
364 # EXTERNAL PRESSURE & GRAVITY: #
365 # NO TIME Load_Factor #
366 THIST 100 0.0 0.5 #
367 1.0 1.0 #
368 100.0 1.0 #
369 # #
370 # Beam (dummy): #
371 # NO TIME Load_Factor #
372 THIST 200 0.0 1.0 #
373 100.0 1.0 #
374 # #
375 # WAVELOAD: #
376 # NO START STOP TYPE Load_Factor #
377 THIST_R 250 0.0 910.0 RAMPCOS 0.0 #
378 910.0 940.0 RAMPCOS 1.0 #
379 # #
380 # CURRENT: #
381 # NO START STOP TYPE Load_Factor #
382 THIST_R 400 0.0 910.0 RAMPCOS 0.0 #
383 910.0 940.0 RAMPCOS 1.0 #
384 # #
385 # #
386 # #
387 # #
388 # CONSTRAINT INPUT #
389 # #
390 # #
391 # Pipe upper-end connected to vessel node: #
392 # #
393 # Constraint equation TYPE NODE DOF NODE fi1 fi2 fi3 ex ey ez #
394 CONSTR PDISP SPECIAL 501 1 5001 0 0 0 -40 0 10.0 #
395 CONSTR PDISP SPECIAL 501 2 5001 0 0 0 -40 0 10.0 #
396 CONSTR PDISP SPECIAL 501 3 5001 0 0 0 -40 0 10.0 #
397 #CONSTR PDISP SPECIAL 501 4 5001 0 0 0 -40 0 10.0 #

```

```

398 # #
399 # #
400 # RAO: #
401 # #
402 # Constraint equation TYPE NODE DOF HEADING WAVENO NAME
403 CONSTR PDISP RAO 5001 1 0.0 100 SURGE
404 CONSTR PDISP RAO 5001 2 0.0 100 SWAY
405 CONSTR PDISP RAO 5001 3 0.0 100 HEAVE
406 CONSTR PDISP RAO 5001 4 0.0 100 ROLL
407 CONSTR PDISP RAO 5001 5 0.0 100 PITCH
408 CONSTR PDISP RAO 5001 6 0.0 100 YAW
409 # #
410 # #
411 # WAVE ELEVATION: #
412 # #
413 # Constraint equation TYPE NODE DOF WAVENO #
414 CONSTR PDISP WAVE 2001 3 100 #
415 REPEAT 4 1 #
416 # #
417 # #
418 # Beam needed to define the turnpoints: #
419 # #
420 # Prescribed displacement TYPE NODE DOF AMPL THIST #
421 CONSTR PDISP GLOBAL 29001 1 0.0 200 #
422 CONSTR PDISP GLOBAL 29001 2 0.0 200 #
423 CONSTR PDISP GLOBAL 29001 3 0.0 200 #
424 CONSTR PDISP GLOBAL 29001 4 0.0 200 #
425 CONSTR PDISP GLOBAL 29001 5 0.0 200 #
426 CONSTR PDISP GLOBAL 29001 6 0.0 200 #
427 # #
428 # #
429 # BOUNDARY CONDITIONS #
430 # #
431 # #
432 # Sea surface: #
433 # #
434 # TYPE NODID DOF #
435 BONCON GLOBAL 2001 1 #
436 REPEAT 4 1 #
437 BONCON GLOBAL 2001 2 #
438 REPEAT 4 1 #
439 # #
440 # #
441 # Pipe bottom end: #
442 # #
443 # TYPE NODID DOF #
444 BONCON GLOBAL 1 1 #
445 BONCON GLOBAL 1 2 #
446 BONCON GLOBAL 1 3 #
447 BONCON GLOBAL 1 4 #
448 BONCON GLOBAL 1 5 #
449 BONCON GLOBAL 1 6 #
450 # #
451 # #
452 # #
453 # #
454 # RAO DEFINITIONS #
455 # #
456 # Read: INPUT-FILE: RIFLEX KinWaterDepth #
457 READTRF ../Seven_Navica_Empty_Reel_RAORiflex.Rif RIF 110 #
458 # #
459 # #
460 # PROPERTY INPUT #
461 # #
  
```

```

462 #-----#
463 # Joint property input: #
464 #-----#
465 # JOINTABNAME ELGRP1 #
466 JOINTPR_APPLY route pipe1 #
467 #-----#
468 # NAME TYPE KP1 KP2 RADIUS THIKNESS #
469 JOINTPR_DEFINE route pipe -100000 100000 0.13975 0.0255 #
470 # CDR CDT CMR CMT Dry_Mass Submerged_Mass #
471 # 1.0 0.1 2.0 1.2 251.03 76.20 #
472 # ODP ODW RKS LABEL #
473 # 0.4658 0.4658 0.5 "FBE/PP" #
474 #-----#
475 #-----#
476 #-----#
477 #-----#
478 # MATERIAL DATA #
479 #-----#
480 #-----#
481 # PIPE: #
482 #-----#
483 # MNAME LINEAR POISS TALFA TECOND HEATC BETA #
484 MATERIAL pipemat linear 0.3 1.17e-5 50 800 0 #
485 # EA EIY EIZ GIT E G #
486 # 4.6349e9 4.5637e7 4.5637e7 3.5105e7 207e9 79.6e9 #
487 #-----#
488 #-----#
489 #-----#
490 # VESSEL: #
491 #-----#
492 # MNAME TYPE XNAME YNAME ZNAME #
493 MATERIAL vessel1 GENSPRING surgespring swayspring heavespring #
494 # XMOMNAME YMOMNAME ZMOMNAME #
495 # rollspring pitchspring yawspring #
496 #-----#
497 # MNAME HYCURVE EPS SIGMA #
498 MATERIAL surgespring hycurve -1000 0 #
499 # 1000 0 #
500 MATERIAL swayspring hycurve -1000 0 #
501 # 1000 0 #
502 MATERIAL heavespring hycurve -1000 0 #
503 # 1000 0 #
504 MATERIAL rollspring hycurve -1000 0 #
505 # 1000 0 #
506 MATERIAL pitchspring hycurve -1000 0 #
507 # 1000 0 #
508 MATERIAL yawspring hycurve -1000 0 #
509 # 1000 0 #
510 #-----#
511 #-----#
512 #-----#
513 # BEAM NEEDED TO DEFINE THE TURNPOINTS: #
514 #-----#
515 # MNAME LINEAR POISS TALFA TECOND HEATC BETA #
516 MATERIAL dummy linear 0.3 1.17e-5 50 800 0 #
517 # EA EIY EIZ GIT E G #
518 # 1e13 3e13 3e13 1e13 210e9 79.6e9 #
519 #-----#
520 #-----#
521 #-----#
522 # ROLLER: #
523 #-----#
524 # MNAME MTYPE MUX MUY XNAME YNAME ZNAME #
525 MATERIAL turnpoints contact 0.3 0.3 turnx turny turnz #

```

```

526 #-----#
527 # Properties for friction in x direction (turned off in contint card): #
528 #           MNAME  HYCURVE           EPS           SIGMA #
529 MATERIAL      turnx  HYCURVE          -10000        -2000000e3 #
530 #           10000           2000000e3 #
531 #-----#
532 # Properties for friction in y direction (turned off in contint card): #
533 #           MNAME  HYCURVE           EPS           SIGMA #
534 MATERIAL      turny  HYCURVE          -10000        -2000000e3 #
535 #           10000           2000000e3 #
536 #-----#
537 # Stiffness of rollers #
538 #           MNAME  HYCURVE           EPS           SIGMA #
539 MATERIAL      turnz  HYCURVE          -10000        -15000000e3 #
540 #           10000           15000000e3 #
541 #-----#
542 #-----#
543 # SOIL: #
544 #-----#
545 #           MNAME  CONTACT  MUX  MUY  XNAME  YNAME  ZNAME #
546 MATERIAL      soil1  contact  0.6  0.6  soilx  soily  soilz #
547 #-----#
548 #-----#
549 # AXIAL-DIRECTION: #
550 #           MNAME  EPCURVE  IHARD  EPS           SIGMA #
551 MATERIAL      soilx  epcurve  1      0.0           0.0 #
552 #           0.005           1.0 #
553 #           100.0           10.0 #
554 #-----#
555 # LATERAL-DIRECTION: #
556 #           MNAME  EPCURVE  IHARD  EPS           SIGMA #
557 MATERIAL      soily  epcurve  1      0.0           0.0 #
558 #           0.1           1.0 #
559 #           1000.0           10.0 #
560 #-----#
561 # Z-DIRECTION: #
562 #           MNAME  HYCURVE           EPS           SIGMA #
563 MATERIAL      soilz  hycurve          -10000.0        -400000.0e3 #
564 #           10000.0           400000.0e3 #
565 #-----#
566 #-----#
567 # SEA: #
568 #           MNAME  MTYPE  RHO #
569 MATERIAL      seamat  sea    1026 #
570 #-----#

```

C MATLAB files

Route Input- and Local Buckling Criteria Calculations in MATLAB are included. The codes can also be found in the attached zip-folder.

C.1 Simla_Route_Input_Calculations

```
1 %% Simla Route Input Calculations
2 % Christian Andersson
3 % Spring 2014
4
5 %% Clear and close previous data
6 clear all
7 close all
8
9 %% Route data
10 KP_start = 0; % Start position
11 KP_tot = 1600; % Route length [m]
12 TP_1 = 748; % KP-value starting the curve radius [m]
13 TP_2 = 1195; % KP-value ending the curve radius [m]
14 r_curve = 400; % Curve Radius [m]
15 z_depth = -110; % Constant Water Depth [m]
16
17 %% Defining the diameter of the roller and pipe:
18 D_roller = 2;
19 D_pipe_total = 0.4658;
20
21 %% Defining arc length and total angle of the arc:
22 s_total = TP_2-TP_1; % Arc length of the curve radius [m]
23 theta = s_total/r_curve; % Total angle of the arc [rad]
24
25 %% Defining the step lengths:
26 ds = 1; % Incremental arc length [m]
27 dtheta = theta*ds/s_total; % Incremental arc angle [rad]
28
29 %% Defines the first straight distance:
30 x1 = (KP_start:TP_1)'; % X-coordinates [m]
31 y1 = zeros(length(x1),1); % Y-coordinates [m]
32
33 %% Defines the curved curvature:
34 x2 = zeros(s_total, 1); % Dummy initial zero-vector
35 y2 = zeros(s_total, 1); % Dummy initial zero-vector
36 x_turn = zeros(s_total, 1);
37 y_turn = zeros(s_total, 1);
38 for i=1:s_total
39     x2(i,1) = TP_1 + r_curve*cos((pi/2)-dtheta*i); % X-coordinates [m]
40     y2(i,1) = -r_curve + r_curve*sin((pi/2)-dtheta*i); % Y-coordinates [m]
41     x_turn(i,1) = x2(i,1) - ((D_roller+D_pipe_total)/2)*cos((pi/2)-dtheta*i);
42     y_turn(i,1) = y2(i,1) - ((D_roller+D_pipe_total)/2)*sin((pi/2)-dtheta*i);
43 end
44 x_origin = TP_1;
45 y_origin = -r_curve;
46
47 %% Defines the last straight distance:
48 L3 = KP_tot - TP_2; % Remaining distance to template L [m]
49 x_temp = x2(length(x2)); % Temporary x given as previous x-value
50 y_temp = y2(length(y2)); % Temporary y given as previous y-value
51 x3 = zeros(L3, 1); % Dummy initial zero-vector
```

```

52 y3 = zeros(L3, 1); % Dummy initial zero-vector
53 for i=1:L3
54     x3(i) = x_temp + cos(theta); % X-coordinates [m]
55     y3(i) = y_temp - sin(theta); % Y-coordinates [m]
56     x_temp = x3(i); % Temporary x given as previous x-value
57     y_temp = y3(i); % Temporary y given as previous y-value
58 end
59
60 %% Coordinates of the entire route:
61 xy = [x1, y1; x2, y2; x3, y3]; % X- and Y-coordinates for entire route
62
63 %% Input to Simla
64 z = z_depth * ones(length(xy),1); % Z-coordinates for entire route
65 nx = zeros(length(xy),1); % Normal vector component x-direction
66 ny = zeros(length(xy),1); % Normal vector component y-direction
67 nz = ones(length(xy),1); % Normal vector component z-direction
68 simla = [xy, z, nx, ny, nz]; % Input Matrix of coordinates to Simla
69
70 %Write to file:
71 fName = 'C:\Marintek\SIMLA\Simla\cases\Masteroppgave\OsebergDelta2\Route_Data_PL←
    .txt';
72 dlmwrite(fName,simla, 'delimiter','\t', 'newline', 'pc', 'precision', 8);
73
74 %% Defines the coordinates of the arc/circle:
75 % Includes the first coordinate that starts the arc:
76 xarc = [x1(length(x1)); x2]; % X-coordinate [m]
77 yarc = [y1(length(y1)); y2]; % Y-coordinate [m]
78
79 x_turn_coor = [x1(length(x1)); x_turn];
80 y_turn_coor = [y1(length(y1))-((D_roller+D_pipe_total)/2); y_turn];
81 n_turncurve = length(x_turn_coor)
82
83 %% Find turnpoints-locations:
84 % n turnpoints:
85 n_turn = 8; % Define number of turnpoints.
86 x_turnpoint = zeros(n_turn, 1);
87 y_turnpoint = zeros(n_turn, 1);
88 theta_turn = zeros(n_turn, 1);
89
90 % Place the turnpoint at beginning and end of the curvature if n_turn>2:
91 if n_turn<=2
92     for i = 1:n_turn
93         % x-coord [m]
94         x_turnpoint(i, 1) = (x_turn_coor(floor(i*n_turncurve/(n_turn+1))) + ...
95         x_turn_coor(ceil(i*n_turncurve/(n_turn+1))))/2;
96         % y-coord [m]
97         y_turnpoint(i, 1) = (y_turn_coor(floor(i*n_turncurve/(n_turn+1))) + ...
98         y_turn_coor(ceil(i*n_turncurve/(n_turn+1))))/2;
99         % Theta:
100        theta_turn(i,1) = tan((y_origin-y_turnpoint(i,1))/...
101        (x_turnpoint(i,1)-x_origin));
102    end
103
104 else
105     x_turnpoint(1,1) = x_turn_coor(1);
106     y_turnpoint(1,1) = y_turn_coor(1);
107     x_turnpoint(n_turn, 1) = x_turn_coor(end);
108     y_turnpoint(n_turn, 1) = y_turn_coor(end);
109     theta_turn(1,1) = pi/2;
110     theta_turn(n_turn,1) = pi/2 - theta;
111
112
113 for i=2:(n_turn-1)
114 % x-coord [m]:

```

```

115 x_turnpoint(i, 1) = (x_turn_coor(floor((i-1)*n_turncurve/(n_turn-1))) + ...
116     x_turn_coor(ceil((i-1)*n_turncurve/(n_turn-1))))/2;
117 % y-corrdr [m]:
118 y_turnpoint(i, 1) = (y_turn_coor(floor((i-1)*n_turncurve/(n_turn-1))) + ...
119     y_turn_coor(ceil((i-1)*n_turncurve/(n_turn-1))))/2;
120 % Theta:
121 theta_turn(i,1) = atan((y_turnpoint(i,1)-y_origin)/...
122     (x_turnpoint(i,1)-x_origin));
123 end
124 end
125 theta_turn
126
127 disp([num2str(n_turn) ...
128     ' Turnpoints, gives the following turnpoint-coordinates:'])
129 Turnpoints = vpa([x_turnpoint, y_turnpoint])
130
131 %% Turnpoint tolerance
132 Tol=1;
133 x_tol = [x_turnpoint + Tol*sin(pi/2 - theta_turn) ,...
134     x_turnpoint ,...
135     x_turnpoint - Tol*sin(pi/2 - theta_turn) ]
136 y_tol = [y_turnpoint + Tol*cos(pi/2 - theta_turn)...
137     , y_turnpoint ,...
138     y_turnpoint - Tol*cos(pi/2 - theta_turn)]
139
140 %% Worst case turnpoint tolerance:
141 xy_tol_worst1 = [x_tol(:,1), y_tol(:,1)];
142 xy_tol_worst2 = [x_tol(:,3), y_tol(:,3)];
143 xy_normal = [x_tol(:,2), y_tol(:,2)];
144 disp('out = ');
145 vpa(xy_tol_worst1, 8)
146 disp('normal = ');
147 vpa(xy_normal,8)
148 disp('inn = ');
149 vpa(xy_tol_worst2,8)
150
151
152
153 %% Plots to verify the Coordinates:
154 % Route:
155 plot(xy(:,1), xy(:,2), 'LineWidth',2)           % Plots the entire route in xy↔
156     plane
157 axis equal;                                     % Defines x- & y-axis to be equal
158 xlabel('x-coordinate', 'FontWeight','bold'); % Label the x-axis.
159 ylabel('y-coordinate', 'FontWeight','bold'); % Label the y-axis.
160 title('Route Coordinates, XY-plane', 'FontWeight','bold');
161
162 % Arc + n turnpoints:
163 figure(2)
164 plot(xy(:,1), xy(:,2), x_turnpoint, y_turnpoint, 'g*', 'LineWidth',2);
165 axis equal,                                     % Defines x- & y-axis to be equal
166
167 % Arc + n turnpoints:
168 figure(3)
169 plot(xarc, yarc, x_turnpoint, y_turnpoint, 'r*', x_turn_coor, y_turn_coor);
170 axis equal;                                     % Defines x- & y-axis to be equal
171
172 % Tolerance:
173 Tolerance_figure=sprintf...
174 ('/Users/Christian/Documents/Skole/Masteroppgave/LaTex/Matlab-plots/↔
175     Route_Tolerance');
176 figure(4)
177 plot(x_tol(:,1), y_tol(:,1), 'r*', ...
178     x_tol(:,3), y_tol(:,3), 'r*', ...

```



```

177     x_tol(:,2), y_tol(:,2), 'k*', ...
178     x_turn_coor, y_turn_coor)
179 axis equal;
180 xlabel('x-coordinate', 'FontSize',12);    % Label the x-axis.
181 ylabel('y-coordinate', 'FontSize',12);    % Label the y-axis.
182 title('Tolerance, XY-plane', 'FontWeight','bold', 'FontSize',14');
183 saveas(gcf,Tolerance_figure,'png')
184 saveas(gcf,Tolerance_figure,'eps')
  
```

C.2 Local_Buckling_Calculations

```

1 %% Local Buckling – Load Controlled Condition
2 % Christian Andersson
3 % Spring 2014
4
5 %% Clear and close previous data
6 clear all
7 close all
8
9 %% Creates Symbolic Variables:
10 syms t
11 %% Input-choice:
12 % Safety Class Resistance Factor:
13 Safety = 1; % 1=Low, 2=Medium, 3=High
14 res_type = 1; % 1=Pressure Containment, 2=Other
15
16 % Material Resistance Factor:
17 gamma_m = 1.15; % 1.15=SLS/ULS/ALS, 1=FLS
18
19 % Load Effect Factor Combination:
20 load_comb = 2; % 1/2=ULS(System/Local Check),3=FLS,4=ALS
21
22 % Condition Load Effect Factor:
23 condition = 1;
24 % 1=UnevenSeabed, 2=Reeling&Pull-in, 3=SystemPressureTest, 4=Other
25
26 %% Input Values:
27 rho_water = 1026; % Water Density [kg/m^3]
28 rho_steel = 7850; % Steel Density [kg/m^3]
29 g = 9.81; % Gravity of Earth [N/kg]
30 h = 110; % Water Depth [m]
31 P_i = 0; % Empty Condition = 0 [Pa]
32 D = 0.305; % Nominal Diameter [m]
33 t2 = 0.0255; % Thickness t2 [m]
34 fy = 450e6; % Yield Stress [Pa], SMYS
35 fu = 535e6; % Tensile Strength [Pa], SMTS
36 nu = 0.3; % Poison ratio [-]
37 E = 207E9; % Youngs Modulus [Pa]
38 alfa_fab = 1; % Fabrication Factor [-]
39 f0 = 0.005; % Ovalization [-]
40
41
42 %% Static Pressure
43 P_e = rho_water*g*h; % Static Pressure [Pa]
44
45 %% Elastic Collapse Pressure:
46 P_el = ((2*E)/(1-nu^2))*(t2/D)^3; % Elastic Collapse Pressure [Pa]
47
  
```

```

48 %% Plastic Collapse Pressure:
49 P_p = 2*alfa_fab*fy*t2/D; % Plastic Collapse Pressure [Pa]
50
51 %% Analytical coefficients:
52 a = 1;
53 b = -P_el;
54 c = -(P_p^2 + P_p*P_el*f0*D/t2);
55 d = P_el*P_p^2;
56
57 %% Analytical Collapse Pressure:
58 u = (1/3)*(-(1/3)*b^2 + c);
59 v = (1/2)*((2/27)*b^3 - (1/3)*b*c + d);
60 Phi = acos(-v/sqrt(-u^3));
61 y = -2*sqrt(-u)*cos((Phi/3) + (60*pi/180));
62 P_c = y - (1/3)*b; % Collapse Pressure [Pa]
63
64 %% Plastic Capacities:
65 S_p = fy*pi*(D-t2)*t2; % Axial Capacity
66 M_p = fy*(D-t2)^2*t2; % Moment Capacity
67
68 %% Resistance Factors:
69 % Safety Class Resistance Factor
70 safe = load('C:\Users\Christian\Documents\Skole\MASTEROPPGAVE\Matlab_inputfiler\←
Safety_Class.txt');
71 gamma_SC = safe(res_type, Safety); % Resistance Factor
72
73 %% Load Effect Factor Combination:
74 load_effects = load('C:\Users\Christian\Documents\Skole\MASTEROPPGAVE\←
Matlab_inputfiler\Load_Effect_Factors.txt');
75 gamma_vec = load_effects(load_comb,:);
76 gamma_F = gamma_vec(1); % Functional Loads
77 gamma_E = gamma_vec(2); % Environmental Load
78 gamma_I = gamma_vec(3); % Interference Loads
79 gamma_A = gamma_vec(4); % Accidental Loads
80 gamma_C = 1.07; % Condition Load Effect Factor
81 gamma_F = 1.1;
82 gamma_E = 1.3;
83 gamma_I = 0;
84 gamma_A = 0
85 gamma_load = [gamma_F*gamma_C; gamma_E; gamma_F; gamma_A*gamma_C];
86
87 %% Factor used in combined loading criteria:
88 beta = (60-(D/t2))/90;
89
90 %% Flow Stress Parameter:
91 alfa_c = (1-beta) + beta*(fu/fy);
92
93 %% Design Loads: Moments and Effective Axial Loads:
94 Static = load('C:\Users\Christian\Documents\Skole\MASTEROPPGAVE\←
Matlab_inputfiler\Static.txt');
95 Dynamic = load('C:\Users\Christian\Documents\Skole\MASTEROPPGAVE\←
Matlab_inputfiler\Dynamic.txt');
96 Tol = load('C:\Users\Christian\Documents\Skole\MASTEROPPGAVE\Matlab_inputfiler\←
Tolerance.txt');
97 for i=1:8
98     if i<=2
99         j=3
100     elseif i<=4
101         j=4
102     else
103         j=5
104     end
105 S_F = Static(i,1)*1e3; % STATIC
106 S_E = Dynamic(i,1)*1e3; % DYNAMIC

```

```

107
108 M_F = Static(i,2)*1e3;           % STATIC
109 M_E = Dynamic(i,2)*1e3;        % DYNAMIC
110
111 S_F_tol = Static(j,1)*1e3;      % STATIC
112 M_F_tol = Static(j,2)*1e3;
113
114 if i<=6
115   S_E_tol = Tol(i,1)*1e3;
116   M_E_tol = Tol(i,2)*1e3;
117   else
118     S_E_tol=0;
119     M_E_tol=0;
120   end
121
122 %disp([S_F, S_E, M_F, M_E]);
123 disp([S_F_tol, S_E_tol, M_F_tol, M_E_tol])
124
125 %% Design Moment and Design Effective Axial Force:
126 M_Sd = [M_F, M_E, 0, 0]*gamma_load;
127 S_Sd = [S_F, S_E, 0, 0]*gamma_load;
128
129 %% TOLERANCE Design Moment and Design Effective Axial Force:
130 M_Sd_tol = [M_F_tol, M_E_tol, 0, 0]*gamma_load;
131 S_Sd_tol = [S_F_tol, S_E_tol, 0, 0]*gamma_load;
132
133 %% External Overpressure:
134 Util_Ext(i) = (gamma_m*gamma_SC*(abs(M_Sd)/(alfa_c*M_p)) + ...
135   (gamma_m*gamma_SC*S_Sd/(alfa_c*S_p))^2)^2 + ...
136   (gamma_m*gamma_SC*P_e/P_c)^2;
137
138 %% External Overpressure:
139 Util_Ext_tol(i) = (gamma_m*gamma_SC*(abs(M_Sd_tol)/(alfa_c*M_p)) + ...
140   (gamma_m*gamma_SC*S_Sd_tol/(alfa_c*S_p))^2)^2 + ...
141   (gamma_m*gamma_SC*P_e/P_c)^2;
142
143 end
144 Turn = (3:10)';
145 disp([Util_Ext', Turn, Util_Ext_tol'])

```